THESIS FOR THE DEGREE OF DOCTOR OF PHILOSOPHY

Voyage Optimization Algorithms for Intelligent Shipping – Considering Energy Efficiency and Collision Avoidance

YUHAN CHEN

Department of Mechanics and Maritime Sciences
CHALMERS UNIVERSITY OF TECHNOLOGY
Gothenburg, Sweden, 2025

Voyage Optimization Algorithm for Intelligent Shipping – Considering Energy Efficiency and Collision Avoidance

YUHAN CHEN

ISBN: 978-91-8103-165-2

© YUHAN CHEN, 2025

Doktorsavhandlingar vid Chalmers tekniska högskola
Ny serie nr 5623
ISSN 0346-718X

Chalmers University of Technology
Department of Mechanics and Maritime Sciences
Division of Marine Technology
SE-412 96, Gothenburg
Sweden
Telephone: + 46 (0)31-772 1000
www.chalmers.se

Printed by Chalmers Reproservice
Gothenburg, Sweden, 2025

To my family

Voyage Optimization Algorithm for Intelligent Shipping – Considering Energy Efficiency and Collision Avoidance

YUHAN CHEN
Chalmers University of Technology
Department of Mechanics and Maritime Sciences
Division of Marine Technology

Abstract

Environmental emissions from shipping pose significant challenges caused by the rapid increase in energy consumption. Voyage optimization system is an valuable tool to address this challenge by enhancing energy efficiency, with optimization algorithms serving as its core, enabling better decision-making. The main objectives of this thesis are to develop voyage optimization algorithms to improve energy efficiency and investigate the capability of voyage optimization algorithms for ship collision avoidance. By achieving these goals, it aims to support intelligent shipping, characterized by enhanced decision-making capabilities. Weather routing, i.e., voyage optimization with the aim to increase energy efficiency in ship operations, rely on ship performance models to estimate energy costs and optimization algorithms to find optimal voyages. However, ship performance models may contain large uncertainties in estimating a ship's energy consumption and emissions. In addition, optimization algorithms should also consider uncertain and dynamic factors, e.g., weather conditions and market fluctuations, to ensure optimal operations.

To achieve the overall objectives, this thesis first conducts a systematical literature review to help researchers and practitioners clearly understand weather routing and identify opportunities in current research for the development of its optimization algorithms. Based on the review, this thesis proposes two innovative approaches to achieve energy-efficient weather routing, an Isochrone-based predictive optimization algorithm (IPO) and a learning-based multi-objective evolutionary algorithm (L-MOEA). They can effectively minimize fuel consumption and optimize energy efficiency, with the aid of emerging machine learning (ML) techniques. In addition, IPO can be conducted in real-time to address uncertainties in weather routing while considering arrival time, and L-MOEA can consider the essential operational uncertainty due to weather forecast. Furthermore, to ensure reliable operations in practice, this thesis investigates the uncertainty of fuel consumption caused by Specific Fuel Oil Consumption (SFOC) in ship performance models, and the impact of this uncertainty on weather routing. Finally, this thesis extends the research outcome on Isochrone-based algorithms to assist shipping in confined waterways. It seeks to achieve real-time voyage optimization for collision avoidance problems while considering the arrival time, assist on-time transport, and ensure ship operational safety.

It can be concluded that the proposed IPO method can achieve an average of 5% energy savings for weather routing, comparable with L-MOEA. It has also been found that the uncertainty due to ship energy performance models should be carefully considered in decision-making to ensure reliable voyage planning. In addition, the proposed IPO-based collision avoidance algorithm can effectively optimize the voyage in real-time to ensure a ship's operational safety and on-time arrival, complying with COLREGs in both confined waterways and open waters.

Keywords: Collision avoidance, energy efficiency, estimated time of arrival (ETA), Isochrone algorithm, machine learning, voyage optimization, weather routing.

Preface

This thesis presents research work performed from March 2022 to February 2025, at the Division of Marine Technology, Department of Mechanics and Maritime Sciences, Chalmers University of Technology, Sweden. Financial support was provided by the AUTOBarge, the European Union's Framework Program for Research and Innovation Horizon 2020 under Grant 955768, the Swedish Vinnova Project under Grant 2021-02768, and the Lighthouse Sustainable Shipping Program.

It was late at night when I nearly finished my thesis, finally having a chance to summarize my PhD experience from a personal perspective. This task feels even more challenging than summarizing my work, but a few words come to mind, "Intensive" and "Unforgettable" may be sufficient to describe both my work and life during the past three years. Studying for a PhD at Chalmers has been a wonderful opportunity and experience, and I feel very fortunate. Everyone I have met has been great, and I am delighted to have met you all.

First, I would like to express my sincere appreciation to my main supervisor, Professor Wengang Mao. I seemed to have faced ongoing challenges ever since starting my PhD, which never ceased throughout these three years. Initially, the difficulties were centered around research, but even after conquering those, tougher issues arose. However, you have always been very supportive and understanding both professionally and personally. I am truly thankful for the opportunity you gave me to pursue my PhD at the very beginning, and for all your insightful and valuable guidance and supervision throughout my research. I have learned so much from my academic studies and am deeply grateful to have you as my main supervisor.

I would also like to extend my appreciation to my co-supervisor Professor Jonas Ringsberg. As my academic supervisor and manager, your well-organized approach to work and passion for efficiency and meticulousness have been an inspiration. Thank you for all your guidance, discussions, warm support, and all the interesting division activities you would often organize, which have left me with many fond memories. I also feel fortunate to have had the opportunity to pursue my PhD studies in such an enjoyable place as our division. Thank you Rikard, Huadong, and Arash, for all the discussions and chats we've had, and thanks to all my friends and colleagues in our division. I know I thanked you all only half a year ago in my licentiate but still thank you Chengqian and your wife Xue, Chi, Xiao, Daniel and Mohammad for all the chats, which I really enjoyed it. Thank you Dhanika, Rana and all our friends in AUTOBarge, every time I participated in our NWEs and the other times I spent with you all brought me great joy. Gratitude also goes to my great but currently cyberfriends in China, Ge, Rui, and her little daughter. Having friends like you all has brightened my days during the hard times.

Similarly, I could not have achieved this PhD and so much more without my partner, Wenting. Having you in my life has been wonderful, and I look forward to our long and wonderful future, along with our little cat, Potato. Thanks to my parents and grandparents. I know over the past

three years, I have been so focused on my own matters, often absent and sometimes neglecting you. I know you do not blame me, with your always present support and understanding, but I still carry the guilt. Maybe one day these hard times will be behind me, but I hope I will still remember that only with your support could I have been able to keep improving, and only with you by my side does everything have meaning.

Finally, I would like to express a few words in memory of my grandfather. This PhD experience is once in a lifetime, with many valuable experiences and gains, but I also lost one of the most irreplaceable people in my life forever. What I regret the most is probably never realizing that many things we take for granted are not unchangeable. This even led me to question the meaning of my life at one point. If such a solid foundation as family is no longer there, other added values seem to lose their significance. However, there is no way for me to find out how you are doing now. In the end, I can only rely on faith and hope, believing that you must be enjoying a better life than ever before. After almost two years, and I could not see you even once, as if by not seeing you I could avoid facing the reality that you are no longer here. Everyone in our family has since been afraid to even look at your twin brother. Everyone in our family misses you. I wish you nothing but all the best, wherever you are. I hope the words written here continue to remind me not to overlook, but to cherish what I have been taking for granted for so long, as they may indeed be lost someday.

Yuhan Chen
Gothenburg, January 2025

Contents

List of appended papers

Paper I **Chen, Y.**, Zhang, C., Guo, Y., Wang, Y., Lang, X., Zhang, M., Mao, W., 2024. State-of-the-art optimization algorithms in weather routing — ship decision support systems: challenge, taxonomy, and review. Submitted to *Journal publication.*

Paper II **Chen, Y.**, Tian, W., Mao, W., 2024. Strategies to improve the Isochrone algorithm for ship voyage optimization. *Ships and Offshore Structures*. pp.1-13. DOI: 10.1080/17445302.2024.2329011.

Paper III **Chen, Y.**, Mao, W., 2024. An Isochrone-based predictive optimization for efficient ship voyage planning and execution. *IEEE Transactions on Intelligent Transportation Systems*. DOI: 10.1109/TITS.2024.3416349.

Paper IV Guo, Y., Wang, Y., **Chen, Y.**, Wu, L., Mao, W., 2024. Learning-based Pareto-optimum routing of ships incorporating uncertain met-ocean forecasts. *Transportation Research Part E: Logistics and Transportation Review.* DOI: 10.1016/j.tre.2024.103786.

Paper V **Chen, Y.**, Zhang, C., Dashtimanesh, A., Wang, H., Mao, W., 2024. A machine learning method to model stochastic Specific Fuel Oil Consumption induced fuel consumption for ship voyage optimization. Submitted to *Journal publication.*

Paper VI **Chen, Y.**, Zhang, C., Mao, W., 2024. Isochrone-based real-time ship collision avoidance complying with COLREGs in confined waterways. *In manuscript for Journal publication*.

Authors' contributions (CRediT):

Yuhan Chen (All papers): Conceptualization, Methodology, Writing - original draft, Writing - review & editing, Investigation, Validation, Visualization, Programming.

Wengang Mao (All papers): Conceptualization, Validation, Writing - review & editing, Supervision, Funding acquisition.

Chi Zhang (Paper I, V, VI): Conceptualization, Methodology, Validation, Writing – review & editing, Supervision.

Yiyang Wang: (**Paper I**) Validation, Supervision, Funding acquisition; (**Paper IV**) Writing – review & editing, Supervision, Methodology, Funding acquisition, Data curation.

Yuhan Guo: (**Paper I**) Investigation, Validation; (**Paper IV**) Writing – original draft, Conceptualization, Investigation, Methodology, Visualization.

Xiao Lang (Paper I): Investigation, Validation, Methodology.

Mingyang Zhang (Paper I): Investigation, Validation, Methodology.

Wuliu Tian (Paper II): Validation, Supervision, Funding acquisition.

Lingxiao Wu (**Paper IV**)**:** Writing – review & editing, Validation, Funding acquisition.

Abbas Dashtimanesh (**Paper V**)**:** Methodology, Validation, Supervision.

Helong Wang (**Paper V**)**:** Methodology, Validation, Supervision.

List of other relevant papers by the author

Paper A **Chen, Y.**, Mao, W., Zhang, C., 2023. Different strategies to improve Isochrone voyage optimization algorithm. In *Advances in the Analysis and Design of Marine Structures* (pp. 53-61). MARSTRUCT 2023, 3-5 April 2023, Gothenburg, Sweden. CRC Press. DOI:10.1201/9781003399759.

Paper B **Chen, Y.**, Mao, W., 2024. Sensitivity of ship voyage optimizations to various energy cost models. *Proceedings of the ASME 2024 43rd International Conference on Ocean, Offshore and Arctic Engineering*. OMAE 2024, 9-14 June 2024, Singapore. Paper no. OMAE2024-127986. DOI: 10.1115/OMAE2024-127986.

Paper C **Chen, Y.,** Zhang, C., Mao, W., 2025. Isochrone-based collision avoidance for enhanced ship safety in confined waterways. Submitted to *The 35th International Ocean and Polar Engineering Conference*. ISOPE 2025, 1-6 June 2025, Seoul/KINTEX, Korean. Paper No. 2025-TPC-0393.

Paper D Zhang, C., **Chen, Y.**, Mao, W., 2025. Identification of tank cleaning operations at sea based on machine learning method using AIS data. Submitted to *The 35th International Ocean and Polar Engineering Conference.* ISOPE 2025, 1-6 June 2025, Seoul/KINTEX, Korean. Paper no. 2025-TPC-0412.

Paper E Xiao, L., **Chen, Y.**, Zhang, M., Zhang, C., Mao, W., 2025. Unsupervised machine learning method for stationary sea state clustering based on gaussian wave surface elevation. Submitted to *The 35th International Ocean and Polar Engineering Conference.* ISOPE 2025, 1-6 June 2025, Seoul/KINTEX, Korean. Paper no. 2025-TPC-0887.

Nomenclature

Greek notations

ΔD	Parameter controlling the searching width of each local subsector [-]
ΔV	Reduction of speed for ship in the water [m/s]
Δt	Sailing time between two adjacent time stages [h]
$\Delta\theta$	Heading increment in angles, between two neighboring sub-routes from each of the current 'optimal' waypoints at each time stage [°]
η	Propulsion efficiency coefficient [-]
θ_c	Speed direction of ocean current [°]
θ_w	Speed direction of wind [°]
θ_{ref}	Reference course at each waypoint for sailing to the next time stage [°]

Latin notations

$C_{inv(ref)}$	Arrival course of GC_{ref} at the destination waypoint $\boldsymbol{P}_f$ [°]
C_f	Carbon dioxide (CO_2) emission factor for the type of fuel used during voyage [-]
C_{ref}	Initial course of GC_{ref} at the departure waypoint $\boldsymbol{P}_0$ [°]
d_{iS}	Current distance to $\boldsymbol{P}_f$ at the i^{th} time stage [km]
d_{total}	Total distance from $\boldsymbol{P}_0$ to $\boldsymbol{P}_f$ [km]
D	Geographical distance between $\boldsymbol{P}_0$ and $\boldsymbol{P}_f$ [km]
F_c	Overall fuel consumption [ton]
GC_{ref}	Great circle reference route between $\boldsymbol{P}_0$ and $\boldsymbol{P}_f$ [-]
H_s	Significant wave height [m]
m	$(2m+1)$ represents the number of successor waypoints for each waypoint at the current stage [-]
m_{cargo}	Cargo weight transported during voyage [ton]
$\boldsymbol{P}$	Waypoint variable in weather routing problem description
$\boldsymbol{P}_0$	Departure waypoint vector of a voyage [-]
$\boldsymbol{P}_i$	Waypoint at the i^{th} time stage between $\boldsymbol{P}_0$ and $\boldsymbol{P}_f$
$\boldsymbol{P}_f$	Destination waypoint vector of a voyage [-]
P^s	Engine propulsion power [kW]
r	$2r$ indicates the number of subsectors [-]
R_{Calm}	Calm water resistance of a ship [kN]
R_{Wave}	Wave resistances of a ship [kN]
R_{Wind}	Added wind resistances of a ship [kN]
R_{Total}	Total resistance of a ship [kN]
$SFOC$	Specific fuel oil consumption [g/kWh]
$\boldsymbol{S}_P$	Feasible solution space for the waypoint optimization variable $\boldsymbol{P}$
$\boldsymbol{S}_U$	Feasible solution space for the operational optimization variable $\boldsymbol{U}$
T_0	Departure time at $\boldsymbol{P_0}$ [h]
T_i	Time at the i^{th} time stage [h]

T_f	Arrival time at $\boldsymbol{P}_f$ [h]
T_z	Wave period [Hz]
$\boldsymbol{U}$	Operational variable in weather routing problem description
V	Ship's speed through water [m/s]
V_c	Speed of ocean current [m/s]
V_g	Ship's speed over ground [m/s]
V_s	Pre-determined reference speed of ship [m/s]

Abbreviations

2D	Two-dimensional
3D	Three-dimensional
ACO	Ant colony optimization
Adam	Adaptive moment estimation
AI	Artificial intelligence
AIS	Automatic identification system
ANN	Artificial neural network
BBM	Black-box model
BP	Back propagation
CA	Collision avoidance
CFD	Computational fluid dynamics
CRI	Collision risk index
DCPA	Distance to closest point of approach
EA	Evolutional algorithm
EEOI	Energy efficiency operational indicator
ETA	Estimated time of arrival [h]
EU	European Union
GA	Genetic algorithm
GAM	Generalized additive model
GBM	Grey-box model
GC	Great circle route
GD	Generational Distance
GHG	Greenhouse gas
GPR	Gaussian process regression
IMO	International Maritime Organization
IPO	Isochrone-based predictive optimization
JIT	Just in time
LR	Linear regression
L-MOEA	Learning-based multi-objective evolutionary algorithm
MASS	Maritime autonomous surface ships
ML	Machine learning
MPC	Model predictive control
OS	Own ship

PF	Pareto front
PR	Polynomial regression
PSO	Particle swarm optimization
ReLU	Rectified linear unit
RPM	Revolutions per minute
SVR	Support vector regression
TCPA	Time to closest point of approach
TS	Target ship
WBM	White-box model
XGBoost	Extreme gradient boosting

1 Introduction

This chapter introduces the background for the research conducted in this thesis. The motivations and objectives are also illustrated, followed by limitations and work scope.

1.1 Background

International shipping has traditionally been considered a cost- and energy-efficient mode of transportation. It accounts for over 80% of global merchandise trade by volume, while contributing nearly 3% of global greenhouse gas (GHG) emissions (UNCTAD, 2023). Between 2016 and 2020, the maritime transportation market nearly doubled, growing from $4.6 billion to $8 billion (Park et al., 2022). However, this rapid expansion was accompanied by a notable rise in GHG emissions as shown in Figure 1.1, with a 20% increase over the past decade (UNCTAD, 2023). Without intervention, the shipping sector's share of global GHG emissions is projected to rise from 3% to 17% by 2050 (Deng & Mi, 2023). The International Maritime Organization's (IMO's) revised GHG strategy lists three phased decarbonization targets: a 20% reduction by 2030, 70% by 2040, and full decarbonization by 2050, relative to 2008 emission levels (IMO, 2023). Despite these goals, only a 3.6% reduction had been achieved by 2023 (DNV, 2024b).

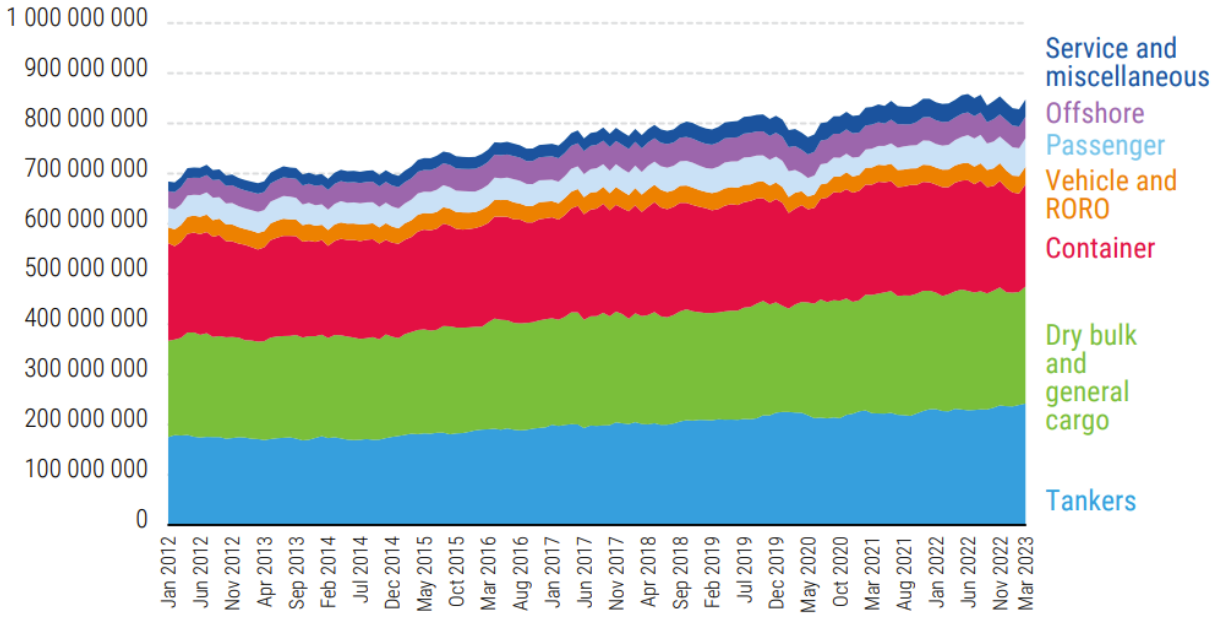

Note: RORO means roll-on/roll-off vehicle carrier.

Figure 1.1: Total carbon dioxide emissions (tons) by vessel type, in January 2012 – March 2023 from UNCTAD based on data provided by Marine Benchmark in July 2023 (UNCTAD, 2023).

Driven by these incentives, the shipping industry is taking serious steps to reduce its carbon footprint and lower emissions. Both technical and operational measures, as well as policy-based strategies, have been developed to increase shipping energy efficiency (Jimenez et al., 2022). Energy transition, e.g., adopting carbon-neutral fuels such as hydrogen, ammonia, and methanol,

is recognized as the most promising solution for shipping decarbonization. However, the production of these alternative fuels is still striving to meet the required demand from the shipping industry (UNCTAD, 2023). Currently, 93% of the global fleet continues to run on conventional fuels (DNV, 2023, 2024). Given the range of uncertainties, the transition will not happen immediately because of great challenges in practical implementation (DNV, 2024b). Before technical measures such as carbon-neutral fuels became more available and affordable, developing and installing energy-efficient operational measures, such as performance monitoring, weather routing, and trim optimization, are essential to meet both short-term environmental goals and long-term economic benefits. Through utilizing these operational energy-efficient measures, 4 – 16% of energy reduction in shipping can be reached by 2030 (DNV, 2024b). Although ship operational measures may not help the shipping industry become fossil free or climate neutral, given the large scale of the global shipping market, only a 1% reduction in fuel consumption can lead to an annual decrease of around 8 million metric tons of CO_2 emissions (IMO, 2020).

Among all available ship operational measures, voyage optimization is one of the most effective that can achieve considerable energy savings (DNV, 2023, 2024). Sea environments can significantly increase the energy consumption of ocean-going ships (Yuan et al., 2022), while voyage optimization, often referred to as weather routing, can help the ship easily avoid heavy metocean environments and maintain an expected time of arrival (ETA) (Zis et al., 2020; Yu et al., 2021). Particularly, it can deliver direct benefits without heavy investment and installation (DNV, 2024a, 2024b). In addition, cargo ships typically spend up to 50% of their time in port or at anchorage (DNV, 2018). They could real-time adjust their voyages to achieve a 'just in time' arrival and slowdown, which would not only reduce fuel consumption but also lessen port congestion. This highlights the significant potential to improve the effectiveness and efficiency of current ship operations through voyage optimizations, such as achieving just-in-time (JIT) arrivals considering ETA (IMO, 2020). Furthermore, voyage optimization is often considered an essential component of other innovative shipping technologies, such as wind-assisted propulsion ships. Studies have shown that combining wind propulsion with weather routing (voyage optimization) offers noticeable benefits in enhancing energy efficiency (Mason et al., 2023; Wang et al., 2022).

A typical voyage optimization process involves ship models and various techniques, such as ship performance modeling and prediction, multi-variable ship/engine control scheme, and multi-objective optimization algorithms. As the maritime industry undergoes digital transformation, large amounts of data are collected onboard today’s ships by sophisticated sensors. These data can be analyzed and leveraged to assist ship operations (DNV, 2024a). This digital shift unlocks the potential for digital-enabled and data-driven techniques in shipping (Lang & Mao, 2022). For example, statistical models have been developed to predict stresses and fatigue damage on ship structures for weather routing (Storhaug, 2007; Mao et al., 2010, 2012, 2015), identify ship speed to power relationships for estimating arrival times (Mao et al., 2016), and,

more recently, provide machine learning (ML) based ship performance prediction and monitoring (Gupta et al., 2022; Lang et al., 2024; Zhang et al., 2024b).

The main objective of today's voyage optimization used in open sea sailing is to minimize ship fuel consumption (Zis et al., 2020). When transportation activities become intensive, involving more complex maritime traffic environments, ship safety in becomes another critical objective. As a result, collision avoidance (CA) has become the most critical problem for voyage optimization, especially for coastal and inland shipping. The decision-making process to avoid collision is generally divided into three stages: motion prediction, collision detection, and collision resolution (Huang et al., 2020). The performance of each stage significantly affects the overall effectiveness of addressing CA problems. Among them, algorithms to assist decision-making in ship safe operations are the core component. For such CA problems, optimization algorithms face challenges from highly dynamic and complex maritime traffic environments surrounding the ship. Those environments should be continuously perceived and processed by the algorithm in real time to assist ship operations for CA. The dynamic factors involved include moving obstacles (e.g., other ships), ship maneuverability, control status, and environmental disturbances (wind and currents). Therefore, the computational efficiency and robustness of the algorithms are crucial for optimization effectiveness (Johansen et al., 2016). For coastal and inland shipping, developing such algorithms also becomes a promising strategy for addressing the CA problems in those complex traffic conditions (He et al., 2023; Hu et al., 2020; Jiang et al., 2022; Tsolakis et al., 2024; Wang et al., 2024).

1.2 Motivation and objectives

To address shipping energy efficiency via weather routing (or voyage optimization), recent development of optimization algorithms has focused on incorporating advancement from other fields such as control engineering, artificial intelligence (AI) and machine learning (ML) technologies. This interdisciplinary approach poses difficulties for the research community of ship voyage optimizations (Zis et al., 2020; Yu et al., 2021), as terminologies from different fields are frequently adopted and mixed used. Meanwhile, the technical pros and cons of those voyage optimization algorithms, as well as their fundamental difference and actual improvement in terms of voyage planning efficiency and effectiveness, are rarely discussed in literature.

In addition, for practical implementation and installation of weather routing systems, the computational efficiency of optimization algorithms in such systems is vital for facilitating real-time decision support of ship operations for each voyage, considering dynamic weather conditions, commercial changes, and other operational uncertainties along the voyage. Therefore, the two-dimensional (2D) Isochrone method, recognized for fast computation for optimization, remains widely used in the commercial weather routing market (Lee et al, 2018). Initially designed to ensure accurate ETAs, the Isochrone method align well with today's IMO promoted JIT ship operations (IMO, 2020). It can quickly generate optimal routes, adapt to changes, and maintain punctuality, making it suitable for both fixed and flexible voyage plans.

One example of this method is that proposed by Hagiwara (1989). However, one notable drawback of this method is the occurrence of "isochrone loops", which are irregular shapes due to the non-convexity of ship performance at sea (Roh, 2013). As the number of isochrones grows, these loops become more prevalent, resulting in impractical outcomes for real operation. Besides the route shape, Hagiwara's 2D Isochrone method (Hagiwara, 1989) also suffers from significant issues with route convergence in its final stages. Many researchers have enhanced the Isochrone method by incorporating speed optimization or advanced ML algorithms. However, they also increase complexity which influences their real-time capabilities.

Furthermore, advanced algorithms, such as emerging AI and ML techniques, can manage a broader range and more flexible variations of optimization parameters (Zis et al., 2020). Significant research efforts have been dedicated to incorporating AI/ML methods to achieve superior optimization results in some fields, e.g., autonomous control systems (Norouzi et al., 2023). However, AI/ML optimization algorithms in weather routing require significant computational efforts (Wang et al., 2020a, 2020c). Additionally, voyage planning results generated from those algorithms may require frequent changes in ship operational conditions, such as speed, course, and power. (Wang et al., 2021). These adjustments are not practical for actual ship operations, as they necessitate continuous ship maneuvering, which can lead to increased fuel consumption, emissions, and maneuvering risks (Baldauf et al., 2018). This approach may further hinder applications of weather routing systems with those complex optimization algorithms (Simonsen et al., 2015). In addition, some advanced meta-heuristic approaches, unlike deterministic methods such as Isochrone algorithms, do not always yield optimal voyage planning solutions (Halim et al., 2021).

Moreover, a ship energy performance model is another crucial component for weather routing systems. Ship energy performance models are used to estimate the fuel costs associated with decisions of maneuvering actions for weather routing systems, to achieve fuel savings. However, within the ship energy performance model, there is a crucial parameter known as the specific fuel oil consumption (SFOC), which is used to estimate a ship's fuel consumption from shaft power (Marques et al., 2019). Different modeling approaches for the SFOC may introduce significant uncertainties into the calculations of fuel consumption in ship performance models. Marine engine SFOC is often provided by engine manufacturers or estimated as statistical averages only in terms of engine shaft power (Degiuli et al, 2023). However, actual SFOC values in ship operations are strongly dependent on engine operation-related control variables (Sarigiannidis et al, 2016), which are normally unknown in advance for voyage planning in ship weather routing systems. This introduces significant uncertainties in ship energy performance models for estimating fuel consumption, possibly rendering ship voyage optimization ineffective. Alternatively, some of the literature has overlooked the role of SFOC, optimizing engine power rather than fuel (Fabbri & Vicen-Bueno, 2021; Lee et al., 2021; Qian et al., 2023), which raises concerns about the potential impact of uncertain models on a ship's voyage optimization results.

Finally, in addition to minimum fuel consumption and strict punctual requirements for ship operations (Lei et al., 2024), voyage optimization systems for inland and coastal shipping need to focus more on collision avoidance due to complex traffic and operation environments. To avoid collisions with the assistance of voyage optimization systems for inland ship operation, the computational efficiency of voyage optimization algorithms is essential to provide real-time optimal voyage planning. Many studies on collision avoidance have been striving to develop algorithms that achieve a balance between real-time performance and optimal outcomes (Zhang et al., 2025; Zhu et al., 2024).

Therefore, to address computational efficiency and optimization effectiveness of ship voyage optimization algorithms, based on a systematical literature review about the status, pros, and cons of current ship voyage optimization algorithms, the main objectives of this thesis are to propose an Isochrone based voyage optimization algorithm that can incorporate ML and exploit the learning-based multi-objective evolutionary algorithm (L-MOEA) to leverage advanced ML methods. These optimization algorithms should ensure optimal voyage planning for both shipping energy efficiency and collision avoidance considering the uncertainties of ship energy performance models in voyage planning. The proposed algorithms aim to assist seafarers with voyage planning for one voyage before departure, based on the provided destination, ETA, and weather forecasts. During the operation, when the ship is en route, the proposed algorithms can also be utilized on board by seafarers to address any uncertainties or to regularly update the voyage, for instance, every 24 to 72 hours when the weather forecast is usually updated (European Centre for Medium-Range Weather Forecasts).

To achieve the overall objectives, this thesis investigated some specific research goals in the appended papers as follows:

1) Clarification of terminologies that are often used interchangeably, a systematic review of optimization algorithms in weather routing, and highlights of recent research trends (Paper I).
2) Proposal of an effective and efficient improved optimization algorithm that leverages the computational efficiency of the Isochrone method to achieve energy-efficient real-time weather routing (Papers II and III).
3) Adoption of advanced ML methods to tackle weather routing, addressing the divergence issues of MOEA, and accounting for uncertainties in weather forecasts (Paper IV).
4) Investigation of the uncertainty of fuel consumption caused by SFOC in ship performance models and its impact on weather routing (Paper V).
5) Application of research on Isochrone-based algorithms to address collision avoidance problems, to assist on-time transport and ensure ship operational safety for inland and coastal shipping (Paper VI).

1.3 Assumptions and delimitations

This thesis investigated and developed several voyage optimization algorithms. The demonstration of such algorithms focus on the proof of concept for their effectiveness and efficiency in ship voyage planning. Some of the delimitations are listed below.

For optimization algorithms in weather routing, whose main objective is to minimize fuel consumption during a voyage:

- The optimization algorithm first aims to assist seafarers with voyage planning before departure based on the provided destination and ETA and enhances energy efficiency for one single voyage.
- Furthermore, the proposed voyage optimization algorithms can consider voyage operational dynamics due to, e.g., market fluctuations (leading to a new port of call or revised ETA, etc.) or dramatic changes in the weather forecast. These dynamics can be considered by restarting the optimization process in real time with updated ETA, weather conditions, or other voyage planning prerequisites. However, simulations of voyage optimization in dynamic environments during execution, i.e., when the ship is en route, are not studied in this thesis.
- Ship safety and practical operation considerations such as traffic separation zones, keel clearance, and real-time operation warnings from an ECDIS (electronic chart display and information system), are not considered for weather routing in this thesis. They can be easily implemented during commercial development.
- For the demonstration of these energy efficiency voyage optimization algorithms, the departure, destination port, and ETA (associated with the service speed or engine speed (RPM)) of case study voyages are assumed to be given as prerequisites, and ship performance models used in these optimization methods have been validated in other studies and assumed accurate in this thesis.
- The parameters of the proposed method defining the waypoint grid resolution are determined based on performance, with discussions provided in the appended papers. However, sensitivity analysis of the parameters and related convergence analysis have not been performed.

For the voyage optimization considering collision avoidance in confined water with dense maritime traffic environment, a linearized model to describe a ship's dynamic is used for demonstration. This model can be replaced with a more accurate model tailored for inland and coastal ships, such as ones that can account for shallow water effects. In addition, the following assumptions have been made for the development of this algorithm for collision avoidance:

- A ship domain is used to define the minimal safety area around the ship during collision avoidance, indicating that any obstacle entering this area is considered to pose a certain collision risk. However, the ship domain in this thesis is based on the definition of Coldwell (1983) and assumed to be static, whereas dynamically adapting it based on

situations when encountering other ships would be more accurate (Szlapczynski & Szlapczynska, 2017).

- The motions and trajectories of the target ships (TSs), i.e., other ships, are assumed to be known to the own ship (OS) through interactions. However, in practice, more reliable solutions can be considered such as using automatic identification system (AIS) data for trajectory prediction for TSs.
- The special hydrodynamic effects in confined waterways, e.g., shallow water effects and bank effects are not considered in this thesis. Thus, the power/energy cost of sailings in confined waterways is not calculated. The current approach uses the shortest distance as a simplified method to estimate the energy cost.

1.4 Outline of the thesis

The thesis consists of two parts: a summary of the research conducted, followed by six appended papers. The research summary section integrates and summarize the work from each appended paper, while also explaining the connections between the appended paper, as illustrated in Figure 1.2. Each appended paper provides more details of approaches presented in this thesis and their intermediate steps.

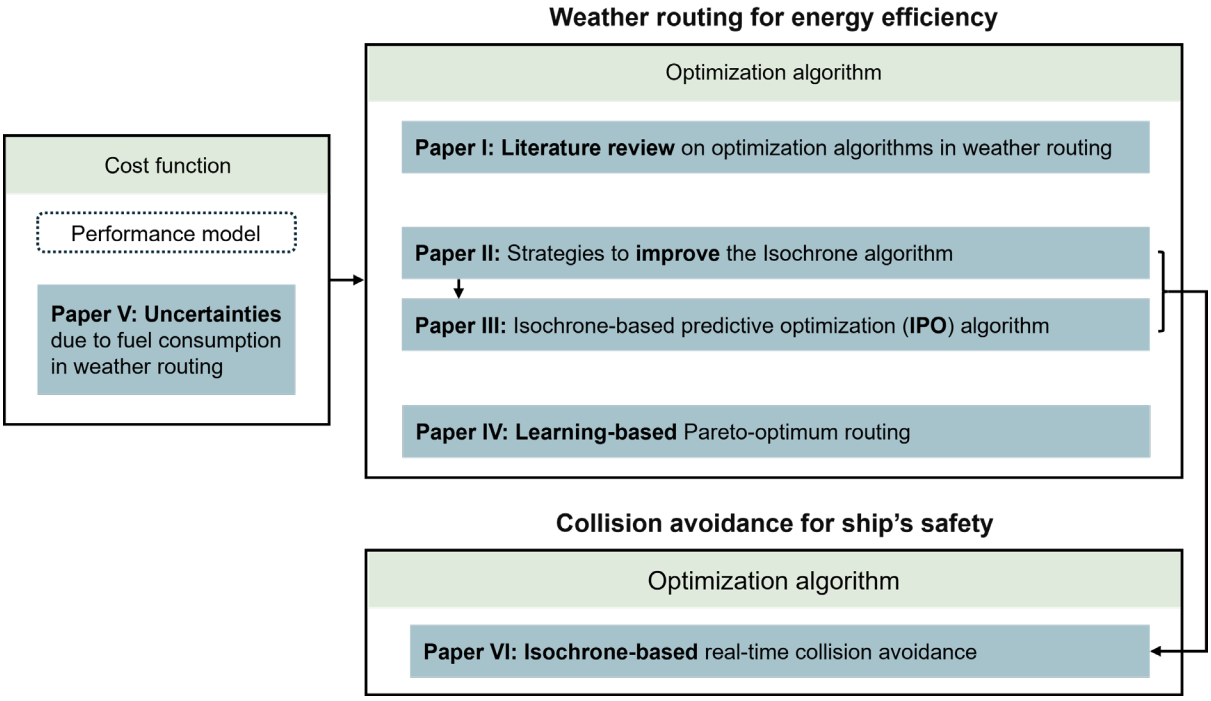

Figure 1.2: Workflow of the appended publications to achieve the objectives of this thesis.

The remainder of this thesis is structured as follows: Chapter 2 clarifies the work scope and some terminologies and presents a literature review of optimization algorithms used in weather routing and collision avoidance problems. Chapter 3 illustrates the optimization algorithms proposed for energy efficient weather routing in this thesis. Chapter 4 investigates the uncertainties

of energy consumption caused by ship models, and Chapter 5 presents the development of optimization algorithm in collision avoidance. Finally, Chapter 6 highlights the main findings and results from the appended publications, Chapter 7 concludes the thesis, and Chapter 8 discusses future work.

2 Literature review

The blurred boundaries of terminologies used within ship voyage optimizations have led to confusion and inconsistency in the methods/algorithms developed for ship weather routing systems. Some confusion problems were presented by Yu et al. (2021) and Zis et al. (2020) to explain and distinguish research fields related to either maritime engineering or maritime management for voyage planning issues. For example, some studies essentially addressed "ship scheduling" problems, while being labeled as weather routing such as in (Lee et al., 2023). To clarify different topics surrounding the research field of ship voyage optimizations, Figure 2.1 presents an overlapping diagram for research topics that often appeared alongside voyage optimization. Path planning and pathfinding problems, as the broadest and most fundamental topics, are extensively studied beyond the maritime sector (Majumder & Majumder, 2021). They apply to moving objects including vehicles and robots, while ship voyage optimization in this thesis focuses on ships. As the objectives of ship voyage planning vary, voyage optimization can be associated with various sub-problems in terms of their implementation scenarios, i.e., **ship routing**, **weather routing**, **collision avoidance**, and **operational optimization**.

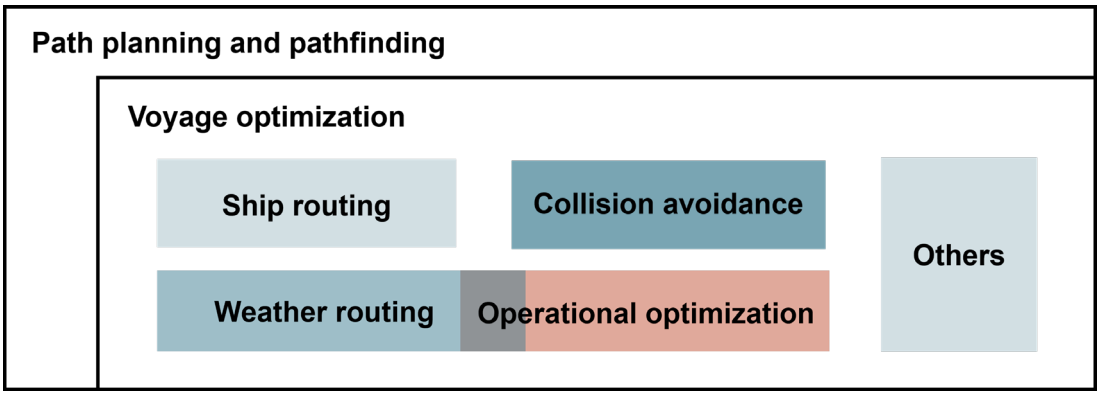

Figure 2.1. Overlapping diagram of common problems related to voyage optimization.

Ship routing often involves multiple voyages between several ports of call, ETAs at each port, or arrival sequences, and it is similar to the vehicle routing problem (VRP) in transportation networks (Zis et al., 2020). It often emphasizes commercial factors, such as freight rate, fuel prices, market fluctuations, and profitability (Lee et al., 2023; Tran & Haasis, 2018). Weather routing and collision avoidance in voyage optimization are significantly different because of different sailing areas with different objectives in focus. **Weather routing** searches for an optimal plan for each voyage from one port of call to another, and weather conditions are the main factors affecting ship operational indexes, such as fuel consumption and ETA. **Collision avoidance** becomes the focus in coastal and inland shipping areas, where maritime traffic density increases (Gao et al., 2023; Zhang et al., 2025). Because of more complex traffic and less pronounced weather impact, ship sailing in these areas prioritize operational safety and traffic regulations compliance, focusing on collision risk and avoiding strategies (Huang et al., 2020; Johansen et al., 2016; Tran et al., 2023). **Operational optimization** focuses on improving ship

operational details (e.g., speed (Li et al., 2024; Sidoti et al., 2023), power (Besikçi et al., 2016; Ma et al., 2023), or trim (Coraddu et al., 2017; Hu et al., 2022)), along a fixed route (e.g., fixed longitudes and latitudes), to optimize, for example, the fuel consumption for a voyage. These problems include voyage division, i.e., separating the entire route into segments, and combinatorial optimization across multiple sub-routes. Clarifying the problem scope is essential for researchers/engineers to choose proper methods to implement or further development for practical maritime operations.

2.1 Optimization algorithms in weather routing

Weather routing algorithms for seagoing ships have been widely investigated throughout the years (Zis et al., 2020). Many well-established methods are available in the maritime transportation community, such as the Isochrone method, dynamic programming (DP), Dijkstra and A* algorithms, and emerging AI and ML algorithms (Wang et al., 2021; Wang et al., 2019). They can be primarily categorized into two-dimensional (2D) or three-dimensional (3D) methods, considering requirements in real applications. Of note, 2D methods are more conventional, simplifying the problem to only involve searching for routes (consisting of longitudes and latitudes of waypoints) along the voyage, and assuming the other inputs such as speed and engine power to be fixed. Alternatively, these optimization methods can also be divided into static and dynamic grid-based methods.

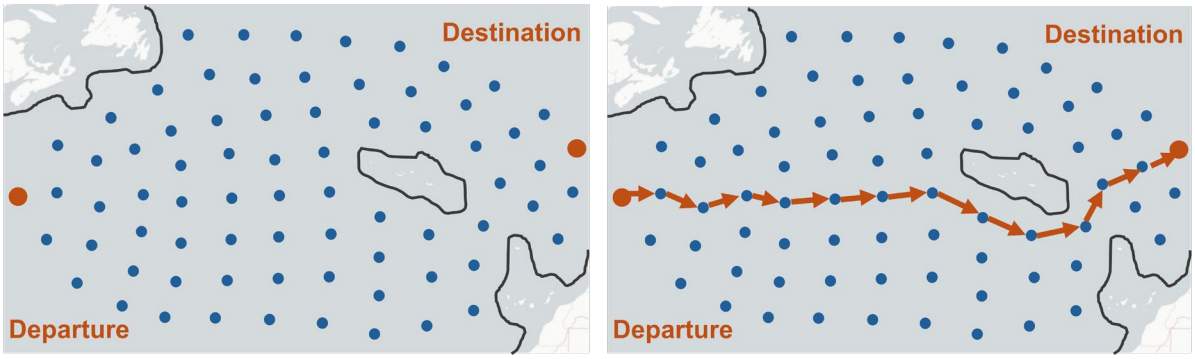

Figure 2.2. Grid system and optimal route (shown as an orange solid line) in the static grid-based voyage optimization methods.

Static grid-based voyage optimization methods discretize the sailing area (a certain range between departure and destination) into small grids and pre-define a grid system based on these grids as illustrated in Figure 2.2. Examples of static grid-bases methods include the DP method (Bellman, 1952) and graph search algorithms, like the Dijkstra (Dijkstra, 1959) and A* algorithms (Hart et al., 1968). DP is based on Bellman's principle of optimality in which one problem is broken down into sub-tasks, and each of them is solved in sequence to obtain the optimal solution for the original problem. De Wit (1990) employed DP for ship sailing, separating voyage planning into a multi-stage process and validating its effectiveness. The Dijkstra algorithm is extended to derive the A* algorithm, by incorporating a heuristic component into the cost function. They have been applied in voyage optimization in recent years, for example, by Shin

et al. (2020a), Ari et al. (2013), Życzkowski et al. (2018), and Gkerekos and Lazakis (2020). These static grid-based algorithms are easy to construct into different forms, and suitable for single and multiple objective optimization problems. However, the result as well as computation loads of static grid-based methods relies heavily on the grid parameters, such as resolution, the number of nodes, and the spatial extent it covers, which makes the grid generation an influencing factor for the algorithm's performance and, therefore, needs to be specifically addressed in each individual voyage.

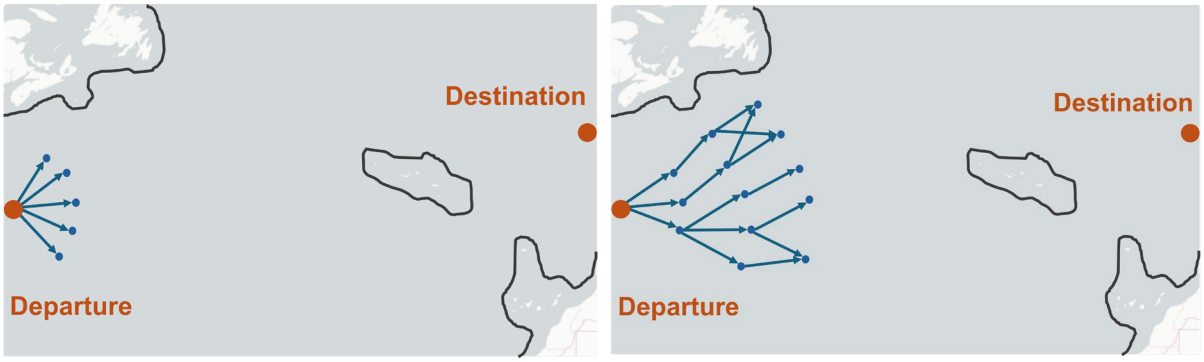

Figure 2.3. Grid system and the evolution process in the dynamic grid-based voyage optimization methods.

Dynamic grid-based voyage optimization methods on the other hand, conduct the optimal voyage search recursively, eliminating the need for a pre-defined grid. At each step, a subsequent node set is generated from the existing nodes, resulting in an iterative grid update, as shown in Figure 2.3. This process continues as routes progressively advance until reaching the destination. A notable example is the Isochrone method, where an isochrone represents a front line encompassing the farthest waypoints, which a ship can reach following different directions within a given sailing time. This method was originally introduced by James (1957a). However, as the number of waypoints in this method grows exponentially, Hagiwara (1989) enhanced it to only keep a specific number of optimal waypoints at each isochrone to resolve the problem of expanded candidate waypoints. This improved Isochrone method (Hagiwara, 1989) was used both manually and on computers for years because of its convenient implementations. However, one drawback of the original Isochrone method by James (1957a) is the phenomenon known as the "isochrone loop". This irregular shape of an isochrone arises from the non-convex nature of a ship's performance (Roh, 2013; Wisniewski, 1991). As the number of isochrones increases, the isochrone loop effect propagates, resulting in impractical outcomes (Roh, 2013). Hagiwara (1989) noticed this problem, however, impractical routes are still yielded by his method. Later, Klompstra et al. (1992) presented a similar approach, the Isopone algorithm, which replaced equal traveling time with fuel consumption. In general, because of the relatively high computational efficiency, the Isochrone method has great value in practical applications. Since it continuously adapts and approaches the destination step by step, it can also handle uncertainty and respond fast to the dynamic weather and business environment.

Table 2.1: Summary for advantage/disadvantage of optimization algorithm types commonly used in weather routing.

Algorithm Type	2D		3D and multi-variables	
Description	Route with fixed speed		Route and speed (or power, RPM, etc.)	
Pros	1) Easy to apply for seafarers 2) Fast for computation		Superior optimization results compared to 2Ds	
Cons	Possible suboptimal and local optimization results due to their simplifications made for fast computations.		1) Slow computation 2) Hard to apply results in real operation	
Method	Deterministic	Stochastic	Deterministic	Stochastic
Pros	Results can be found if they exist.	Stochastic nature helps avoid local optimization.	1) Result can be found if it exists. 2) Improved optimization capability is achieved by including more variations than 2D.	1) Stochastic nature helps avoid local optimization. 2) More improved optimization capability, compared with deterministic methods.
Cons	1) Discretized nature can lead to suboptimality. 2) Optimization result improves with high grid resolution, but computation load also increases.	1) It cannot guarantee an optimized result even if one exists. 2) Same input may not give the same results.	1) It has heavier computation load by using extra variables than 2D. 2) Applying results in real operation is challenging.	1) Computation load increases heavily. 2) Same input may not give the same results. 3) Applying results in real operation is challenging.
Examples	(Hagiwara, 1989) (De Wit, 1990)	(Tsou, 2010) (Li et al., 2018) (Xue, 2022)	(Jeong et al., 2019) (Bahrami & Siadatmousavi, 2024)	(Ma et al., 2021) (Wang et al., 2021) (Ma et al., 2024)

A summary of the advantages and disadvantages of these algorithms is presented in Table 2.1. For more complicated cases and advanced planning, **3D algorithms** have been developed to consider additional variables, such as speed, and time. For example, Choi et al. (2023), Du et al. (2022a), and Zaccone et al. (2018) developed a 3D DP algorithm; Lin et al. (2013), Fang and

Lin (2015), and Lin (2018) improved a 3D Isochrone method; Mannarini and Carelli (2019), Mannarini et al. (2023), Zyczkowski and Szlapczynski (2023), and Wang et al. (2019) developed the 3D Dijkstra algorithms.

Voyage optimization typically requires handling extensive data, adapting to dynamic changes, and making predictions under uncertainty, which renders the problem large-scale and complex. Consequently, alongside the advancement of AI and ML techniques, more sophisticated methods have been developed in recent years, such as the utilization of the genetic algorithm (GA), evolutionary algorithm (EA), ant colony optimization (ACO), particle swarm optimization (PSO), and their variants. Examples include 3D EAs/GAs (Ma et al., 2021; Szlapczynska & Szlapczynski, 2019; Wang et al., 2021) and 3D ACO (Dong et al., 2021). Zhang et al. (2022) proposed a 3D ACO customized for ice routing. Chen and Tan (2023), and Wang et al. (2022) proposed 3D PSO for decision-making; Gkerekos and Lazakis (2020), and Moradi et al. (2022) deployed a 3D artificial neural network (ANN) to predict fuel consumption of ships for optimization. These algorithms consider speed/time variations along the voyage and, therefore, have greater capabilities to achieve more competitive performance.

However, a tradeoff exists between performance and efficiency, and because of the complexity, the computation loads also increase dramatically. Moreover, stochastic methods, such as GA, EA, ACO, and PSO, if given the same specific input, can generate different outputs for each execution they operate because of the stochastic nature of these algorithms.

2.2 Ship performance model for weather routing

To minimize energy consumption along a voyage to achieve efficient ship operations, researchers have established optimization objectives, such as minimizing power (Fabbri & Vicen-Bueno, 2021; Lee et al., 2021; Qian et al., 2023), fuel (Chen & Mao, 2024; Wang et al., 2021; Wang et al., 2019), emission (Lee et al., 2023; Yu et al., 2021), and economic/operational costs (Ma et al., 2024). Ship performance models estimate corresponding optimization-related costs using cost functions to achieve these objectives. As an individual research topic, performance modeling has developed various approaches, such as empirical/semi-empirical methods, computational fluid dynamics (CFD), model testing, and ML methods. These suitable ship models used in today's weather routing can be generally categorized into white-box models (WBMs), black-box models (BBMs), and gray-box models (GBMs) (Lang et al., 2024; Yan et al., 2024).

WBMs rely on established shipping knowledge and physical principles, offering transparency, interpretability and good extrapolation ability. Examples include the models developed by Holtrop and Mennen (1982), Huang et al. (2018), Tillig and Ringsberg (2019), Mao and Rychlik (2017), and Lang and Mao (2020). As WBMs depend on prior knowledge, they are highly suitable for predictions in the ship's early design phase or if measurement data is insufficient. However, their accuracy may be constrained by assumptions inherent in the model. In contrast, **BBMs** utilize extensive operational data and advanced ML techniques, such as ANNs (Bassam

et al., 2023; Du et al., 2019), tree-based models (Soner et al., 2018; Yan et al., 2020), support vector machines (Ahlgren et al., 2019), and others (Lang et al., 2021, 2022) to predict ship performance. These models are praised for their superior fitting capability compared to WBMs, and their generalization capabilities which do not require prior knowledge. However, their complexity and interpretability can limit their acceptance in industry applications. Additionally, they may have difficulty providing accurate predictions for unmeasured conditions, limiting their practical application in unpredictable dynamic sea environments.

In addition to WBMs and BBMs, researchers have also developed **GBMs**, which can combine the theoretical foundations of WBMs with the data-driven insights of BBMs, such as those by Yang et al. (2019) and Wang et al. (2023). These approaches allow for both accurate and theoretically explainable predictions. GBMs have two forms: sequential, where WBMs and BBMs are applied in sequence, and parallel, where WBMs provide the theoretical framework and BBMs refine parameters based on empirical data (Yan et al., 2024).

These types of ship models have been used in weather routing, as demonstrated by Tzortzis and Sakalis (2021), Wang et al. (2020b), and Li et al. (2020), who used WBMs; Beşikçi et al. (2016), Du et al. (2019), and Moradi et al. (2022) who used BBMs; and Coraddu et al. (2017) who used a GBM. However, to the author's knowledge, no previous study has comprehensively considered a critical issue: the uncertainty in the energy transfer processes within the ship's main engine system, specifically SFOC, which leads to uncertainties in ship fuel consumption (Guo et al., 2024). Additionally, no studies have verified the extent to which this stochastic and uncertainty affects weather routing with the objective of saving fuel. This motivates research into the uncertainties in weather routing caused by the stochastic ship fuel consumption models, which is further detailed in Chapter 4.

2.3 Collision avoidance for ship safety

Collision avoidance (CA) problems have been critical for maritime traffic safety, particularly for coastal and inland shipping with complex and high-density transport activities. The process of collision avoidance can generally be divided into three stages: motion prediction, collision detection, and collision resolution (Huang et al., 2020). The performance of each stage can significantly affect the overall effectiveness of addressing CA problems, with optimization algorithms inside the stage of collision resolution serving as a key component because of their responsibility for decision-making.

CA problems remain highly challenging for optimization algorithms, mainly stemming from the dynamic and complex sailing environments of ships, necessitating real-time perception and decision-making during operations. These dynamic factors include moving obstacles such as TSs, ship maneuverability, and environmental disturbances from wind and currents. As such, the computational efficiency and robustness of the optimization algorithms are crucial for their effectiveness (Johansen et al., 2016). Many studies have contributed to addressing CA problems

with a focus on algorithm development, and readers interested in further details can refer to comprehensive review papers by Huang et al. (2020), Zhu et al. (2024), and Zhang et al. (2025).

Generally, based on their optimization or control variables which are outlined by the solution space, optimization algorithms to address CA problems can be categorized into **continuous** and **discrete** search methods. As the name suggests, continuous search methods refer to those where the optimization variables can change continuously, meaning the feasible values for the optimization variables are theoretically infinite. Discrete search methods, on the other hand, typically specify the step size and the range for variable changes or provide only a finite set of choices for the optimization variables. From the perspective of algorithm processes, each of these methods can further be classified as **global** or **stepwise**. Global search algorithms first identify a collision-free solution space, i.e., the space containing all solutions that satisfy constraints, and then conduct search and optimization within this space. Stepwise search progresses iteratively, performing collision checks and optimization at each step, advancing only one step length at a time, and repeating the process until completion.

As presented in Table 2.2, if using continuous spaces, global search examples include the velocity obstacle algorithm (Alonso-Mora et al., 2018; Fiorini & Shiller, 1998; Zhuang et al., 2016) and cone-based approaches (Chakravarthy & Ghose, 1998; Fan et al., 2019). Stepwise search is exemplified by model predictive control (MPC) - based strategies (Abdelaal et al., 2018; Chen et al., 2018). Discrete input-based algorithms use limited variations in optimization to enhance computational efficiency and responsiveness. Examples of global search using discrete inputs includes grid-based methods (Shah et al., 2016; Svec et al., 2014), and stepwise search methods include the dynamic window approach (Fox et al., 1997; Serigstad, 2017) and MPC-based strategies (Johansen et al., 2016). Other algorithms, such as artificial potential fields (He et al., 2023; Li et al., 2021) and ML approaches like reinforcement learning (Jiang et al., 2022; Wang et al., 2024), are applicable to both continuous and discrete inputs.

Global search algorithms can often present better outcomes as they comprehensively assess the problem that appears particularly effective in complex environments. However, achieving efficiency while maintaining optimality is difficult, making them less suitable for real-time operations. On the contrary, stepwise search algorithms sacrifice some computational intensity to achieve much faster execution speeds, but their limited solution space and common reliance on greedy strategies may lead to suboptimal outcomes.

Table 2.2: Examples of different methods used in collision avoidance.

Type	Global	Stepwise
Continuous	Velocity obstacle algorithm, vision cone	MPC-based
Discrete	Grid-based methods	Dynamic window approach, MPC based
Others	Artificial potential field, ML (reinforcement learning algorithms)	

3 Methods of weather routing for energy efficiency

This chapter summarizes the optimization algorithms developed in Papers II, III, and IV to solve weather routing problems. For the completeness of the thesis, a general overview of weather routing is first described. Then, the contributions and dedicated development of optimization algorithms in this thesis are presented afterwards.

3.1 An overview of the weather routing problem

In a ship's weather routing system, a voyage is normally discretized into a series of waypoints accompanied by operational parameters defined for each sub-route between every two waypoints, as shown in Figure 3.1.

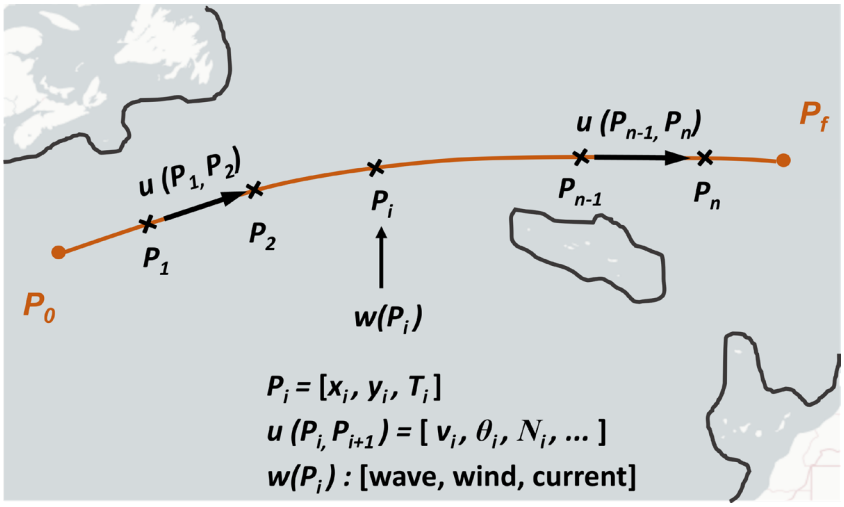

Figure 3.1: An illustration of a ship voyage with its waypoints, operational parameters and sailing sea conditions.

Let $\boldsymbol{P}_0$ denote the departure and $\boldsymbol{P}_f$ the destination. A waypoint at the i^{th} time stage between $\boldsymbol{P}_0$ and $\boldsymbol{P}_f$ is defined as:

$$\boldsymbol{P}_i = [\, x_i, y_i, T_i \,] \tag{3.1}$$

where x_i, y_i and T_i are the longitude, latitude, and the time that ship passes this waypoint respectively. The sea condition $\boldsymbol{w}$ at the waypoint $\boldsymbol{P}$ are described by the wave, wind and current as:

$$\boldsymbol{w} = [\, S\,(\omega\,|H_s, T_z), V_c, \theta_c, V_w, \theta_w \,] \tag{3.2}$$

where $S\,(\omega\,|H_s, T_z)$ is the wave given by significant wave height H_s and wave period T_z. Ocean current and wind are represented by V_c, θ_c, V_w and θ_w, where V and θ denote their speed and direction respectively. The operational parameters along the sub-route from $\boldsymbol{P}_i$ to the next waypoint $\boldsymbol{P}_{i+1}$ at the $(i+1)^{th}$ time stage are defined as:

$$\boldsymbol{u}(\boldsymbol{P}_i, \boldsymbol{P}_{i+1}) = [v_i, \theta_i, N_i, \dots] \tag{3.3}$$

where $\boldsymbol{u}(\boldsymbol{P}_i, \boldsymbol{P}_{i+1})$ includes parameters that can guide the ship's sailing, such as the sailing speed v_i, heading θ_i, engine speed (RPM) N_i, etc.

The optimization **variables** of the weather routing are the set of waypoints $\boldsymbol{P}$ and their corresponding operational parameter $\boldsymbol{U}$:

$$\begin{aligned} \boldsymbol{P} &= [\boldsymbol{P}_0, \boldsymbol{P}_1, \boldsymbol{P}_2, \dots \boldsymbol{P}_{n-1}, \boldsymbol{P}_n] \\ \boldsymbol{U} &= [\boldsymbol{u}(\boldsymbol{P}_0, \boldsymbol{P}_1), \dots, \boldsymbol{u}(\boldsymbol{P}_n, \boldsymbol{P}_f)] \end{aligned} \tag{3.4}$$

where n indicates the last time stage before $\boldsymbol{P}_f$, and $\boldsymbol{P}_n$ denotes the last waypoint before $\boldsymbol{P}_f$. A general framework for weather routing is outlined in Figure 3.2, featuring four key components: constraints, objectives, cost function, and optimization algorithm.

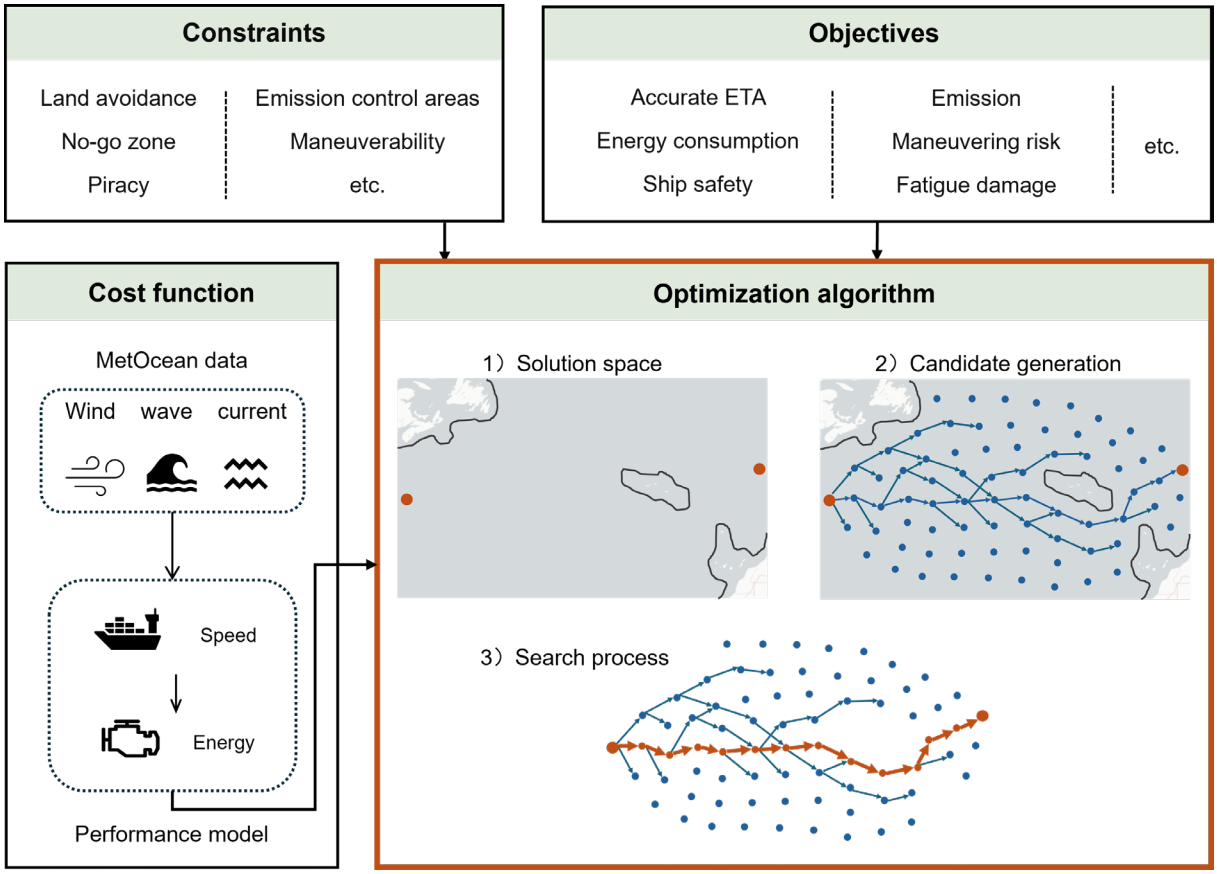

Figure 3.2: A general framework of weather routing problem.

The **constraints** outline the solution space where optimization variables $\boldsymbol{P}$ and $\boldsymbol{U}$ choose feasible values. Assume $\boldsymbol{S}_P$ is the feasible solution space for $\boldsymbol{P}$, i.e., the allowed sailing area between $\boldsymbol{P}_0$ and $\boldsymbol{P}_f$; and $\boldsymbol{S}_U$ is the feasible solution space for $\boldsymbol{U}$, i.e., the ship's allowed range of operational settings. $\boldsymbol{S}_P$ excludes areas such as land, no-go zones, shallow water or emission control areas, and $\boldsymbol{S}_U$ considers ship's specific maneuverability, etc. The aim of weather routing is to find the

optimal set of $\boldsymbol{P}$ and $\boldsymbol{U}$, i.e., $\boldsymbol{P}^*$ and $\boldsymbol{U}^*$, which optimizes pre-defined optimization **objectives**. Some common objectives are energy efficiency, accurate ETA, emission or ship safety at sea. A **total cost function** should be defined to evaluate if such objectives are achieved:

$$J_n = \sum_{i=0}^{n} L_i(\boldsymbol{P}_i, \boldsymbol{u}(\boldsymbol{P}_i, \boldsymbol{P}_{i+1})|\boldsymbol{w}) \tag{3.5}$$

where L_i ($\boldsymbol{P}_i$, $\boldsymbol{u}$ ($\boldsymbol{P}_i$, $\boldsymbol{P}_{i+1}$) |$\boldsymbol{w}$) is the instantaneous cost function, calculating the one step's cost at the i^{th} time stage or sub-route. For example, if the optimization objective is to achieve minimal fuel consumption, L_i ($\boldsymbol{P}_i$, $\boldsymbol{u}$ ($\boldsymbol{P}_i$, $\boldsymbol{P}_{i+1}$) |$\boldsymbol{w}$) will calculate the fuel consumed at the sub-route following waypoint $\boldsymbol{P}_i$ to $\boldsymbol{P}_{i+1}$, by sailing with operational parameter $\boldsymbol{u}$ ($\boldsymbol{P}_i$, $\boldsymbol{P}_{i+1}$) at the local sea states $\boldsymbol{w}$. Correspondingly, J_n is the accumulated cost function, presenting the accumulative cost from $\boldsymbol{P}_0$ to the final n^{th} time stage. J_i indicates the current accumulated cost function at the i^{th} time stage.

The ship performance model is incorporated in the instantaneous cost function L_i given in Eq. (3.5) to numerically evaluate the impact of weather on the ship's sailing. Specifically, the ship model calculates the energy that the ship needs to consume, to sail at the given speed under the local weather conditions. That is, the ship model presents a speed to energy mathematical relationship. This energy needed by sailing could be defined by fuel consumption, power of engine, or emissions, etc. The cost function needs the ship model to calculate an energy cost for algorithm, however, the formulation of the cost function can be problem specific.

In the end, constraints, objectives and the cost function are given to the optimization algorithm, and the algorithm searches for the $\boldsymbol{P}^*$ and $\boldsymbol{U}^*$, that can lead to the minimal value of the total cost function J_n given in the previous Eq. (3.5):

$$\boldsymbol{P}^*, \boldsymbol{U}^* = \underset{\boldsymbol{P}_i \in \boldsymbol{S}_P, \boldsymbol{u}(\boldsymbol{P}_i, \boldsymbol{P}_{i+1}) \in \boldsymbol{S}_U}{\arg\min} \sum_{i=0}^{n} L_i(\boldsymbol{P}_i, \boldsymbol{u}(\boldsymbol{P}_i, \boldsymbol{P}_{i+1})|\boldsymbol{w}) \tag{3.6}$$

where $\boldsymbol{P}^*$ and $\boldsymbol{U}^*$ are the final output of the weather routing.

Optimization algorithms are the core of enabling intelligent decision-making in weather routing. They involve three key processes: 1) defining the solution space, 2) generating feasible solution candidates, and 3) searching for the optimal solution. Different algorithms employ various strategies to execute and integrate these processes. Typically, the solution space is first defined based on constraints. Feasible candidate solutions are generated within this space and their costs are evaluated. The search is conducted in all candidates to identify the optimal one based on their cost, to meet optimization objectives. Thus, the effectiveness of weather routing highly depends on the optimization algorithms, as well as the accuracy of weather forecasts and ship performance models (Tsai et al., 2021). As weather forecasting belongs to the domain of meteorological expertise, it falls outside the scope of this thesis. The later chapters will present research on optimization algorithms, followed by ship performance model given in Chapter 4.

3.2 The process of the Isochrone algorithm

The Isochrone algorithm is a long-established ship weather routing method, which was first proposed in 1957 (James, 1957b; Wisniewski, 1991). Different from other methods, it was developed for marine applications in the first place with specific consideration for ETA. An isochrone is a contour line or isopleth showing the farthest distance that a ship can reach in an equal sailing time, as shown in Figure 3.3 a). The general procedures of the Isochrone method are shown in Figure 3.3.

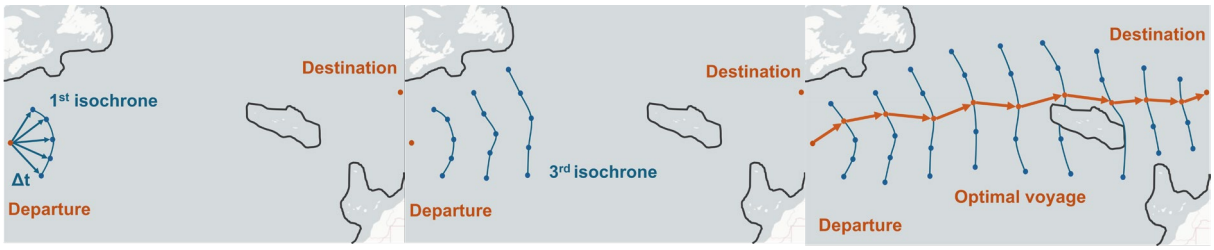

(a) (b) (c)

Figure 3.3: Graphical illustrations for the processes of the Isochrone algorithm.

How to generate a new isochrone based on the current one (i.e., moving from (a) to (b) in Figure 3.3) has always been a core issue in improving this algorithm. Hagiwara (1989) refined the method and proposed a practical approach for the development, while effectively controlling the computational load. He introduced the concept of a "subsector". In his method, some waypoints are first generated based on the current isochrone, then the subsector is used to select some of the best ones from these waypoints. This process is repeated iteratively until reaching the destination. His method (referred to as the Isochrone method hereafter) serves as the main reference for improving the Isochrone method in this thesis, with the detailed steps outlined below.

Denote the departure as $\boldsymbol{P}_0$ and the destination as $\boldsymbol{P}_f$, following Eq. (3.1). The great circle (GC) route between $\boldsymbol{P}_0$ and $\boldsymbol{P}_f$ is chosen as the reference route, denoted as GC_{ref}. For each (i^{th}) time stage, waypoints are given as $\boldsymbol{P}_{i,j}^{k}$, and it is derived from the latest ((i-1)$^{\text{th}}$) stage's point $\boldsymbol{P}_{i-1,\,k}$. Here, j in $\boldsymbol{P}_{i,j}^{k}$ means the j^{th} new point generated from the waypoint $\boldsymbol{P}_{i-1,\,k}$, where k refers to the k^{th} pre-reserved point at the (i-1)$^{\text{th}}$ isochrone $\{\boldsymbol{P}_{i-1}\}$. The ship's speed is assumed to remain constant throughout the voyage. If engine limitations prevent maintaining this speed under certain weather conditions, the ship will operate at the maximum allowable speed. The parameters that need to be initialized are listed in Table 3.1 which is introduced in the following process.

The voyage is segmented into a sequence of time stages, i.e., T_i, where $i = 0, 1, \ldots, n, f$, from $\boldsymbol{P}_0$ to $\boldsymbol{P}_f$, as shown in Figure 3.1. T_0 represents the departure time and T_f represents the required time of arrival of the voyage. Let a ship's initial service speed be denoted by V_s:

$$V_s = D/(T_f - T_0) \tag{3.7}$$

where D is the length of the reference great circle route GC_{ref}. The other inputs and outputs of the Isochrone algorithm are listed together in Table 3.1.

Table 3.1: Parameters to initialize the Isochrone algorithm with its input and output features.

Parameter and descriptions		
Δt	Sailing time between two adjacent time stages	
$\Delta\theta$	Change in heading angles between two consecutive sub-routes from each of the 'optimal' waypoints at the current time stage.	
$2m+1$	Number of successor waypoints for each waypoint at the current stage	
$2r$	Number of subsectors	
ΔD	Width of the searching limit within each local subsector	
Input and output features		
Input	Parameters to be initialized	As listed above
	Departure waypoint	$\boldsymbol{P}_0 = [x_0, y_0, T_0]$
	Destination waypoint	$\boldsymbol{P}_f = [x_f, y_f, T_f]$
	Service speed	V_s
Output	A series of waypoints consisting of the optimal voyage	$\boldsymbol{P}_0, \boldsymbol{P}_1, \boldsymbol{P}_2, \ldots, \boldsymbol{P}_n, \boldsymbol{P}_f$

The process of the Isochrone voyage optimization (Hagiwara, 1989) is illustrated in Figure 3.4. The first step is to generate the first isochrone $\{\boldsymbol{P}_1\}$ starting from $\boldsymbol{P}_0$ (Figure 3.4 (a)). At $\boldsymbol{P}_0$, head forward in the initial headings $\theta = \theta_{ref} \pm j \cdot \Delta\theta$ ($j = 0, 1, \ldots, m$) using the GC route to find new points for $\{\boldsymbol{P}_1\}$. At this step, θ_{ref} is C_{ref} at $\boldsymbol{P}_0$, and C_{ref} is the initial course of GC_{ref} at $\boldsymbol{P}_0$.

1) Check the sailing constraints:
   a) Check if V_s can be achieved with the headings θ under the weather at $\boldsymbol{P}_0$. If not, adjust the speed V_s in accordance with engine limitations.
   b) Check for land-crossing, shallow water, no-go zones, etc.
2) Proceed from $\boldsymbol{P}_0$ for Δt hours, with headings θ and speed V using the GC route. Way-points of the first isochrone $\{\boldsymbol{P}_1\}$, i.e., $\{\boldsymbol{P}_{1,k}, k = 1, 2, \ldots, 2m+1\}$ are found. Link $\boldsymbol{P}_0$ to every $\boldsymbol{P}_{1,k}$ with directions from $\boldsymbol{P}_0$ to $\{\boldsymbol{P}_1\}$ using an edge/sub-route.

The next step is to generate $\{\boldsymbol{P}_2\}$ based on $\{\boldsymbol{P}_1\}$. Start from each waypoint in $\{\boldsymbol{P}_1\}$ following the same steps as above, candidate waypoints $\{\boldsymbol{P}_{2,j}^{k}, k = 1, 2, \ldots, 2m+1, j = 1, 2, \ldots, 2m+1\}$ is obtained. To prevent the excessive growth, the sub-sector is introduced to select waypoints (Hagiwara, 1989), which is sub-areas distributed evenly around GC_{ref}. Thus, starting from $\{\boldsymbol{P}_1\}$, the following voyage search is carried out as given in Figure 3.4:

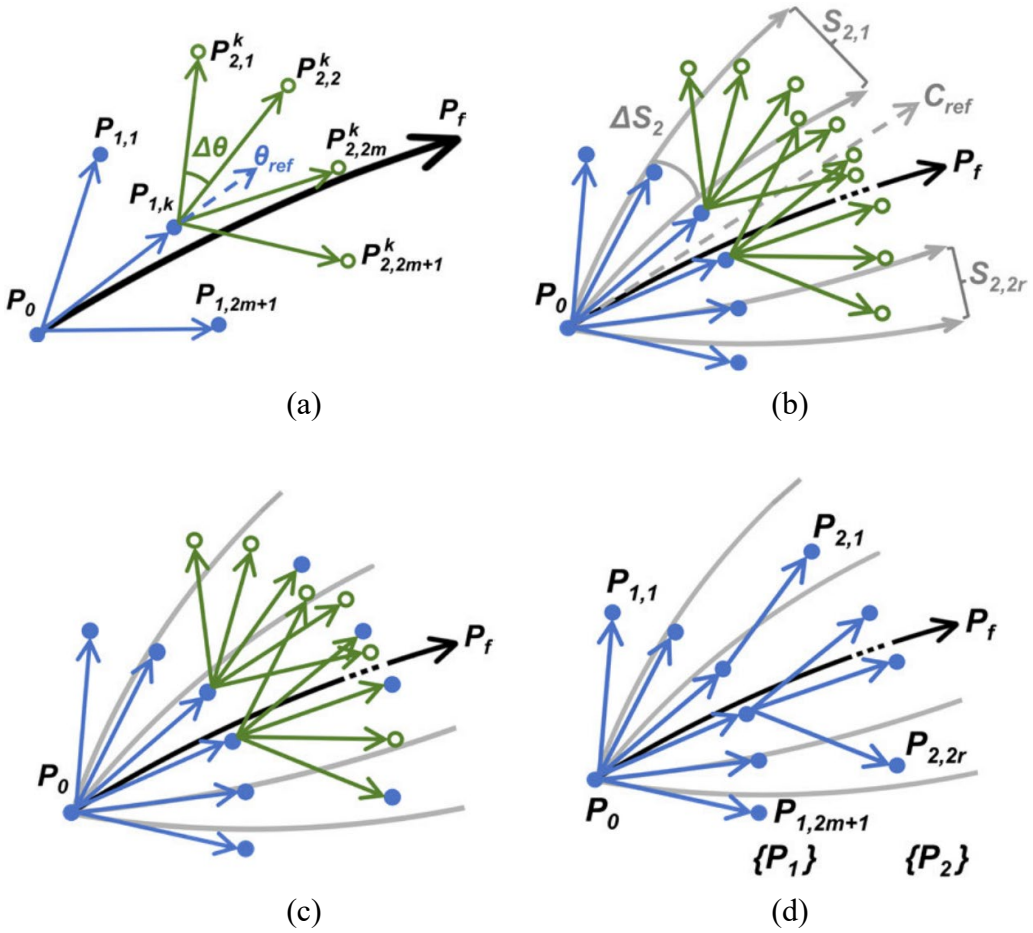

Figure 3.4: Generation of waypoints in the Isochrone algorithm.

1) Repeat the processes above as in Figure 3.4 (a) at each (k^{th}) waypoint $\boldsymbol{P}_{1,k}$. The reference heading θ_{ref} is the arrival course at $\boldsymbol{P}_{1,k}$ from $\boldsymbol{P}_0$. Each $\boldsymbol{P}_{1,k}$ leads to $2m+1$ potential waypoints $\{\boldsymbol{P}^k_{2,j}, j = 1, 2, \ldots, 2m+1\}$.
   Sub-sectors are defined based on $2r+1$ initial courses $C_{ref} \pm k{\cdot}\Delta S_i$ ($k= 0, 1, \ldots, r$) of the GC route from $\boldsymbol{P}_0$, shown as grey lines in Figure 3.4 (b).
2) The increment ΔS_i ($i = 2$, indicating the second time stage) is defined following (Hagiwara, 1989):

$$\Delta S_i = c \cdot \Delta D \;/\; \sin(c \cdot d_i),\; c = \pi \;/\; (60 \cdot 180) \tag{3.8}$$

   where d_i ($i = 2$) is the expected traveled distance equal to $i{\cdot}\Delta t{\cdot}V_s$ ($i = 2$).
   Then, subsectors $\{\boldsymbol{S}_{i,k}\}$ are given based on sub-areas between GC routes with adjacent initial headings, i.e., $[C_{ref} + (k\text{-}r\text{-}1){\cdot}\Delta S_i,\ C_{ref} + (k\text{-}r){\cdot}\Delta S_i]$, ($i = 2$, $k = 1, 2, \ldots, 2r$).
3) In each (k^{th}) sub-sector $S_{2,k}$, identify the optimal waypoint $\boldsymbol{P}_{2,k}$ with the optimum cost given by the cost function in Eq. (3.5), shown as blue dots in Figure 3.4 (c).
4) Only optimal waypoints $\{\boldsymbol{P}_{2,k}, k = 1, 2, \ldots, 2r\}$ are pre-reserved. Connect by directed edges with its predecessor in $\{\boldsymbol{P}_1\}$ respectively, as shown in Figure 3.4 (d). The second isochrone $\{\boldsymbol{P}_2\}$ is obtained.

Repeatably, based on the isochrone $\{\boldsymbol{P}_2\}$, and follow the above steps in recursion: at the i^{th} time stage, generate waypoints $\{\boldsymbol{P}_{i,j}^{k},\ k = 1, 2, \ldots, 2r, j = 1, 2, \ldots, 2m+1\}$, and identify the isochrone $\{\boldsymbol{P}_{i,k},\ k = 1, 2, \ldots, 2r\}$ from $\{\boldsymbol{P}_{i,j}^{k}\}$ using sub-sectors $\{\boldsymbol{S}_{i,k}\}$. New isochrones are generated in sequence, until the destination is reached.

3.3 Isochrone-based predictive optimization

Hagiwara's improvements have been proven to perform well in practice with computational efficiency (Lee et al., 2018). However, some shortcomings are still evident, such as it often generates sharp turning routes as shown in Figure 3.5, which are not suitable for operations.

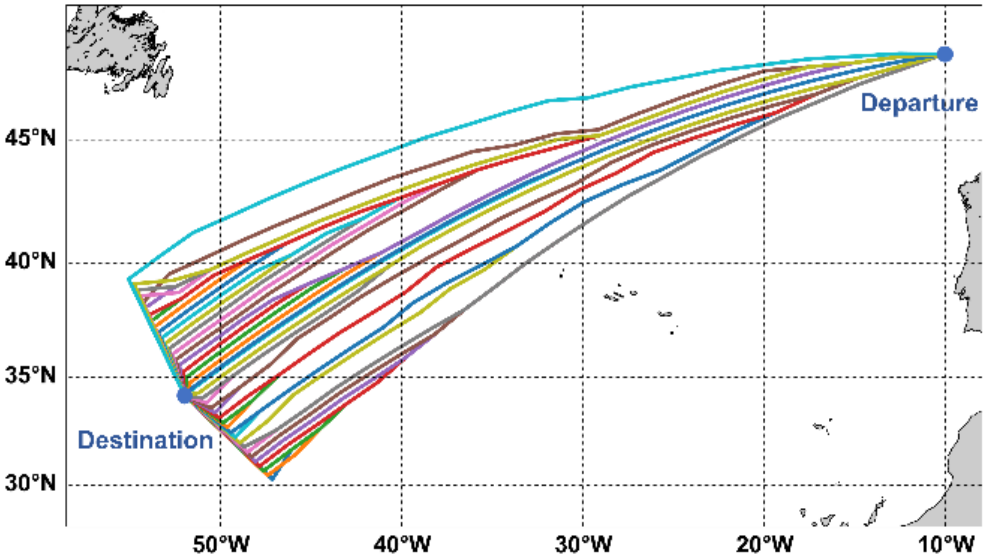

Figure 3.5: Routes given by the Isochrone method with sharp turns.

To solve this problem, an Isochrone-based predictive optimization (IPO) is proposed to improve the Isochrone method, addressing the following research objectives, and achieving real-time energy efficient weather routing:

1) Remain computationally efficient,
2) Avoid the route convergence problem in Figure 3.5,
3) Improve optimization performance and avoid local optimization.

The proposed IPO method is briefly introduced in the following, based on above introduction for the Isochrone method (Hagiwara, 1989).

Isochrones of the first half voyage in the IPO method

The first phase of the IPO method proceeds following steps illustrated in Figure 3.4. The cost function is defined to identify the waypoint nearest to $\boldsymbol{P}_f$, and the objective is to minimize the deviation from $\boldsymbol{P}_f$, as deviations at early stages can result in long and fuel-consuming routes.

Isochrones of the second half voyage in the IPO method

When $d_{iS} < 0.5D$, the second half of the voyage search begins. At this stage, special attention needs to be given to two problems: (1) smooth convergence towards P_f, and (2) avoiding local optimization as depicted in Figure 3.6.

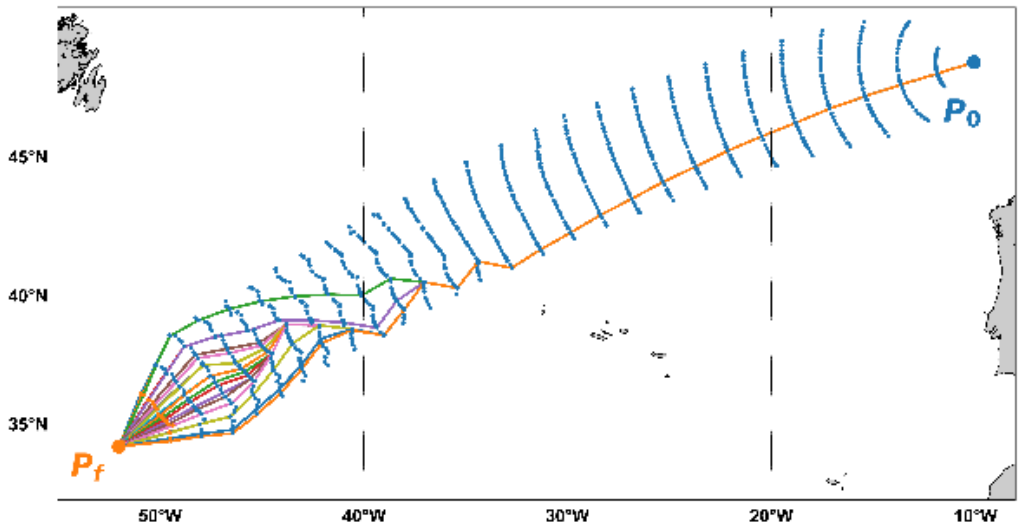

Figure 3.6: Example of a local optimized result giving overlapped candidate routes.

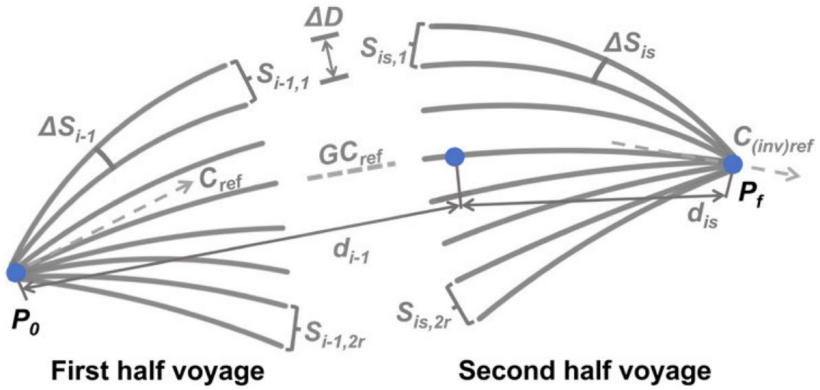

Figure 3.7: Reversed subsectors generated during the second half voyage.

To solve problem (1), the reversed subsectors are adopted, as shown on the right side in Figure 3.7. The subsectors introduced in Eq. (3.8) are reformulated, making it converging toward $\boldsymbol{P_f}$ in the late stages. In the second half of the voyage, the distance from the departure $\boldsymbol{P_0}$ is calculated, i.e., d_i is replaced by the current distance to $\boldsymbol{P_f}$ (denoted as d_{iS}), which is used to define the width of subsectors in the second half of a voyage:

$$d_{iS} = d_{total} - d_i, \Delta S_{iS} = \frac{c \cdot \Delta D}{\sin(c \cdot d_{iS})} \tag{3.9}$$

where d_{total} is the total distance from $\boldsymbol{P_0}$ to $\boldsymbol{P_f}$ along the reference route. A symmetric subsector set is generated as shown in Figure 3.7, which reduces its range when approaching $\boldsymbol{P_f}$.

Further to address problem (2), predictive optimization is conducted referring to the A* algorithm, which includes a heuristic term in its cost function, to account for future predictions:

$$f(n) = g(n) + h(n), \tag{3.10}$$

where usually for A*, $g(n)$ is defined as the accumulative cost from departure, $h(n)$ is the estimated cost to the destination, and $f(n)$ is the estimated cost for entire route. Based on Eq. (3.10), the cost/evaluation function C_p for choosing waypoints in each subsector in the proposed IPO, is augmented with a heuristic term $h(\boldsymbol{S})$:

$$C_p = \int_{T_0}^{T_i} j(\boldsymbol{S})dt + h(\boldsymbol{S}) \tag{3.11}$$

where $\int_{T_0}^{T_n} j(\boldsymbol{S})dt$ accumulates the consumed fuel from $\boldsymbol{P}_0$ to $\boldsymbol{P}_{i,k}$, $h(\boldsymbol{S})$ predicts the future fuel needed to reach $\boldsymbol{P}_f$ from $\boldsymbol{P}_{i,k}$. This prediction relies on a ship model and weather forecasts, assuming the ships adheres to the GC route and incorporates dynamic weather updates at each time stage. Consequently, C_p estimates total fuel consumption from $\boldsymbol{P}_0$ to $\boldsymbol{P}_f$.

The complete IPO methods are outlined as follows, assuming the current i^{th} isochrone:

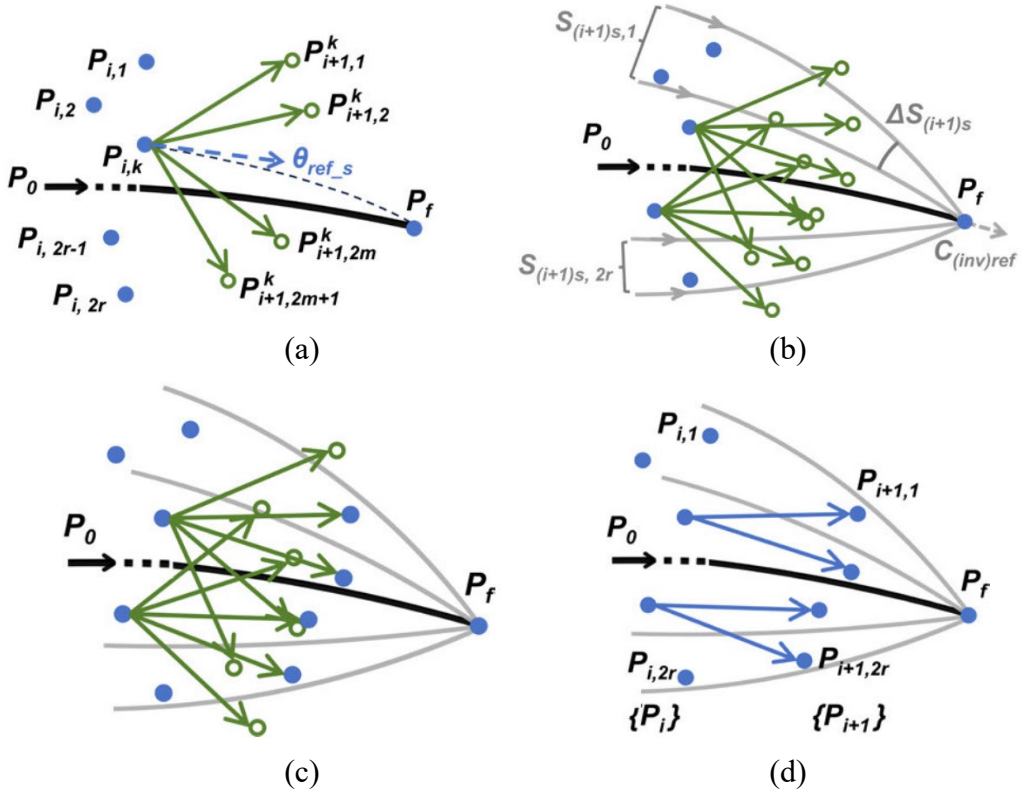

Figure 3.8: Generation of isochrones in the second half of the voyage using the IPO method.

1) At current waypoint $\boldsymbol{P}_{i,k}$ (k^{th} waypoint in the i^{th} isochrone), follow the heading $\theta=\theta_{ref\_s} \pm j\cdot\Delta\theta (j= 0, 1, \ldots, m)$ and obtain the new waypoints for the next/$(i+1)^{\text{th}}$ stage.
θ_{ref_s} is the initial course of the GC route from $\boldsymbol{P}_{i,k}$ to $\boldsymbol{P}_f$. Each $\boldsymbol{P}_{i,k}$ generates $2m+1$ new points $\{\boldsymbol{P}^{k}_{i+1,j}, j = 1, 2, \ldots, 2m+1\}$ as shown in Figure 3.8 (a).
2) The reversed sub-sectors are indicated by $2r+1$ GC routes with arrival courses $C_{inv(ref)} \pm k\cdot\Delta S_{(i+1)\,s}$ ($k= 0, 1, \ldots, r$) at $\boldsymbol{P}_f$, as shown by the grey lines in Figure 3.8 (b). $\Delta S_{(i+1)\,s}$ can be calculated following Eq. (3.9).
Define the sub-sectors $\{S_{(i+1)\,s,\,k}\}$ as sub-areas between adjacent arrival headings at $\boldsymbol{P}_f$, i.e., $[C_{inv(ref)}+(k-r-1)\cdot\Delta S_{(i+1)\,s}, C_{inv(ref)}+(k-r)\cdot\Delta S_{(i+1)\,s}]$, ($k =1, 2, \ldots, 2r$).
3) In each sub-sector $S_{(i+1)\,s,\,k}$ (k^{th} sub-sector at $(i+1)^{\text{th}}$ time stage), choose the optimal point $\boldsymbol{P}_{i+1,\,k}$ as the one with the lowest cost, using the function C_p defined in Eq. (3.11), as shown by the blue dots in Figure 3.8 (c).
4) Connect each optimal points $\{\boldsymbol{P}_{i+1,\,k}, k =1, 2, \ldots, 2r\}$ with its predecessor, as shown in Figure 3.8 (d), and obtain the next/$(i+1)^{\text{th}}$ isochrone $\{\boldsymbol{P}_{i+1}\}$.
5) Continue from Step 1) until $\boldsymbol{P}_f$ is closer than one stage's sailing. Connect directly to $\boldsymbol{P}_f$.

A feasible route set $\{\boldsymbol{R}\}$ is generated, with all candidate routes having comparable ETAs. The total fuel consumption is the sum of all sub-routes' cost, i.e., a sequence from $\boldsymbol{P}_0$ to $\{\boldsymbol{P}_1\}$, $\{\boldsymbol{P}_1\}$ to $\{\boldsymbol{P}_2\}$, …, $\{\boldsymbol{P}_n\}$ to $\boldsymbol{P}_f$, as shown in Figure 3.9, and the optimal voyage $\boldsymbol{R}^*$ has the lowest accumulative fuel in $\{\boldsymbol{R}\}$.

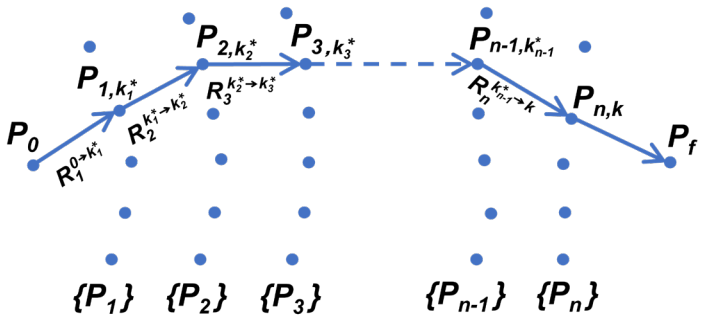

Figure 3.9: Examples of the optimal route $\boldsymbol{R}^*$.

3.4 Learning-based Pareto optimum weather routing

In this thesis, the application of an advanced ML method, specifically an innovative multi-objective evolutionary algorithm (MOEA), is explored to address weather routing challenges by proposing a learning-based EA approach, L-MOEA.

Evolutionary learning network

MOEAs are population-based metaheuristic methods inspired by biological evolution. Typically, based on a set of initial solutions, MOEA finds their potential directions for effective evolution through random exploration, aiming to achieve optimal objectives. However, it can

be inefficient with slow convergence. This thesis introduces an intelligent learning network capable of capturing knowledge about positive evolutionary directions. This drives more aimed searches to generate new solutions, achieving efficient search than random exploration.

The **Pareto front (PF)** is a set of non-dominated solutions in multi-objective optimization, considered optimal when no objective can be improved without worsening at least one other objective. In this thesis, the proposed algorithm is anticipated to efficiently converge towards the real Pareto front (PF*), to achieve superior optimization performance. A learning network activated by rectified linear units (ReLU) is implemented to achieve this goal as illustrated in Figure 3.10. A dataset is used to gather successful instances that emerge from previous populations, where offspring Pareto dominate their parents. Then the network learns the evolutionary characteristics of these samples, with the input and output representing the parents and offspring in the evolutionary process.

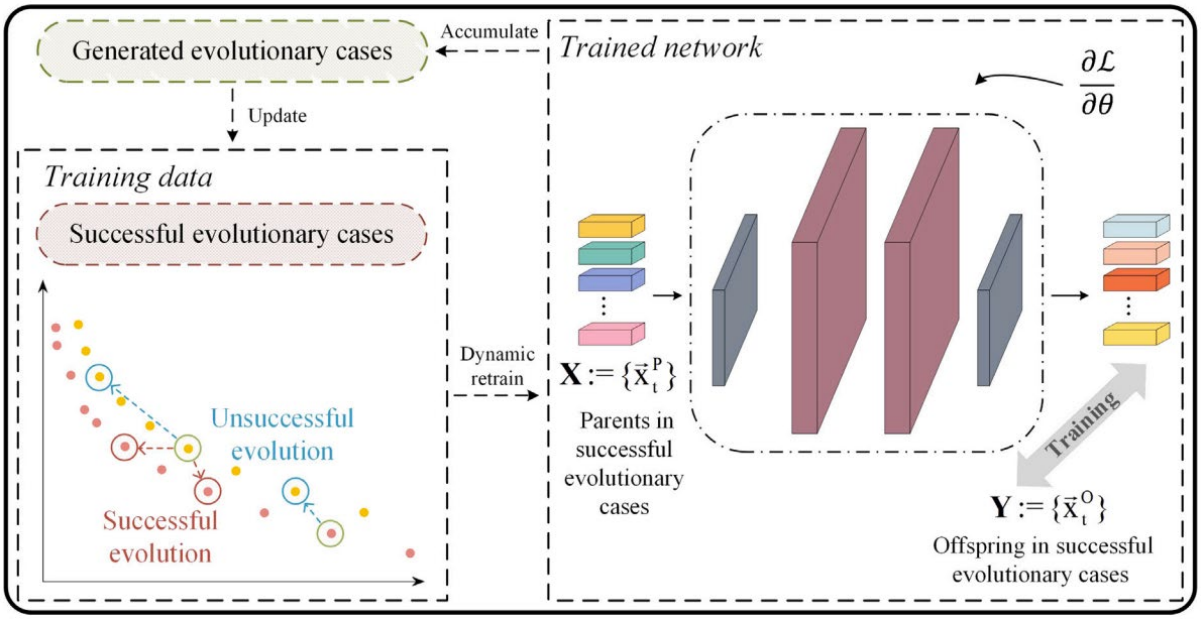

Figure 3.10: The evolutionary learning network and dynamic retraining mechanism of the proposed L-MOEA.

An individual $\vec{\boldsymbol{x}}$ in the population of MOEA is a feasible voyage from $\boldsymbol{P}_0$ to $\boldsymbol{P}_f$ in a predefined static grid, consisting of waypoints $\boldsymbol{P}$ and operational parameters $\boldsymbol{U}$ defined in Eq. (3.4), i.e., $\vec{\boldsymbol{x}} = \{\boldsymbol{P}, \boldsymbol{U}\}$. Denote $\boldsymbol{P}_t^i$ $(0 < t \leq i)$ and $\boldsymbol{O}_t^i (0 < t \leq i)$ as the parent and offspring sets at each (t^{th}) generation in the past, till the current (i^{th}) generation. The initial learning network takes all the parental samples $\boldsymbol{X}$ from successful evolutions as input, and their offsprings $\boldsymbol{Y}$ as output, to fit the latent evolution directions, i.e.:

$$\begin{aligned} \boldsymbol{X} &= \{\, \vec{x}_t^P \mid \vec{x}_t^P \in \boldsymbol{P}_t^i \,\}_{t=1}^i \\ \boldsymbol{Y} &= \{\, \vec{x}_t^O \mid \vec{x}_t^O \in \boldsymbol{O}_t^i \,\}_{t=1}^i \end{aligned} \tag{3.12}$$

The signal forward propagation in this network is as follows:

$$\begin{aligned} \boldsymbol{Z}^{(l)} &= \boldsymbol{A}^{(l-1)} \cdot \boldsymbol{W}^{(l-1)} + \boldsymbol{B}^{(l-1)}, && l = 2, 3 \\ \boldsymbol{A}^{(l)} &= \begin{cases} \mathrm{ReLU}\left(\boldsymbol{Z}^{(l)}\right), & l = 2, 3 \\ \mathrm{linear}\left(\boldsymbol{Z}^{(l)}\right), & l = 4 \end{cases} \end{aligned} \tag{3.13}$$

where $\boldsymbol{Z}^{(l)}$and $\boldsymbol{A}^{(l)}$denote the input and output at the l^{th} layer in the network and is $\boldsymbol{A}^{(l)}$ an encoding result of the input $\boldsymbol{X}$. $\boldsymbol{W}$ and $\boldsymbol{B}$ are the weight matrix and the bias vector respectively. With the loss function based on the mean squared error, the network is guided to minimize the difference between the output and the ground truth by adjusting its weights and biases:

$$\begin{aligned} \Delta^{(l)} &= \begin{cases} \Delta^{(l+1)} \cdot \boldsymbol{W}^{(l)^{\mathrm{T}}} \odot \mathrm{ReLU}'\left(\boldsymbol{Z}^{(l)}\right), & l = 2, 3 \\ \left(\mathbf{Y} - \boldsymbol{A}^{(l)}\right) \odot \mathrm{ReLU}'\left(\boldsymbol{Z}^{(l)}\right), & l = 4 \end{cases} \\ \boldsymbol{W}^{(l)} &\leftarrow \boldsymbol{W}^{(l)} + \alpha \boldsymbol{A}^{(l)} \cdot \Delta^{(l)}, && l = 2, 3, 4, \\ \boldsymbol{B}^{(l)} &\leftarrow \boldsymbol{B}^{(l)} + \alpha \Delta^{(l)}, && l = 2, 3, 4, \end{aligned} \tag{3.14}$$

where ReLU′is the derivative of the activation function, and α denotes the learning rate.

In subsequent iterations, to track changes in the positive evolutionary direction during the process, a dynamic retraining mechanism is introduced, which will continuously accumulate successful cases from the process and regularly refresh the training dataset.

Multi-objective evolutionary processes

Combined with the above evolutionary learning network, L-MOEA follows the integrated framework illustrated in the flowchart shown in Figure 3.11.

- **Initial population generation**

Initially, each individual is represented as a set of waypoints from $\boldsymbol{P}_0$ to $\boldsymbol{P}_f$ and the RPM of the ship's engine at each sub-route. The initialization employs the GC route and several random routes, and routes optimized for the shortest duration and minimal fuel consumption, each determined through single-objective optimization at constant RPM. They (denoted as DRs) are also incorporated into the initial population $\boldsymbol{G}_0$.

- **Population renewal**

A clustering-based crowding distance sorting method is developed, as illustrated in the population renewal module in Figure 3.11, to enhance the diversity of solutions. First, an unlimited-capacity archive $\boldsymbol{A}_t$ is established to filter all the non-dominated solutions to date. Further, the elite archive $\boldsymbol{A}_t^e$ is used to select solutions from $\boldsymbol{A}_t$ that have superior crowding distances. The

crowding distances are calculated and ranked on a regional basis. Then the solutions with superior distances in each region are extracted into $\boldsymbol{A}_t^e$ until it reaches maximum capacity.

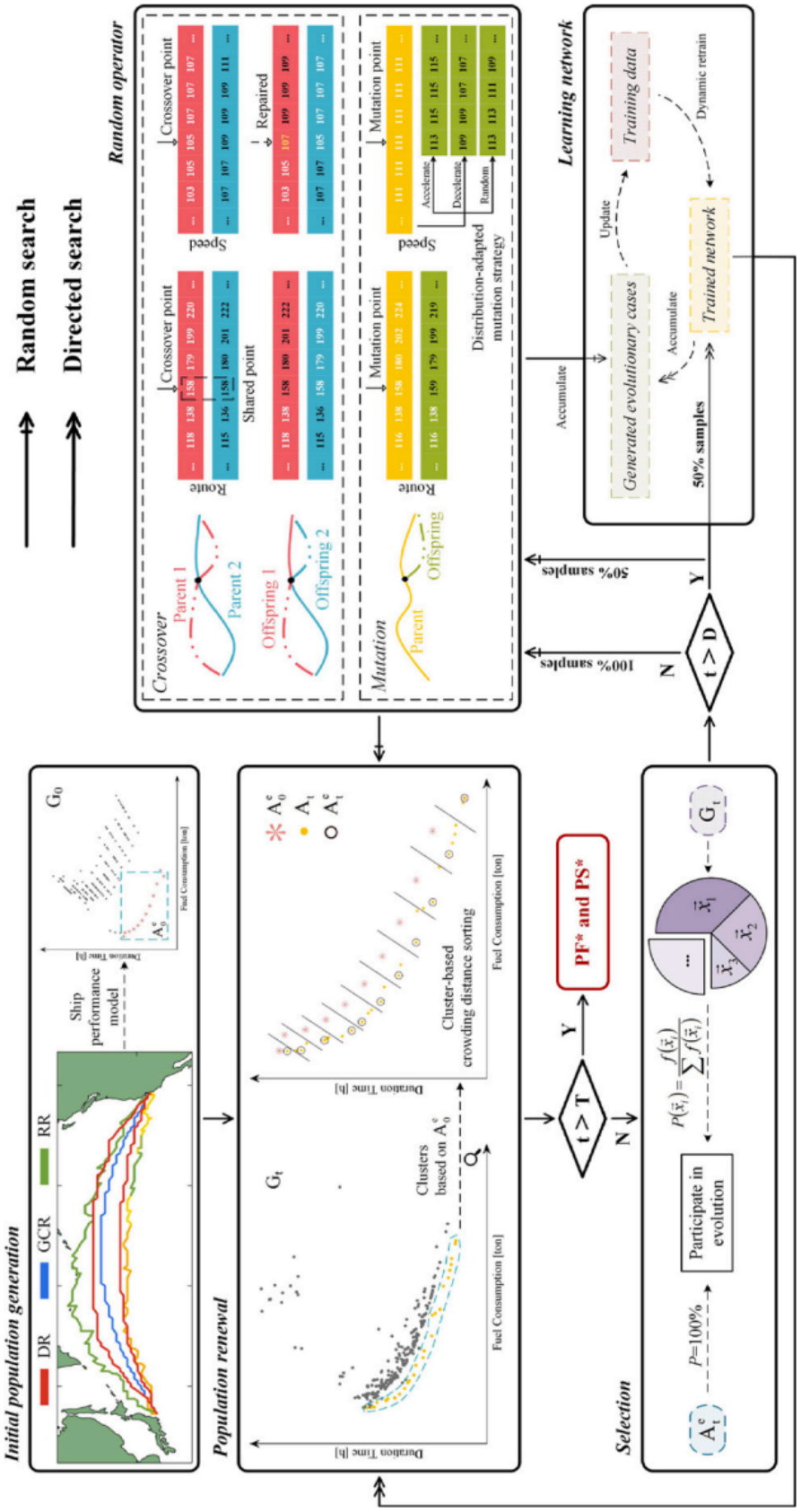

Figure 3.11: Flowchart of the proposed L-MOEA framework.

- **Selection, crossover and mutation**

For selection, fitness-based roulette selection is implemented in $\boldsymbol{A}_t^e$ to select populations to produce next generations, ensuring the quality of solutions. For route crossing, a common point is randomly selected as the breakpoint, then two parental routes exchange segments at this point to create new offspring routes. For route mutation, identifying a random point allows for the regeneration of the route. For RPM, the same crossing and mutation are conducted. But since it cannot change instantaneously, the offspring will undergo a repair to ensure a gradual change, as shown in the crossover module in Figure 3.11. The RPM will undergo acceleration, deceleration, or random changes, continuing for a certain duration.

- **Uncertainty-driven optimization**

This thesis aims to select a voyage that has the lowest uncertainty in achieving the optimization objectives under dynamic weather impacts. As shown in Figure 3.12, $f_k^u(\vec{x}) = s(\sigma_k)$ denote the uncertain results of a sailing plan $\vec{x}$, σ_k represents the standard deviation of $f_k^u(\vec{x})$ based on the ensemble forecast, k = 1, 2 is the fuel cost and duration time. The function s (·) is the Min–Max normalization (Kiran & Vasumathi, 2020), to mitigate the interference of magnitude.

L-MOEA first employs the expectations of ensemble forecast data during the process. In the end (i.e., when t reaches the terminating threshold T) for each solution in the optimal set $\boldsymbol{A}_t$, all members of the ensemble forecast are input into the performance model, generating multiple f_k^u values. If replacing crowding distance with f_k^u values as introduced in the population renewal, the solution with lowest uncertainty will be identified.

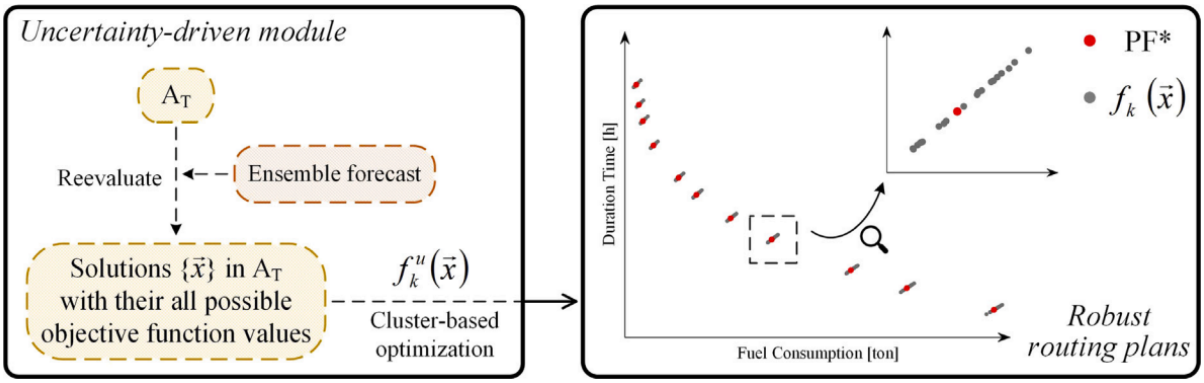

Figure 3.12: Robust optimization based on the proposed uncertainty-driven module.

4 Ship performance model in weather routing

From the above research in optimization algorithms, a crucial observation is that the weather routing exhibits significant uncertainty, which may have a substantial impact on the effectiveness of their applications. Besides the dynamic weather condition which was investigated in Chapter 3.4, another source of uncertainty stems from the estimation of fuel consumption due to the ship performance model.

This thesis aims to investigate the uncertainty in fuel consumption due to the ship performance model and its impact on weather routing. An artificial neural network (ANN) is used to model the speed-to-power performance of the ship, as it is widely recognized for its strong ability to fit complex models. A Gaussian Process Regression (GPR) model is used to estimate the distribution of SFOC, as it can provide probabilistic predictions along with uncertainty estimation without specifying a specific functional form (Zhang et al., 2023). Three main steps is illustrated with more details in Figure 4.1.

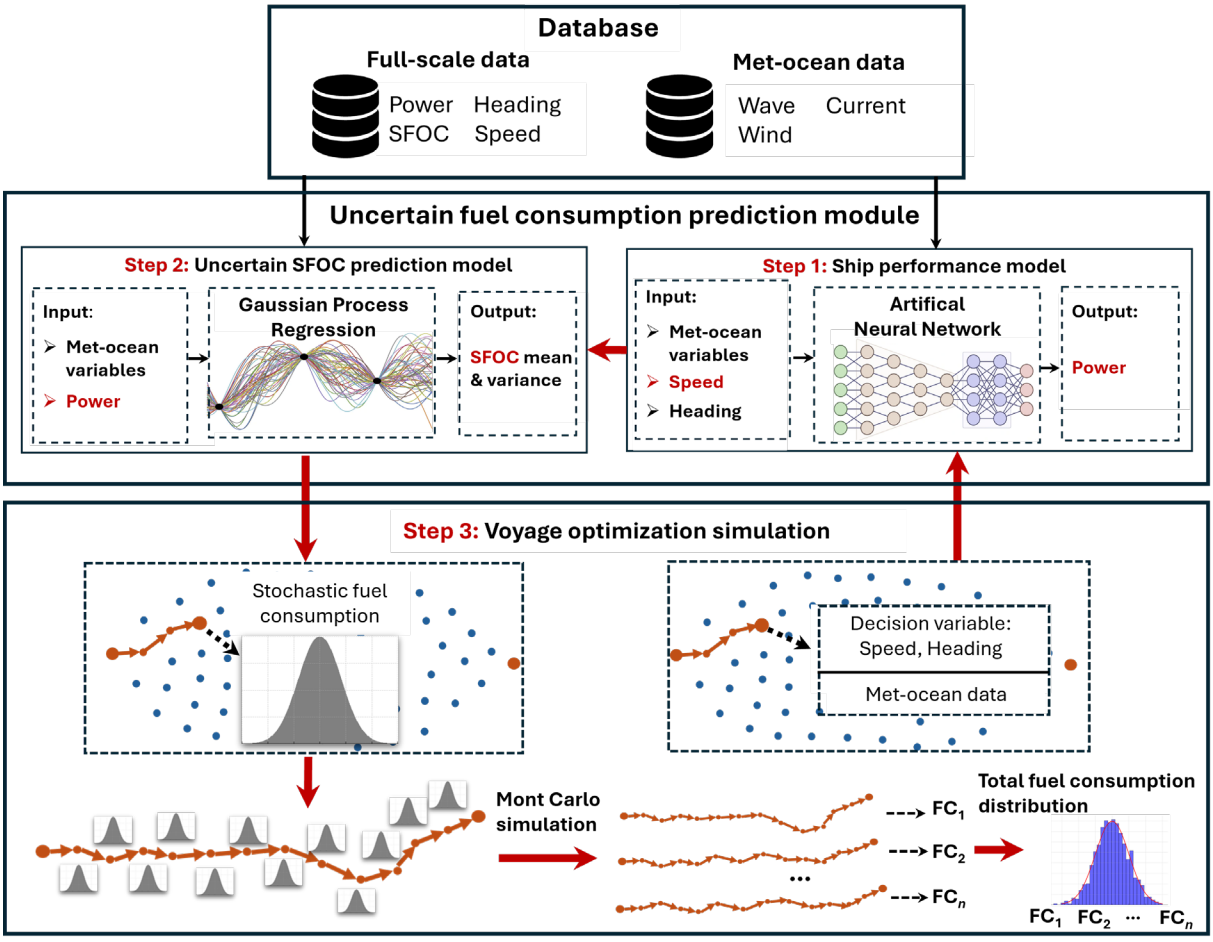

Figure 4.1: Steps of uncertainty investigation conducted in this thesis.

- ***Step 1*** - Develop a genetic algorithm – back propagation (GA-BP) neural network (NN) model to predict ship power in terms of speeds and weather conditions. (Chapter 4.1)

- ***Step 2*** – Develop a Gaussian Process Regression (GPR) model, to establish a model that predicts SFOC, and its uncertainty based on power and weather conditions (Chapter 4.2).
- ***Step 3*** - The ship performance GA-BP model (*Step 1*) and the stochastic SFOC GPR model (*Step 2*) are integrated into a voyage optimization method (e.g., the 3D-Dijkstra algorithm (3DDA)). Monte Carlo simulations are conducted to analyze the impact of uncertainty in fuel consumption based on the optimization results (Chapter 4.3).

4.1 Model for ship speed-power performance

ANNs are renowned ML methods for developing complex data-driven models (Du et al., 2019; Yan et al., 2024). This thesis employs an ANN, specifically a BP-NN, to establish a ship performance model. The proposed performance model is used to predict the engine power P^S based on the ship speed, heading, and metocean conditions, etc. Based on the i^{th} input $\boldsymbol{\alpha}_i$ among all the inputs, the GA-BP model can be represented as:

$$P^S = f_p(\boldsymbol{\alpha}_i) + \rho_i \tag{4.1}$$

where ρ_i denotes the prediction error; $f_p(\cdot)$ is a function mapping the n-dimensional input $\boldsymbol{\alpha}_i$ to the 1-dimensional output power P^S. The attributes in the input $\boldsymbol{\alpha}_i$ are listed in Table 4.1.

Table 4.1: Attributes used as input features and outputs for the proposed GA-BP model.

Class	Description	Attributes
Input	Speed through water [knots]	V_s
	Heading [°]	θ
	Significant wave height [m]	H_s
	Mean wave period [s]	T_z
	Mean wave direction [°]	D_{wave}
	Current speed [m/s]	V_c
	Current direction [°]	θ_c
	Wind speed [m/s]	V_w
	Wind direction [°]	θ_w
Output	Propulsion power [kW]	P^s

BP-NN is a variant of ANN which features an input layer and output layer, with multiple hidden layers in between. Each layer is associated with network parameters such as weight and threshold. BP-NN adjusts these network parameters via the gradient descent method during training, making it particularly sensitive to the initial values. Inappropriate initial weights and thresholds may lead to slow convergence during training. Thus, GA is initially employed to address the issue of choosing initial weights and thresholds, before further refinement through BP-NN.

The general process of this GA-BP model is presented in Figure 4.2. GA is inspired by the process of natural selection. For each generation of population, GA iterates through the following steps: individuals are selected from the population based on their fitness; selected individuals undergo crossover to exchange information; mutations are applied to introduce random variations; and fitness-based selection continues. Gradually, GA improves the quality of the solutions until a predefined termination criterion is met, at which point the best individual in the population represents the optimal solution.

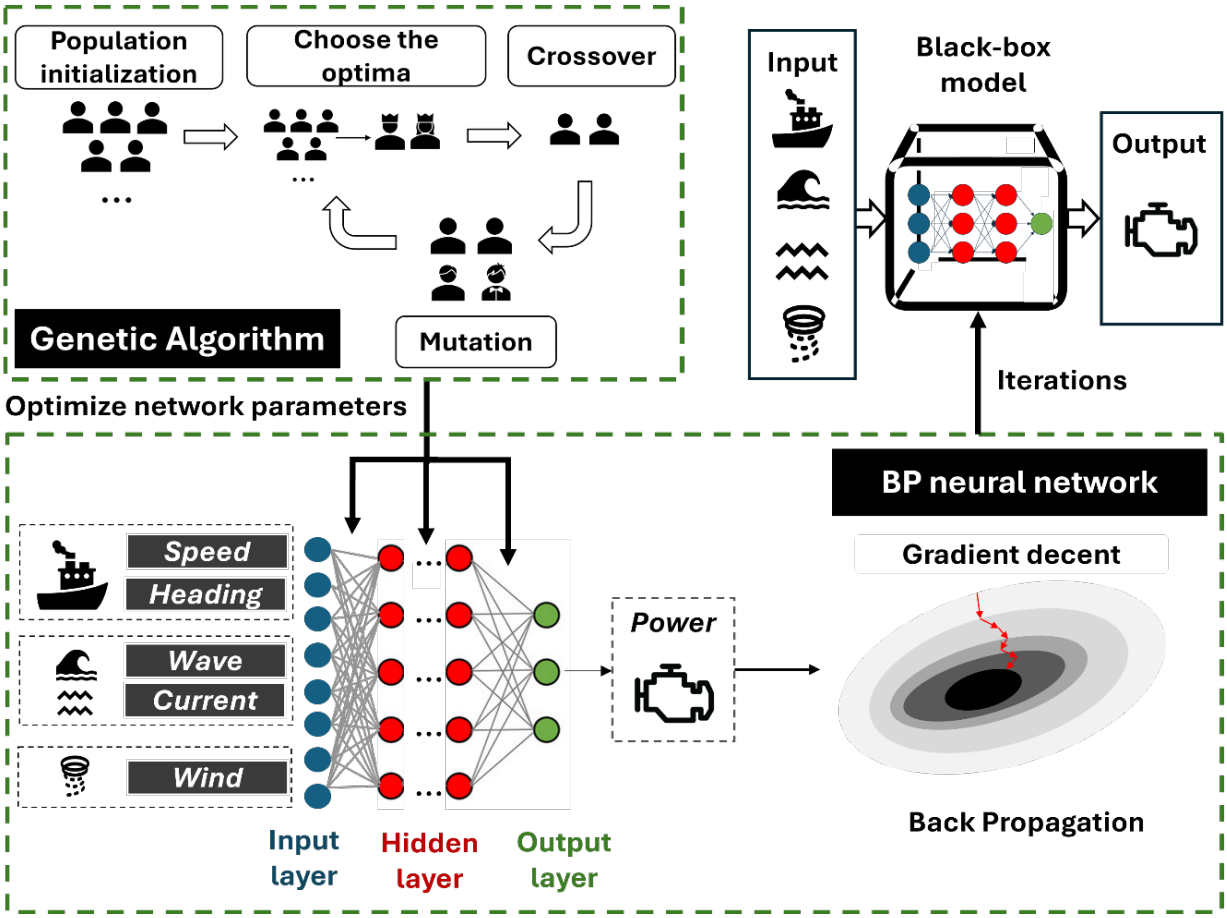

Figure 4.2: Structure of the proposed GA-BP Neural Network ship performance model.

For this GA-BP model, network parameters of the BP-NN (weights and thresholds of all layers) are first encoded into GA to obtain optimal values to start BP-NN. The training residual of the BP-NN is taken into the fitness function:

$$F_{fitness} = \left| P^S - \widehat{P^S} \right| \tag{4.2}$$

The fitness of each population will be evaluated, where one population consists of a series of network parameters (weights and thresholds) for BP-NN. Through selection, crossover, and mutation, the new populations are iteratively generated, evaluated, and selected until the requirements are met:

$$\boldsymbol{w}^* = \arg\min_{\boldsymbol{w}} \mathcal{L}(\boldsymbol{w}) \tag{4.3}$$

where $\boldsymbol{w}^*$ is optimized values for initial network parameters (weights and thresholds); $\mathcal{L}(\cdot)$ indicates objective function, which is the fitness function $F_{fitness}$.

In the above process, GA offers an approximate global search, while the fine-tuning of parameters is performed by subsequent BP-NN using gradient descent during the backpropagation process. As the BP-NN network features multiple hidden layers between input layer and output layer, after obtaining initial weights and thresholds for each hidden layer which has been optimized by GA, the output for a single hidden layer can be defined as follows:

$$h_j = f_a(\sum_{i=1}^{n} \omega_{ij}\boldsymbol{\alpha}_i - \theta_{ij}) \tag{4.4}$$

where h_j represents the output from the hidden layer; f_a represents the activation function of the hidden layer; ω_{ij} and θ_{ij} represent its weights and thresholds. The output of the overall network can be calculated as follows:

$$\widehat{P^s} = g_a(\sum_{j=1}^{l} \omega_j h_j - b_j) \tag{4.5}$$

where $\widehat{P_s}$ represents the predicted power given by the overall network; $g_a(\cdot)$ represents the activation function of the output layer; ω_j and b_j represent the weights and thresholds of the output layer. The prediction residual ε can be calculated as:

$$\varepsilon = \frac{1}{2}(P^s - \widehat{P^s})^2 = \frac{1}{2}\sum_{k=1}^{n} \left[P^s - g_a\left(\sum_{j=1}^{l} \omega_j f_a\left(\sum_{i=1}^{n} \omega_{ij}\boldsymbol{\alpha}_i - \theta_{ij}\right) - b_j\right)\right]^2 \tag{4.6}$$

The total error of the BP-NN is accumulated from all the output errors of each individual neuron. This total error will propagate backward from the output layer to the input layer, according to a specified learning rate. All the weights and thresholds in the network will be updated through gradient descent, to reduce the overall error until the terminating criteria is met.

4.2 Model for stochastic fuel consumption

Uncertain SFOC modeling using GPR

SFOC indicates the fuel consumption per kilowatt-hour (kWh) of power, which is a critical measure for evaluating energy performance of an engine. Typically, fuel consumption is calculated using a SFOC regression curve which relates power to SFOC. The general process is as follows, as shown in Figure 4.3.

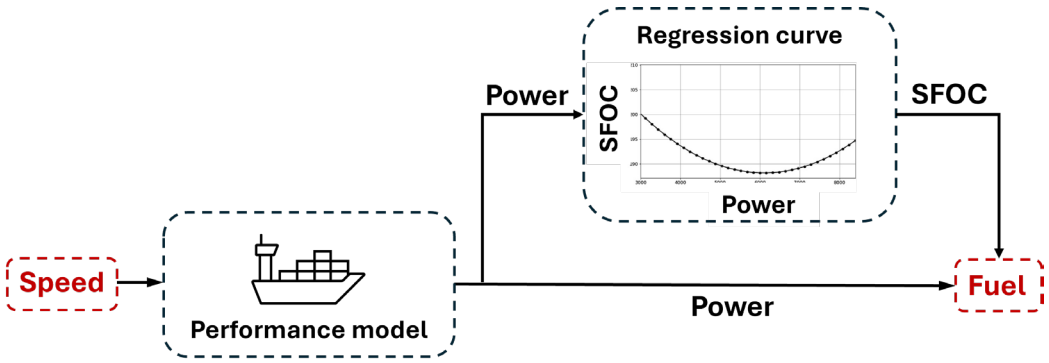

Figure 4.3: Theoretical calculations for fuel costs using a regressed power - SFOC curve.

First, based on a ship speed-power performance model introduced in Chapter 4.1, the power required for a given speed is determined. The corresponding SFOC can be found using the regressed curve of power to SFOC. Finally, multiplying the power P^s by the SFOC yields the fuel consumption F_c for a voyage segment:

$$F_c = P^S \cdot SFOC \tag{4.7}$$

However, factors influencing SFOC values extend beyond only power P^s, and for each power level, SFOC is in fact a probabilistic distribution rather than a deterministic value, as shown in Figure 4.4.

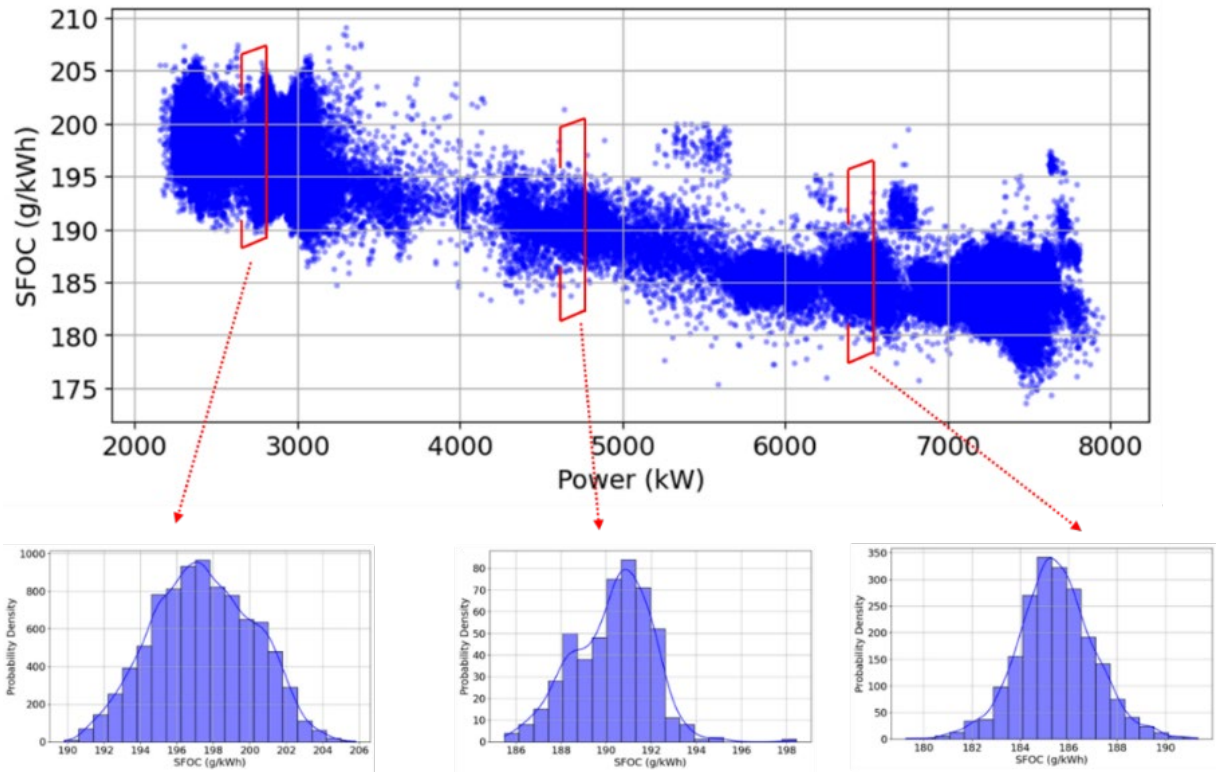

Figure 4.4: SFOC measurement data under different operation conditions.

This thesis employs a Gaussian Process Regression (GPR) model to estimate the distribution of SFOC, modeling it with power and metocean conditions as input variables. GPR is a non-parametric Bayesian approach to address regression problems (Zhang et al., 2023), providing probabilistic predictions along with uncertainty estimation without specifying a specific functional form. In this thesis, the GPR model for SFOC can be defined as:

$$c_i^{SFOC} = f(\boldsymbol{x}_i) + \varepsilon_i \tag{4.8}$$

where $\varepsilon_i \sim \mathcal{N}(0, \sigma_n^2)$ and σ_n^2 is the noise variance. The unknown latent function $f(\cdot)$ is assumed Gaussian process prior, i.e., $f(\cdot) \sim \mathcal{GP}(\mu(\cdot), k(\cdot))$, where $\mu(\cdot)$ refers to the mean function, which is usually assumed zero for simplicity, and $k(\cdot)$ is the covariance (kernel) function. The formulation of $f(\cdot)$ is unknown, and the value of $f(\boldsymbol{x}_i)$ follows a joint Gaussian distribution. The input $\boldsymbol{x}_i$ and output features are listed in detail in Table 4.2.

Table 4.2: Attributes used as input and output features for the proposed GPR model of SFOC prediction.

Class	Description	Attributes
Input	Propulsion power [kW]	P^s
	Significant wave height [m]	H_s
	Mean wave period [s]	T_z
	Mean wave direction [°]	D_{wave}
	Current speed [m/s]	V_c
	Current direction [°]	θ_c
	Wind speed [m/s]	V_w
	Wind direction [°]	θ_w
Output	The observed corresponding SFOC value	c_i^{SFOC}

Further, let denote:

$$\boldsymbol{X} = \{\boldsymbol{x}_i, i = 1, \ldots, n\} \tag{4.9}$$

$$\mathbf{f} = [\mathrm{f}_1, \mathrm{f}_2, \mathrm{f}_3, \ldots, \mathrm{f}_n]^T = [f(\boldsymbol{x}_1), f(\boldsymbol{x}_2), f(\boldsymbol{x}_3), \ldots, f(\boldsymbol{x}_n)]^T \tag{4.10}$$

where $\mathbf{f} \sim \mathcal{N}(\boldsymbol{\mu}(\boldsymbol{X}), \boldsymbol{K}(\boldsymbol{X}, \boldsymbol{X}))$. All the observed values of SFOC can be defined as:

$$\boldsymbol{c}^{SFOC} = \{c_i^{SFOC}, i = 1, \ldots, n\} \tag{4.11}$$

where $\boldsymbol{c}^{SFOC}$ is joint Gaussian distributed, i.e., $\boldsymbol{c}^{SFOC} \sim \mathcal{N}(\boldsymbol{\mu}(\boldsymbol{X}), \boldsymbol{K}(\boldsymbol{X}, \boldsymbol{X}) + \sigma_n^2 \boldsymbol{I})$, and $\boldsymbol{I}$ denotes an identity matrix. For a new input $\boldsymbol{x}_*$, the prior assumption is that there exists the same

Gaussian distribution between the training and the testing data sets, $\boldsymbol{c}^{SFOC}$ and $f(\boldsymbol{x}_*)$ follow the joint Gaussian prior distribution:

$$\begin{bmatrix} \boldsymbol{c}^{SFOC} \\ \mathrm{f}_* \end{bmatrix} \sim \mathcal{N}\left(\begin{pmatrix} \boldsymbol{\mu}(\boldsymbol{X}) \\ \mu(\boldsymbol{x}_*) \end{pmatrix}, \begin{pmatrix} \boldsymbol{K}(\boldsymbol{X},\boldsymbol{X}) + \sigma_n^2 \boldsymbol{I} & \boldsymbol{K}(\boldsymbol{X},\boldsymbol{x}_*) \\ \boldsymbol{K}(\boldsymbol{x}_*,\boldsymbol{X}) & k(\boldsymbol{x}_*,\boldsymbol{x}_*) \end{pmatrix} \right) \tag{4.12}$$

Finally, in a Bayesian framework, the key equation of GPR is the conditional distribution given the observed data samples described as:

$$\mathrm{f}_* \mid \boldsymbol{X}, \boldsymbol{c}^{SFOC}, \boldsymbol{x}_* \sim \mathcal{N}\left(\bar{\mathrm{f}}_*, \Sigma_{\mathrm{f}_*}\right) \tag{4.13}$$

where:

$$\bar{\mathrm{f}}_* = \boldsymbol{K}(\boldsymbol{x}_*,\boldsymbol{X})[\boldsymbol{K}(\boldsymbol{X},\boldsymbol{X}) + \sigma_n^2 \boldsymbol{I}]^{-1}\, \boldsymbol{c}^{SFOC} \tag{4.14}$$

$$\mathrm{Var}\,(\mathrm{f}_*) = k(\boldsymbol{x}_*,\boldsymbol{x}_*) - \boldsymbol{K}(\boldsymbol{x}_*,\boldsymbol{X})\,[\boldsymbol{K}(\boldsymbol{X},\boldsymbol{X}) + \sigma_n^2 \boldsymbol{I}]^{-1} \boldsymbol{K}(\boldsymbol{X},\boldsymbol{x}_*) \tag{4.15}$$

where $\bar{\mathrm{f}}_*$ is the predicted SFOC mean value based on input $\boldsymbol{x}_*$, and $\mathrm{Var}\,(\mathrm{f}_*)$ is the variance to incorporate the uncertainty into the predictions.

Using this method, the mean value $\bar{\mathrm{f}}_*$ and variance $\mathrm{Var}\,(\mathrm{f}_*)$ of SFOC at different power levels under various metocean conditions can be predicted (Luo et al., 2024). The predicted SFOC represents a distribution that accounts for its uncertainty, and it can be used in weather routing to investigate the reliability of the optimization results.

4.3 Uncertainty of fuel consumption in weather routing

In this part, the GA-BP performance model and stochastic GPR SFOC model are used for the calculation of fuel consumption. They are employed in 3DDA to estimate fuel, further investigating the impact of uncertainty on weather routing. 3DDA is an optimization algorithm for weather routing where speed is one of the optimization variables. During the optimization process, each time a waypoint and speed need to be determined, uncertainty arises due to the stochastic SFOC GPR model. This uncertainty accumulates and may eventually lead to different fuel consumptions.

This thesis aims to analyze this uncertainty and investigate its impact. By calculating the fuel consumption for each sub-route using the mean and variance of the SFOC distribution, and integrating the fuel consumption of each sub-route, the uncertainty of the entire voyage can be calculated, as illustrated in Figure 4.5.

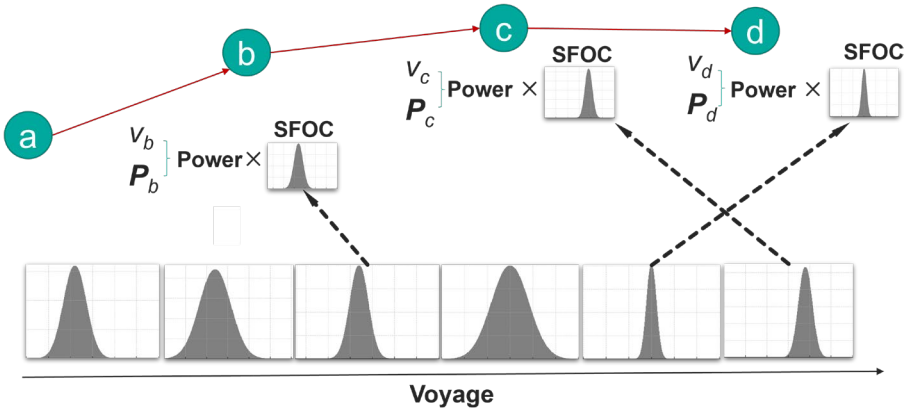

Figure 4.5: The impact of the stochastic SFOC on fuel consumption in weather routing.

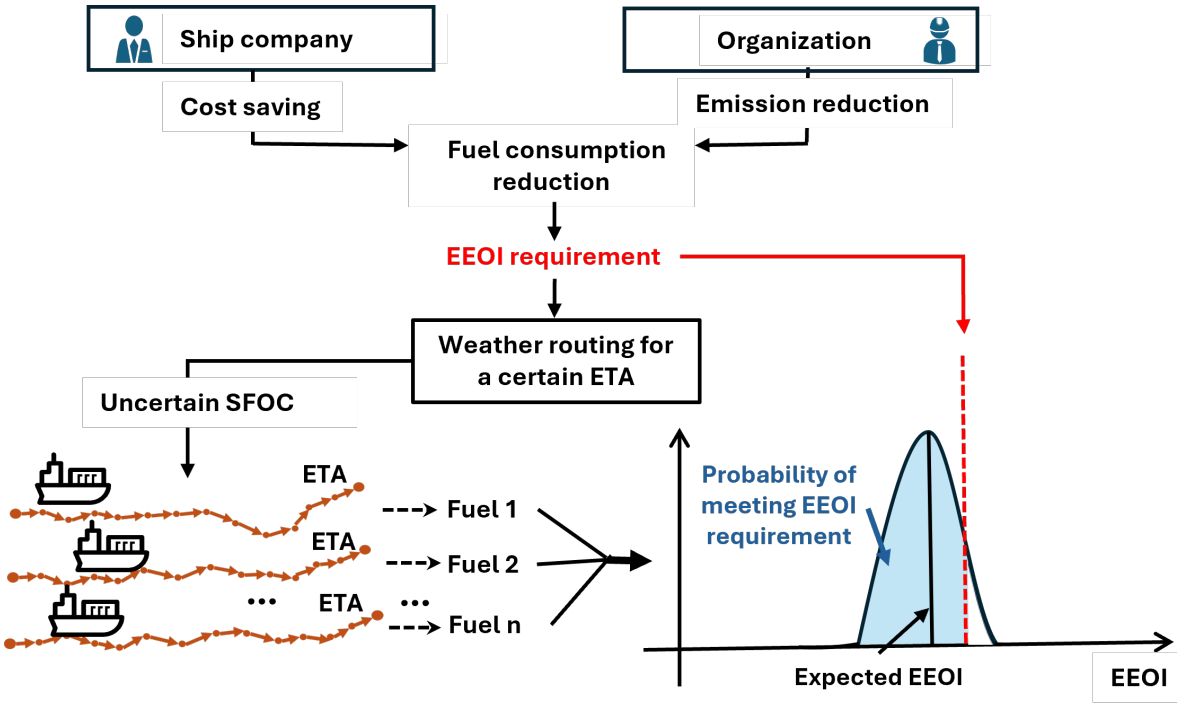

Figure 4.6: The impact of SFOC induced uncertain fuel consumptions on weather routing.

This approach enables not only the optimization for fuel consumption, but also the assessment of the reliability of the potential voyage in actual operations as illustrated in Figure 4.6. Reducing fuel consumption and emissions has always been crucial goals of IMO, which introduced the Energy Efficiency Operational Indicator (EEOI) to regulate the energy efficiency of ships during their operational phase. The formula for calculating EEOI is:

$$EEOI = \frac{F_c \times C_f}{m_{cargo} \times D} \tag{4.16}$$

where F_c is the fuel consumption of the voyage, C_f is the carbon dioxide (CO_2) emission factor for the type of fuel used during voyage, m_{cargo} is the cargo weight transported during voyage,

and D is the distance traveled during voyage. EEOI measures the CO_2 emissions per ton of cargo transported over one nautical mile. As illustrated in Figure 4.6, incorporating the uncertainty of fuel consumption further introduces uncertainty about whether the targets for EEOI set by shipping companies or maritime authorities can be met. The lower the EEOI the better, as it indicates that the ship is using energy more efficiently during transportation, which results in less CO_2 and smaller environmental impact.

Monte Carlo simulation

The Monte Carlo method uses random sampling to estimate the probabilities of different outcomes, or to approximate numerical solutions of complex problems. Due to computational speed, or when faced with uncertainties that are difficult to describe clearly, deterministic methods can sometimes be limited. The Monte Carlo method, relying on randomness to evaluate solutions for nonlinear and uncertain problems, becomes very effective. This thesis employs Monte Carlo simulation to incorporate the uncertainty of SFOC, systematically analyzing the uncertainty of weather routing results.

5 Method of collision avoidance for ship safety

Based on the above research outcome in weather routing, the Isochrone algorithm is further improved to address the collision avoidance (CA) problems, leveraging its computational efficiency and ETA considerations. In the following, an overview of CA problems is first presented. Then, the proposed Isochrone method to address CA problems to assist intelligent ship operations in coastal and inland waterways is briefly described.

5.1 Overview of the collision avoidance problem

Figure 5.1 illustrates the structure of a typical ship collision avoidance problem. This CA problem is treated as a voyage optimization problem in this thesis. The optimization algorithm to address CA problems will consider constraints such as avoiding riverbanks, shallow waters, obstacles, and compliance with traffic regulations. By satisfying these constraints, a collision-free voyage can further be optimized for factors such as safety, estimated time of arrival (ETA), or energy consumption, etc.

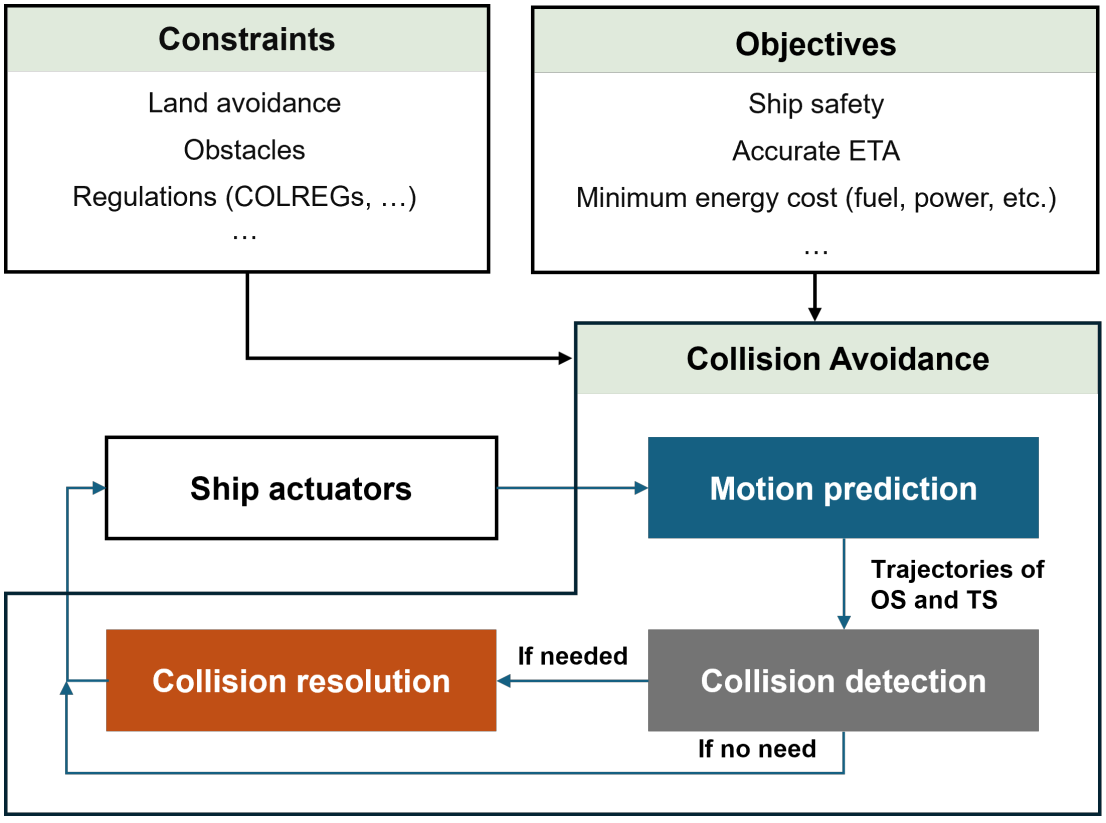

Figure 5.1: Framework for a typical collision avoidance problem.

CA problems mainly involve three steps: motion prediction, collision detection, and collision resolution (Huang et al., 2020). Figure 5.2 further illustrates these steps in detail. Assume the own ship (OS) is currently at $\boldsymbol{P}_0$, aiming to reach the target $\boldsymbol{P}_f$. In the first step, based on observational data, the **motion prediction** module predicts trajectories of all moving objects within

a specified future period. This includes the trajectory of the OS (e.g., the gray dashed line including the coordinates of $\boldsymbol{P}_I$ as depicted in Figure 5.2 (a)) and the trajectories of other target ships (TSs) (e.g., orange dashed lines as depicted in Figure 5.2 (a)). Details of motion prediction will be introduced later. Using the predicted trajectories of the OS and TSs, the **collision detection** module decides whether a collision is likely to occur or if any evasive action is needed by the OS. If a potential collision or need for avoidance is identified, the **collision resolution** module responds by calculating and generating collision-free trajectories (gray dashed lines as illustrated in Figure 5.2 (b)), and determine the optimal collision-free trajectory for the OS to follow. This updated trajectory is then provided to the ship's actuators for operation.

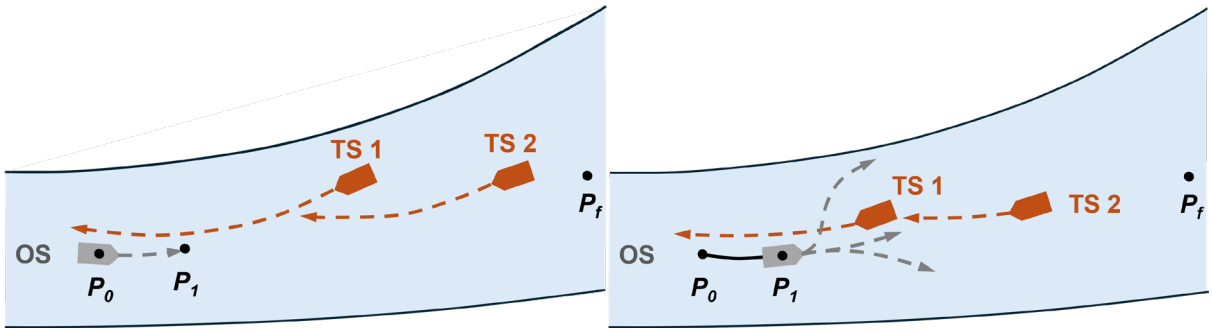

(a) (b)

Figure 5.2: Graphical illustration of collision avoidance processes.

5.2 Isochrone-based real-time CA in confined waterways

Based on the framework presented in the Figure 5.1, this thesis proposes an Isochrone-based real-time optimization algorithm addressing CA problems in both open water and confined waterways. The method comprises three steps: motion prediction, collision detection, and collision resolution, following the structure presented in Figure 5.1. Each of these three steps will be illustrated in detail below, with the core innovation residing in the stage of collision resolution.

Motion prediction

- **Own ships (OS)**

The trajectory prediction of the OS (gray dashed lines in Figure 5.2) requires a ship dynamics model. This model predicts the ship's future motion under specific control commands and environmental disturbances from wind and currents. A linear maneuvering model is used in this thesis, which is a classical model describing the basic maneuverability of a ship under hydrodynamic forces proposed by Clarke et al. (1983):

$$(M_{RB} + M_A)\,\dot{v}_r + (C^*_{RB} + C^*_A)\,v_r = \tau + \tau_{wind} \tag{5.1}$$

where v_r represents the relative velocity of the ship with respect to the current. M_{RB} and M_A denote the rigid-body and added mass matrix respectively, while C_{RB}^* and C_A^* represent the Coriolis and centripetal matrices for the rigid-body and added mass. τ denotes the thrust, and τ_{wind} represents the wind force. The ship model is based on the Python toolbox developed by Fossen, which accounts for the dynamic behaviors of the propulsion and steering systems. However, as listed in limitations in Chapter 1.3, it does not include bank and shallow water effects.

- **Target ships (TSs)**

The trajectory prediction of target ships (TSs) (orange dashed lines in Figure 5.2) are treated as moving obstacles whose characteristics are unknown to the OS. In this thesis, it is assumed that the motion of the target ships is known to the OS through communication and interaction.

Collision detection

Collision detection determines whether a collision is likely to occur and when evasive measures need to be taken, based on the predicted motions of OS and TSs. In this thesis, the ship's arena and domain are adopted to detect collisions. The ship domain defines the minimal safety zone around the ship, indicating that any obstacle entering this area is considered to pose a certain probability of collision accident (Hörteborn et al., 2019). The ship arena is an extended version of the ship domain, representing an area where any violation would necessitate collision avoidance actions (Davis et al., 1980).

In this thesis, the ship domain is constructed based on the definition of Coldwell (1983) and simplified into a static ellipse, as shown by the orange ellipse in Figure 5.3. *L* and *B* represent the length and width of the OS. For the ship arena, it is dynamically defined based on DCPA (Distance to Closest Point of Approach) and TCPA (Time to Closest Point of Approach) as given in Eq. (5.2).

$$0 < \text{DCPA} < 6L,\ 0 < \text{TCPA} < 120\text{s} \tag{5.2}$$

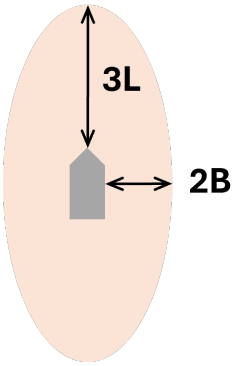

Figure 5.3: Definitions of ship domain in the simulations of CA in this thesis.

Collision resolution

In this thesis, the contribution of the proposed optimization algorithm for CA focuses on the collision resolution strategy, with its problem formulation given in Table 5.1, and the general workflow is given in Figure 5.4.

Table 5.1: The input, optimization formulation, and output of the proposed optimization algorithm to address CA problem.

Input		
Departure	$\boldsymbol{P}_0 = \{x_0, y_0, t_0\}$	
Destination	$\boldsymbol{P}_f = \{x_f, y_f, t_f\}$	
Parameters	Δt	Time interval in each isochrone [s]
	$2r$	Number of sub-sectors [-]
	$\Delta\theta$	Increments in heading [°]
	$2m+1$	Number of candidates generated for one waypoint [-]
	Thrust power	Constant thrust in each time interval [N]
Optimization formulation		
Variables	Ship heading θ	
Objectives	Lowest probability of collision accidents, accurate ETA, and shortest travelling distance	
Constraints	Shallow water, static obstacles, COLREGs rules	
Cost functions	Collision probability OR travelling distance OR deviations from reference route (depending on sailing situations)	
Output		
Optimal voyage	$\theta^* = \{\theta_0, \theta_1, \ldots, \theta_2, \theta_f\}$ which gives $\boldsymbol{R}^* = \{\boldsymbol{P}_0, \boldsymbol{P}_1^*, \boldsymbol{P}_2^*, \ldots, \boldsymbol{P}_i^*, \ldots, \boldsymbol{P}_f\}$	

1) Determine the time interval (Δt) and the constant ship propulsion power for each interval.
2) If the stopping condition is met (e.g., reaching $\boldsymbol{P}_f$ within the time less than Δt), connect to $\boldsymbol{P}_f$ and terminate the process; otherwise, proceed to the next step.
3) For each waypoint in the current (i^{th}) isochrone $\{\boldsymbol{P}_i\}$, generate new waypoints for the next isochrone $\{\boldsymbol{P}_{i+1}\}$, which stay the same as in Figure 3.4.
4) Check whether the generated candidate waypoints satisfy the constraints, including avoidances of static obstacles, and COLREGs compliance in the presence of any TS, as shown in Figure 5.6.
5) Divide the waterway into *2r* parallel subsectors as shown in Figure 5.5. Retain one optimal candidate waypoint in each subsector.
6) The retained candidate points form the next isochrone $\{\boldsymbol{P}_{i+1}\}$. Repeat from Step 2).

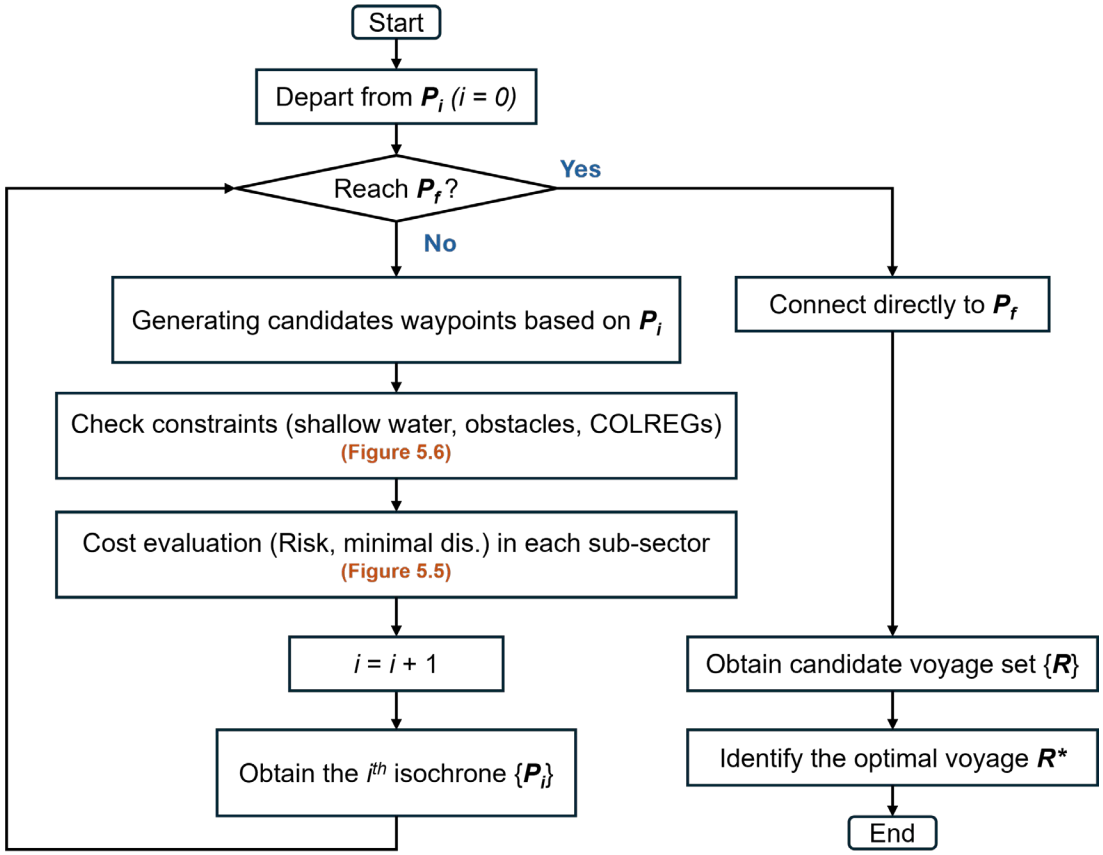

Figure 5.4: Flowchart for the collision resolution process in the proposed method.

- **Parallel sub-sectors**

The grid partition by parallel subsectors is illustrated in Figure 5.5. It is important to note that black lines along the outermost exclude areas containing shallow water, not the riverbanks. The division of parallel subsectors is based on the width of this operating area, with the river evenly partitioned into $2r$ intervals along its width.

In each subsector, the optimal waypoint is selected based on the criteria listed in Table 5.2. This thesis assumes that, in the absence of any obstacles, OS will sail along the centerline of the river, which serves as the OS's reference route (shown as the green dashed line in Figure 5.5).

Table 5.2: Waypoint evaluation criteria in subsectors to achieve the optimization objective

Scenarios	Open area	Confined waterway
No encountering	Shortest distance to P_f	Least deviation to the reference route
Encountering	Lowest probability of collision accident	Lowest probability of collision accident

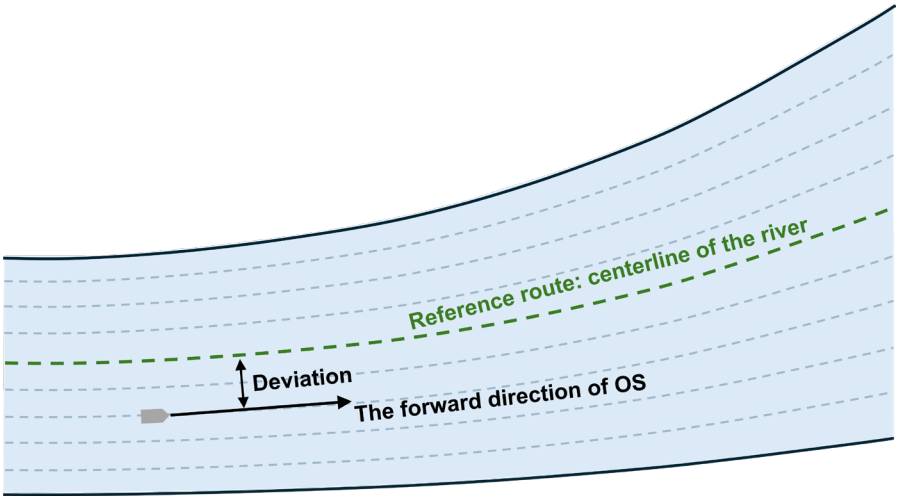

Figure 5.5: Illustration of parallel sub-sectors based on topography of confined waterways.

For sailing in open areas, the parallel subsectors are replaced with open subsectors as proposed in Figure 3.7 in previous studies in Chapter 3.3. When avoiding collisions, the waypoint with the lowest probability of collision accident is chosen. To evaluate the collision probability, a Collision Risk Index (CRI) is calculated using DCPA and TCPA, following the method outlined in (Hu et al., 2020).

- **COLREGs compliance**

This thesis follows the work of Johansen et al. (2016) for COLREGs compliance. Figure 5.6 illustrates an example of waypoint generation for a head-on situation in compliance with COLREGs. Waypoints that fail to satisfy the COLREGs rules for head-on encounters are removed, which are shown in transparency in Figure 5.6.

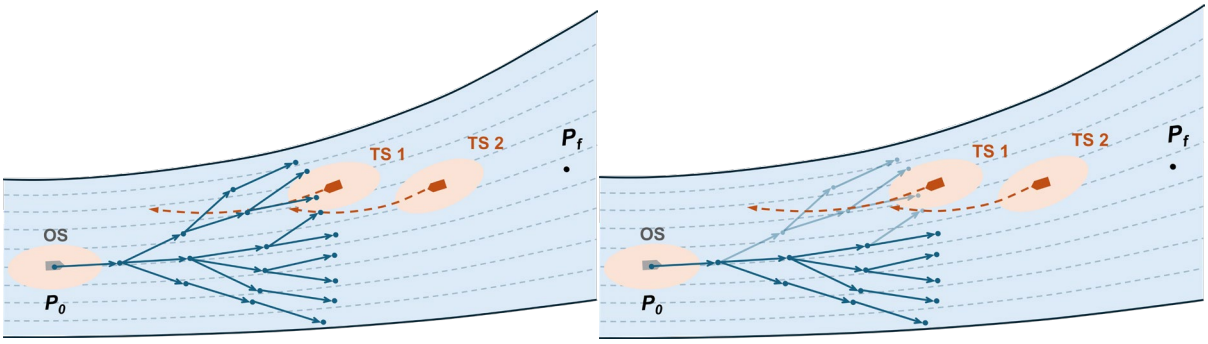

(a) (b)

Figure 5.6: Graphical illustration of COLREGs compliance for the head-on encountering.

6 Summary of appended papers

This chapter summarizes the major findings and results from the studies of the appended papers. In addition, case studies are conducted to investigate the effectiveness of methods in Papers II, III, and V, using a chemical tanker with full-scale measurements operating in the North Atlantic. The ship was guided by a conventional weather routing system and the ship crews onboard, with its specifications detailed in Table 6.1. Its actual routes were planned and chosen based on the crew's experience, and the actual ship had certain weather routing capabilities.

Table 6.1: Principal particulars of the chemical tanker ship.

Length	178.4 m	Design draft	10.98 m
Length	174.8 m	Block coefficient	0.8005
Beam	32.2 m	Deadweight	50752 t
Depth	17.0 m		

These studies include six voyages in 2015 and 2016 of the ship as shown in Figure 6.1. These voyages include eastbound and westbound trips throughout winter and summer, covering a wide range of environmental conditions with Beaufort Scale ratings from 0 to 10. The scale extends up to 12, indicating exceptionally strong hurricane-force conditions (National Weather Service Portland). Additionally, weather data, including wind, waves, and currents, are necessary to describe sailing environments and estimate ship performance. Historical meteorological and oceanographic data from 2015 and 2016 were retrieved in 2023 from the ECMWF ERA-5 dataset for wind (speed and direction) and wave (height, direction, and period), and from the Copernicus 2023 server (http://marine.copernicus.eu/) for current.

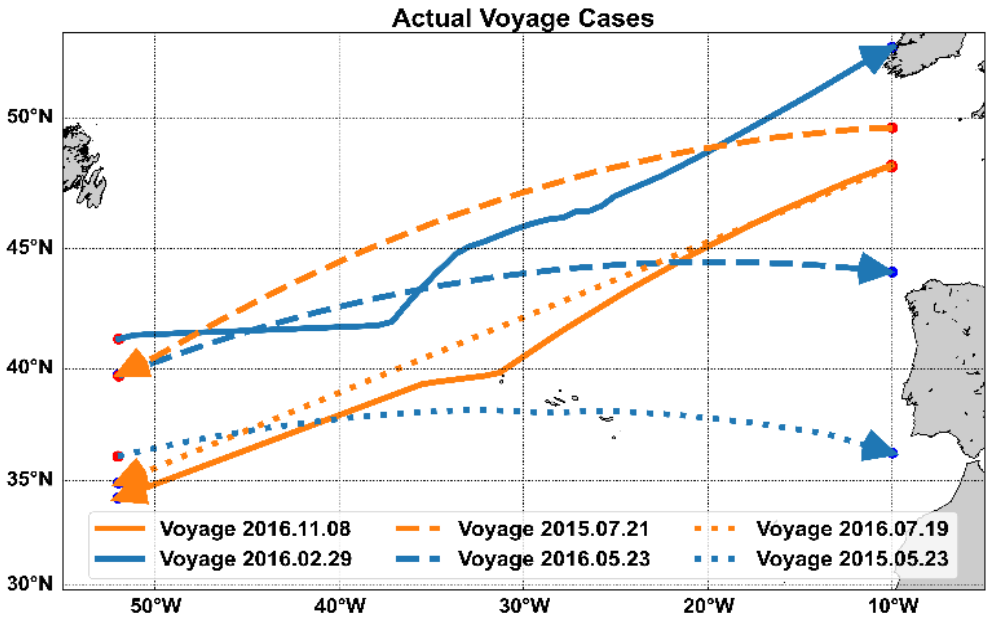

Figure 6.1: Actual case study voyages used in the thesis for validations.

6.1 Summary of Paper I

State-of-the-art optimization algorithms in weather routing — ship decision support systems: challenge, taxonomy, and review.

This paper summarized in Chapter 2.1 provides a systematic review and highlights recent research trends of optimization algorithms applied in weather routing, including the influence of AI and ML technologies since 2020.

Motivations and objectives

Noticeable inconsistencies and confusions are in the literature regarding the use of common terminologies within the weather routing research community, which has led to misunderstandings about weather routing and, possibly, resulted in incorrect solutions. In addition, to the author's knowledge, no existing review has comprehensively summarized the evolution of weather routing optimization algorithms over the years. This paper aims to help researchers and practitioners gain a clear understanding of weather routing, identify the correct problem-solving approaches, and avoid misunderstandings to facilitate the efficient development of weather routing services. Furthermore, it aims to identify gaps in current research and opportunities for future development of optimization algorithms by presenting a comprehensive review of the scientific literature published in recent years on this topic and discussing future directions for the development of weather routing algorithms.

Results and conclusion remarks

Several commonly confused subtopics are briefly summarized in Chapter 2. In this part, the main types of optimization algorithms used in related literature are first summarized. Subsequently, some research results on optimization algorithms are shown in Table 6.2, followed by a summary of the discussions for future research directions.

Table 6.2: Average quantitative optimization results reported from literature compared with real voyage cases.

Metrics	Average results with references from full-scale measurement
Fuel savings	1%-10% (Chen & Mao, 2024), 9.4% (Du et al., 2022b), 9% (Lee et al., 2018)
Time savings	1.65% (Shin et al., 2020), 5% (Du et al., 2022a)
Economics profit	2.55% (Du et al., 2023), 1.5% (Ma et al., 2024), 7.9% (Bahrami & Siadatmousavi, 2024)
Emission reductions	19% (Du et al., 2022a), 6.4% (Du et al., 2022b), 2% -12.5% (Wang et al., 2021)
Fatigue	50% - 90% (Lang et al., 2021), 50% (Wang et al., 2019)

The literature review reveals that four main types of algorithms are mostly studied in weather routing: the Isochrone algorithms, DP-based algorithms, PSOs/ACOs, and EAs/GAs. Some

examples of optimization results from the literature are presented in Table 6.2. When illustrating the effectiveness of their proposed approaches, many studies evaluated their proposed algorithms against established methods, with some also incorporating comparisons using real sailing data. The benchmarks used for comparison vary across studies,complicating the assessment of these algorithms' performance. Additionally, the optimization results reported vary significantly across studies as detailed in Table 6.2.

The potential research directions in the future can be summarized as follows.

1) Algorithm performance improvement, which includes developing enhanced heuristic and learning-based methods.
2) Applicability in real-world operations, such as handling uncertainty, and supporting clean fuel-powered ships.
3) Benchmark studies, which may provide valuable insights for the application of weather routing.

6.2 Summary of Paper II

Strategies to improve the Isochrone algorithm for ship voyage optimization.

This paper investigates the improvement of the Isochrone method (Hagiwara, 1989) by proposing five strategies. Subsequently, this paper compares these strategies to identify the most effective ones. The findings serve as an intermediate step that contributes to proposing the IPO method in Paper III, which is summarized in Chapter 3.3.

Motivations and objectives

Real-time algorithms are valuable in weather routing as they can effectively handle uncertainties. The Isochrone algorithm is commonly used in weather routing applications because of its high computational efficiency and ETA considerations. However, it also has significant drawbacks, including impractical routes and results from local optimization that may not save fuel. Thus, this paper aims to propose an optimization algorithm based on the Isochrone method that can effectively minimize fuel consumption in real-time, while considering ETA and optimizing energy efficiency. More specifically, this paper aims to explore effective strategies to leverage the advantages of the Isochrone algorithm while addressing its shortcomings.

Summary of five strategies proposed in Paper II

The proposed five strategies are presented in Figure 6.2, each with a focus on improving the optimization process in the second half of the voyage search. Each strategy is introduced respectively in the following context.

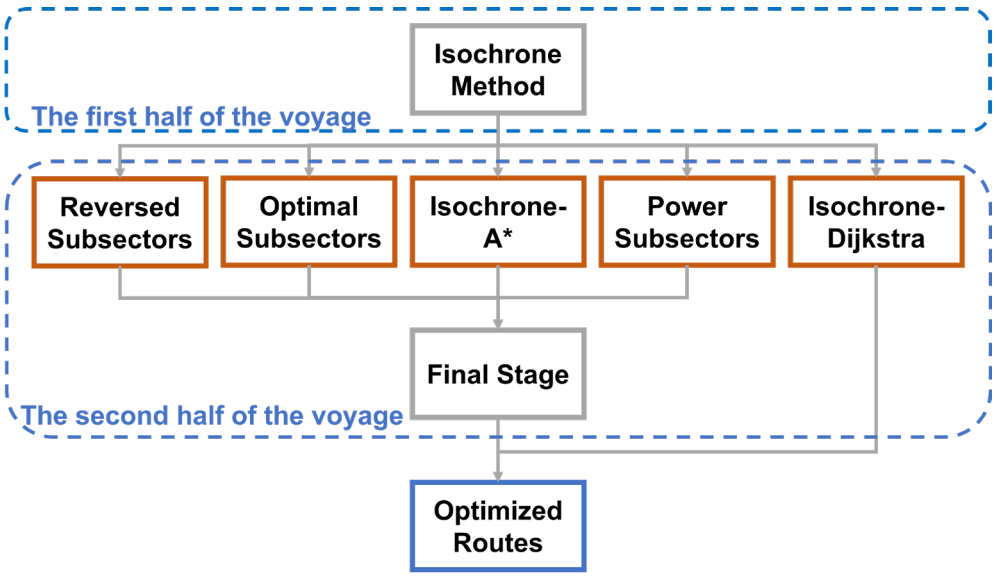

Figure 6.2: Five improvement strategies of the Isochrone method proposed in Paper II.

- **Reversed subsectors**

The "Reversed subsectors" strategy focuses on solving the route convergence problem, by proposing the reversed subsectors defined in Eq. (3.9). The overall procedure of this improved method follows the steps of the Isochrone method (Hagiwara, 1989) which is illustrated in Figure 3.4. The change is that when reaching the second half of the voyage, the subsector defined in Eq. (3.9) will be used.

- **Optimal subsectors**

The reversed subsectors given above, however, may cause the subsectors to become very narrow at a late stage, and locally optimal routes would be chosen because of these compact subsectors. The following method to define optimal subsections is proposed to solve the above problem:

1) In the latter half of the voyage, generate the waypoint grid following the "Reversed subsectors" strategy. The optimal waypoint in each subsector is chosen as the closest one to the destination.
2) Define the number of waypoints that can be chosen in each subsector, instead of only one in "Reversed subsectors" strategy. Restrict the number of successors that can be reserved for one predecessor to prevent dominance. These values are set to three and five in this thesis, respectively.

- **Isochrone-A***

Another approach to resolving the local optimization is to explore more comprehensive criteria to select optimal waypoints in subsectors, i.e., changing cost functions. This "Isochrone-A*"

strategy proposes the cost function defined in Eq. (3.11) to be used in the second half of the voyage search. The other steps are the same as given in the strategy of "Reversed subsectors".

- **Power subsectors**

An alternative method is also proposed to resolve the local optimization, referred to as "Power subsectors". This method removes the subsectors but selects the optimal point among the successors for each waypoint. The procedure is as follows:

1) In the first half of the voyage, conduct the same procedures as in "Reverse subsectors".
2) In the latter half, every waypoint proceeds toward $\boldsymbol{P}_f$ following the heading $C_{ni} \pm j \cdot \Delta\theta$ ($j = 0, 1, \ldots, m$). Then, among $2m+1$ successors, keep the point with the lowest fuel cost, and append it as the optimal one. Continue toward $\boldsymbol{P}_f$.

- **Isochrone-Dijkstra**

In the Isochrone algorithm, waypoints are generated following a tree structure. Removing one waypoint may lead to removing a route and causing local optimization. To address this issue, this approach combines Dijkstra's algorithm in the second half of the voyage to cover a sufficient search range during the search. Based on this static grid illustrated in Figure 6.3, the Dijkstra algorithm can enumerate the lowest cost route by evaluating every possible solution. This approach is as follows.

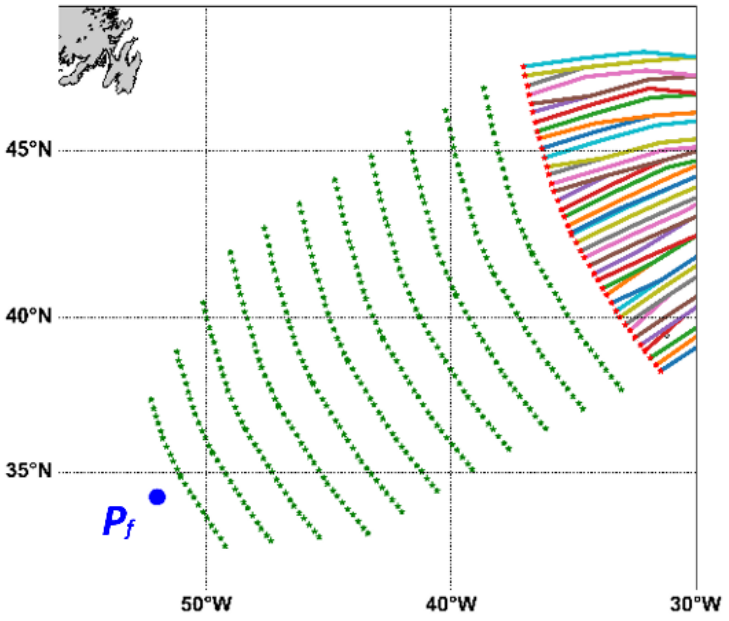

Figure 6.3: Static grid initialized at the latter half voyage for the Dijkstra algorithm.

1) In the first half of the voyage, apply the same procedures as with "Reverse subsectors".
2) In the second half, generate a static grid as shown in Figure 6.3. The waypoints in subsequent stages are obtained by translating the latest isochrone following the direction of the GC_{ref} toward $\boldsymbol{P}_f$.

3) Assign a cost for all sub-routes based on the estimated fuel cost. Apply the Dijkstra algorithm to find the lowest cost route, starting from each waypoint in the latest isochrone to $\boldsymbol{P}_f$ respectively.
4) This yields several potential sailing routes. These candidate half-routes possess different ETAs as the distance varies in sub-routes, and the sailing speed is constant. Choose the optimal route as the one with the closest ETA to the required arrival time.

Results and conclusion remarks

The effectiveness of these five strategies is compared using the case study chemical tanker and its measurement data. The results of two case study voyages, Voyages 2016.11.08 (winter) and 2015.07.21 (summer), are summarized. The optimization results of fuel consumption, sailing time (ETA), and sailing distance are listed in Table 6.3, with the highlighted cells showing the most fuel reductions.

Table 6.3: Results from the improved Isochrone algorithms for the two case study voyages.

Optimization Methods	Voyage 2016.11.08				Voyage 2015.07.21			
	ETA [h]	Fuel [ton]	Dis. [km]	Average Speed [knot]	ETA [h]	Fuel [ton]	Dis. [km]	Average Speed [knot]
Actual Route	164.3	159.7	3877.5	12.8	139.8	177.7	3453.6	13.4
Isochrone method	167.8	162.0	3896.1	12.5	142.4	170.8	3533.5	13.4
Reversed subsectors	164.8	163.2	3807.2	12.5	139.8	168.5	3474.3	13.4
Optimal subsectors	164.4	162.9	3798.5	12.5	139.8	168.5	3474.3	13.4
Power subsectors	165.4	156.1	3840.7	12.5	139.9	168.3	3482.3	13.4
Isochrone-A*	165.1	155.6	3836.1	12.5	140.0	167.5	3487.1	13.5
Isochrone-Dijkstra	165.1	155.7	3834.3	12.5	140.0	168.7	3478.0	13.4

For Voyage 2015.07.21, all improved Isochrone methods successfully reduced fuel consumption compared to the actual route, achieving savings between 3.9% and 5.7%. In contrast, for Voyage 2016.11.08, certain modified Isochrone methods performed better, notably the "Isochrone-A*", "Power subsectors", and "Isochrone-Dijkstra" methods. Specifically, "Isochrone-A*" demonstrated the best performance with 2.6% energy improvement. From these two westbound cases, the "Isochrone-A*" method provided the most energy-efficient route for voyage optimization. The Isochrone method, however, did not perform well, resulting in the highest fuel consumption, longer sailing distances, and sharp turns near the destination in both cases, as shown in Figure 6.4. Additionally, the "Optimal subsectors" method behaved similarly to the "Reversed subsectors" method, with nearly identical routes and comparable fuel expenses in both cases.

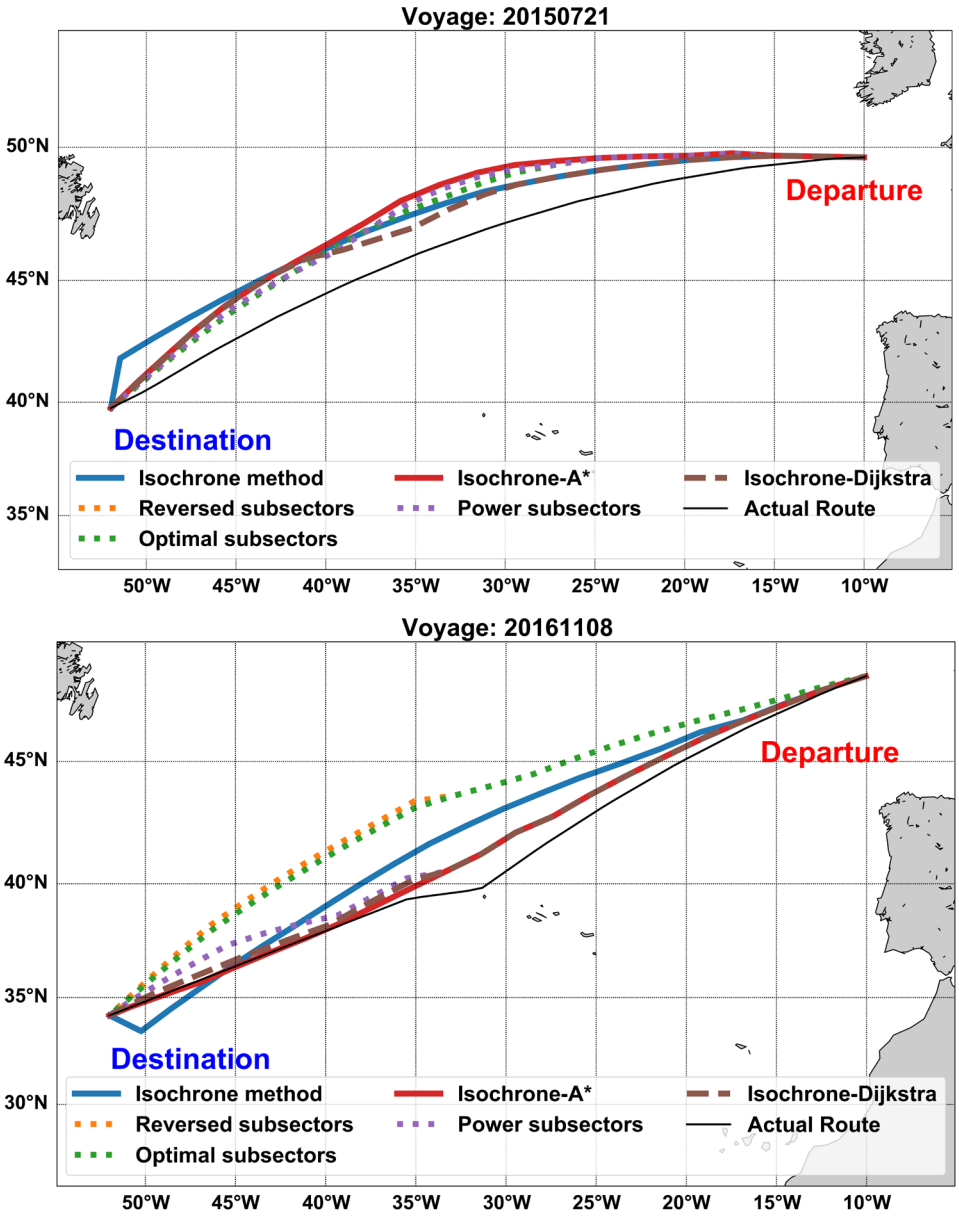

Figure 6.4: Optimization for Voyage 2015.07.21 (above) and 2016.11.08 (below) using different methods.

6.3 Summary of Paper III

An Isochrone-based predictive optimization for efficient ship voyage planning and execution.

Based on the strategies in Paper II, this paper further proposes the IPO algorithm as previously introduced in Chapter 3.3.

Motivations and objectives

Paper II demonstrated that the strategies "Reversed Subsectors" and "Isochrone-A*" effectively improve the Isochrone method, highlighting the importance of heuristics in enhancing

optimization performance. Based on this finding, to facilitate timely and energy-efficient weather routing, this paper aims to propose an Isochrone-based algorithm that can effectively minimize fuel consumption in real-time while considering ETA. Furthermore, this paper seeks to achieve predictive optimization by utilizing ML-enhanced heuristics to improve the Isochrone algorithm. Additionally, it aims to maintain computational efficiency, enabling real-time executions to handle potential uncertainties in operations.

Results and conclusion remarks

The IPO method is proposed in this paper, featuring ML-enhanced heuristics to achieve predictive optimizations. The efficiency and effectiveness of the proposed IPO method are compared using six actual voyages in Figure 6.1, and four weather routing methods detailed in Table 6.4.

Great Circle (GC) routing is a traditional manual voyage planning method used in industrial practice. It follows the shortest GC route as a fixed path and divides the route into several stages based on the ETA. The speed of the sub-routes can be adjusted according to local sea conditions to ensure punctuality. It serves as a baseline to verify the practicality of the proposed method for real operations. The proposed IPO method is derived from MI (modified Isochrone), allowing for a comparison to demonstrate the IPO's improvements. The 2D Dijkstra algorithm (2DDA) is a widely used method known for its optimization capability and generalization, and the 3D Dijkstra algorithm (3DDA) is an enhanced version of 2DDA that includes speed optimization. They can provide a standard for comparison outside of Isochrone types.

Table 6.4: Four voyage optimization methods used in the comparison.

Method	Description	Reference
GC	Traditional GC routing	-
MI	Modified Isochrone method	(Hagiwara, 1989)
2DDA	Conventional 2D Dijkstra algorithm	(Dijkstra, 1959)
3DDA	3D Dijkstra algorithm	(Wang et al., 2019)

- **Highlighted results from three case study voyages**

In the North Atlantic, storms driven by the prevailing westerly generally move from west to east, resulting in ships facing more head-on waves on westbound voyages. This makes westbound sailings more challenging and fuel-intensive, necessitating careful planning to improve efficiency and safety. This paper investigates three westbound voyage cases: one in winter and two in summer. The optimization results are summarized in Table 6.5, with ETA, fuel consumption, sailing distance, average speed, and runtime for each voyage. The actual voyage is highlighted in gray, and the proposed method's result is highlighted in green. The optimized routes generated by each method are illustrated in Figure 6.5.

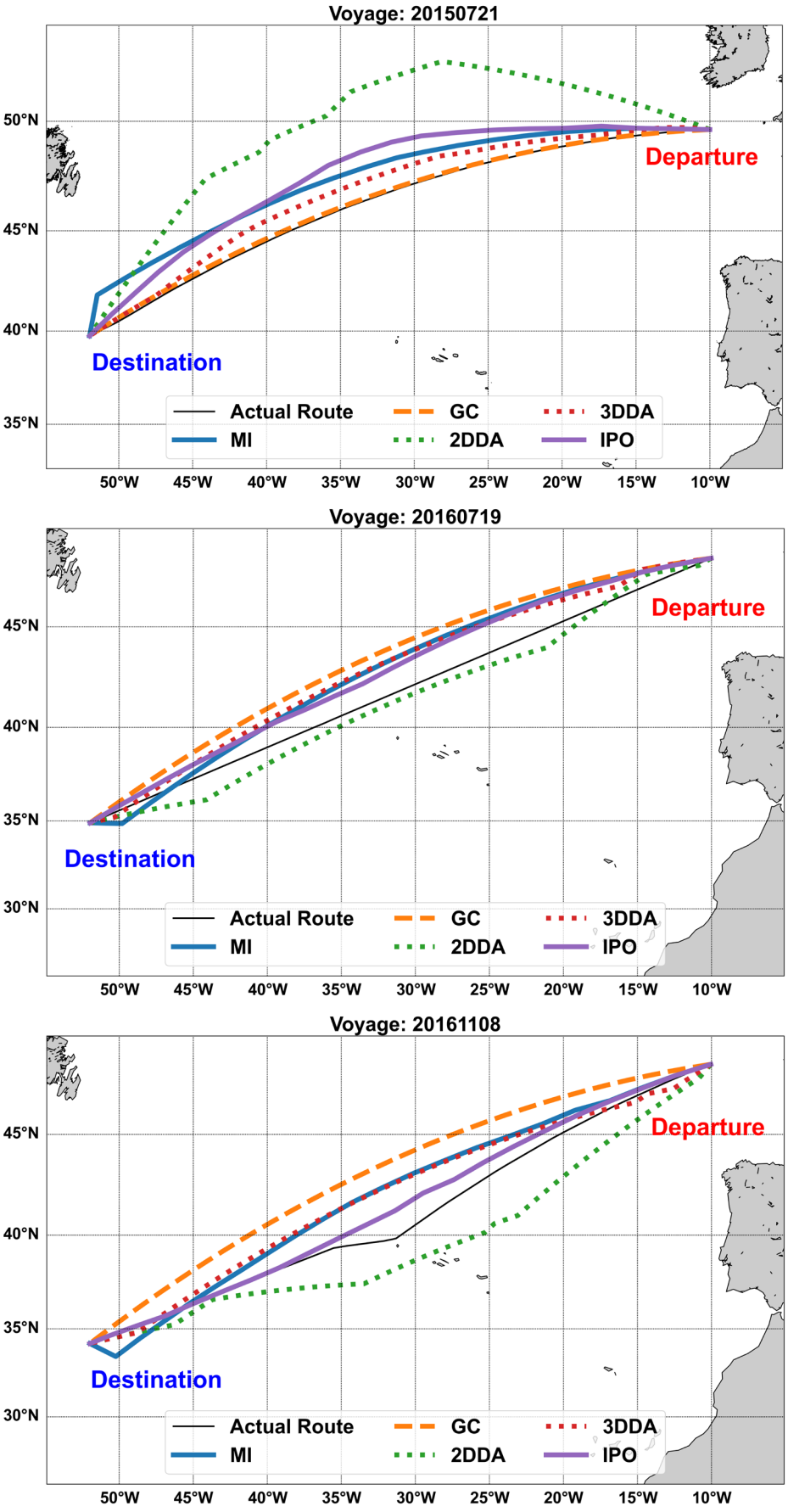

Figure 6.5: Optimized voyages for three westbound cases.

Table 6.5: Optimization results of the three case study voyages.

Voyage	Category	ETA [h]	Fuel [ton]	Dis. [km]	Ave. Speed [knots/h]	Runtime [s]
2015.07.21	Actual route	139.8	180.6	3453.6	13.3	-
	GC	138.7	180.8	3452.4	13.4	5
	MI	142.4	170.7	3533.5	13.4	25
	2DDA	146.5	161.6	3660.9	13.5	80
	3DDA	142.0	165.9	3462.1	13.2	3432
	IPO	140.0	167.5	3487.1	13.5	40
2016.07.19	Actual route	168.8	141.4	3780.3	12.1	-
	GC	168.5	139.7	3741.8	12.0	4
	MI	168.8	139.5	3783.1	12.1	28
	2DDA	173.4	136.3	3852.4	12.0	76
	3DDA	168.5	137.2	3765.8	12.1	4189
	IPO	168.8	137.4	3749.8	12.0	45
2016.11.08	Actual route	164.3	160.2	3877.5	12.7	-
	GC	163.8	164.1	3789.3	12.5	5
	MI	167.8	162.0	3896.1	12.5	30
	2DDA	172.5	154.2	4024.3	12.6	100
	3DDA	164.0	162.4	3838.4	12.6	4921
	IPO	165.1	155.6	3836.1	12.5	48

For Voyage 2015.07.21, 2DDA and 3DDA show the least fuel consumption but with seven- and two-hour arrival delays respectively. Considering punctuality, the IPO method achieves the most significant fuel reduction at 7.3%. For Voyage 2016.07.19, IPO and 3DDA closely result in the largest reductions at 3.0% with accurate ETAs. For Voyage 2016.11.08, IPO and 2DDA provide the most fuel savings at around 3.0%, and 2DDA again fails to meet the ETA.

In summary, across the three voyages, IPO consistently delivers the most energy-efficient routes with on-time arrivals. Although IPO and 3DDA result in similar fuel cost, the IPO method operates roughly 90 times faster than 3DDA and twice as fast as 2DDA in terms of runtime. Although 2DDA can offer considerable fuel savings, it frequently fails to guarantee the ETA and often suggests longer sailing routes. GC routing does not demonstrate significant improvements in energy efficiency compared to the actual routes, and the MI method also does not perform well, showing similar fuel consumption to the actual routes with abrupt turns near the destination in all three cases, as depicted in Figure 6.5.

6.4 Summary of Paper IV

Learning-based Pareto-optimum routing of ships incorporating uncertain met-ocean forecasts.

The exploration of a sophisticated ML algorithm, notably an MOEA (multi-objective evolutionary algorithm), is conducted to tackle the challenges of weather routing. An L-MOEA is presented in this paper, as introduced in Chapter 3.4.

Motivations and objectives

The application of emerging ML methods in weather routing, specifically MOEA, presents powerful optimization capabilities. However, typical MOEAs face challenges with convergence due to their reliance on random evolutionary processes. Additionally, the uncertainty of weather conditions significantly impacts the effectiveness of weather routing. This paper aims to achieve energy-efficient weather routing with the aid of emerging ML-based MOEA, while considering the essential operational uncertainty caused by dynamic weather. Furthermore, this paper aims to address the challenging convergence problem of MOEA, achieving efficient and effective optimization performance.

Results and conclusion remarks

The effectiveness of L-MOEA is compared with several widely concerned algorithms for multi-objective optimization from relevant studies. Firstly, the multi-objective optimization performance of the proposed L-MOEA is evaluated by presenting outcomes of weather routing. Then the uncertainty of the optimization results due to dynamic weather is also examined.

- **Results of weather routing**

Overall, compared to the other algorithms, the proposed L-MOEA achieves an average saving of approximately 2.5% in fuel consumption and a 2.0% reduction in travel time per voyage. An optimized route is depicted in Figure 6.6, accompanied by the met-ocean conditions encountered by the ship, which are illustrated with color-coded segments..

The voyage for comparison, i.e., the original route given in green involves a ship sailing at a fixed engine speed (set at 111 rpm) along the GC route between the port of origin and the destination. It can be observed that the original plan led the ship through an area with waves exceeding six meters, posing a significant potential threat to the ship crew and cargo. However, the optimized plan guides the ship to sail along the edge of the high-wave zone and experience a deceleration, returning to the originally set engine speed. In the end, the optimized voyage further suggests reducing the engine to 109 rpm. From a numerical standpoint, the optimized voyage achieves almost 2% savings in fuel consumption while arriving five hours earlier.

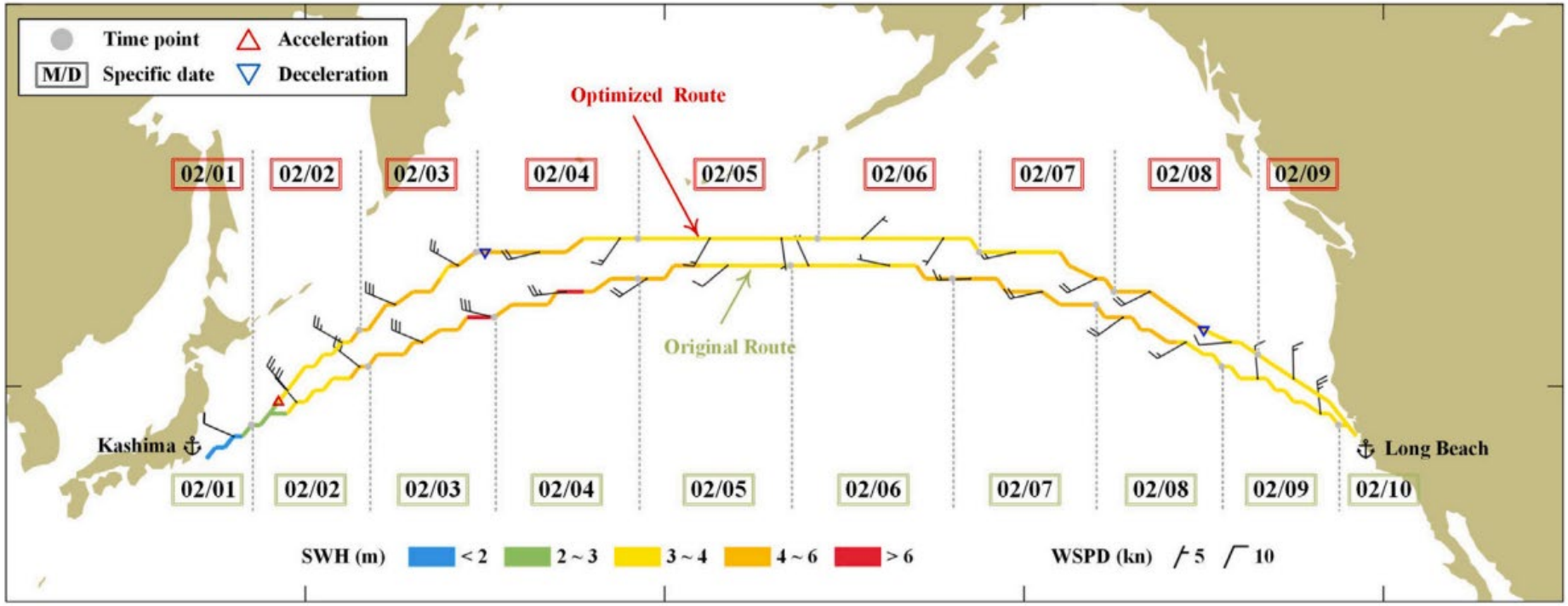

Figure 6.6: An optimization example for a voyage in February, including the route and sailing speed of the case ship, as well as the encountered met-ocean conditions.

- **Results of uncertainty-integrated optimization**

The uncertainty evaluation module is integrated into L-MOEA (abbreviated as L-MOEA-U) and further compared. Three results, i.e., sailing with the shortest duration but highest fuel consumption (DT-Opt), the least fuel consumption but longest duration (FC-Opt), and a balance between fuel consumption and duration (BL-Opt), are selected.

Table 6.6: Optimization results under uncertain met-ocean forecasts from weather routing.

Algorithm	Route	Aggregated objective value							
		FC_{max}	FC_{min}	FC_{mean}	FC_{var}	DT_{max}	DT_{min}	DT_{mean}	DT_{var}
NSGA-II	DT-Opt	1167.24	1153.39	1159.69	12.76 (+23%)	174.91	172.83	173.78	0.29 (+26%)
	BL-Opt	1033.82	1019.96	1025.43	15.10 (+397%)	187.42	185.16	186.06	0.42 (+180%)
	FC-Opt	874.24	868.80	871.55	1.71 (+11%)	220.30	218.94	219.62	0.13 (+86%)
SPEA2	DT-Opt	1188.13	1175.46	1180.72	12.81 (+24%)	180.62	178.58	179.42	0.28 (+22%)
	BL-Opt	913.32	905.70	908.84	6.21 (+100%)	201.18	199.49	200.18	0.26 (+73%)
	FC-Opt	894.44	889.58	891.08	1.81 (+18%)	218.41	216.72	217.24	0.14 (+100%)
KnEA	DT-Opt	1167.04	1153.39	1159.29	12.56 (+21%)	178.17	176.15	177.02	0.28 (+22%)
	BL-Opt	1017.92	1006.80	1010.92	8.58 (+168%)	186.72	184.77	185.51	0.27 (+80%)
	FC-Opt	876.58	871.65	873.90	1.85 (+20%)	219.26	217.03	218.60	0.13 (+86%)
MGA	DT-Opt	1163.22	1149.24	1155.62	12.85 (+24%)	174.31	172.21	173.17	0.29 (+26%)
	BL-Opt	932.08	925.57	928.07	7.74 (+142%)	198.26	196.78	197.35	0.20 (+33%)
	FC-Opt	871.51	866.00	868.61	1.89 (+23%)	218.39	217.03	217.67	0.12 (+71%)
MOEA-LS	DT-Opt	1145.74	1131.99	1138.04	12.56 (+21%)	177.66	175.61	176.51	0.28 (+22%)
	BL-Opt	921.28	914.74	917.52	6.15 (+92%)	202.52	201.01	201.65	0.22 (+47%)
	FC-Opt	892.64	887.54	889.56	2.11 (+37%)	216.62	215.37	216.87	0.13 (+86%)
L-MOEA-U	DT-Opt	1136.59	1124.45	1131.60	**10.38**	170.62	168.80	169.87	**0.23**
	BL-Opt	890.37	883.86	886.70	**3.20**	196.55	195.15	195.76	**0.15**
	FC-Opt	858.39	852.92	855.14	**1.54**	215.28	213.92	214.48	**0.07**

Note that FC and DT denote fuel consumption and duration time, respectively. The subscripts *max*, *min*, *mean*, and *var* represent the corresponding statis-

As shown in Table 6.6, the percentages in parentheses indicate the increases in uncertainties generated by other algorithms compared to L-MOEA-U. The voyages given by L-MOEA-U demonstrate more stable time and fuel savings under uncertain met-ocean conditions. The variances in voyage costs generated by other algorithms are significantly higher, generally exceeding 20% more than those of L-MOEA-U, and in some cases, nearly quadruple. Such unstable voyage plans can significantly affect the supply chain system. Thus, the application of these algorithms with high uncertainty can be severely limited. Taking the BL-Opt route as an example, qualitative results are presented in Figure 6.7. The optimized voyage recommended by L-MOEA-U exhibits a more concentrated distribution in objective functions. In other words, while ensuring optimal convergence of the solution set, it can also recommend more reliable plans to decision-makers.

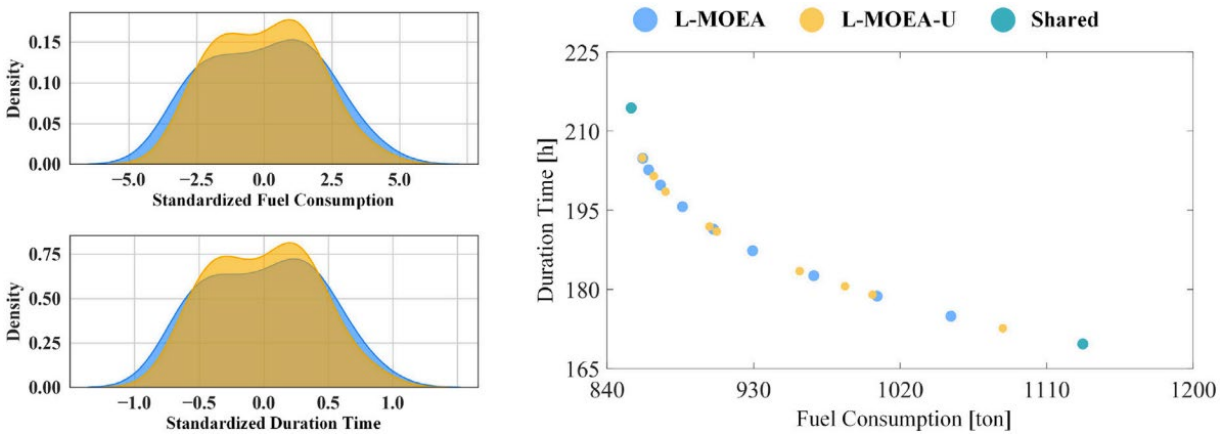

Figure 6.7: Standardized kernel density histograms and PF*.

6.5 Summary of Paper V

A machine learning method to model stochastic Specific Fuel Oil Consumption induced fuel consumption for ship voyage optimization.

Paper V investigates uncertainties of weather routing due to the stochastic fuel consumption model and develops an ML ship performance model to comprehensively consider uncertainties due to SFOC, as presented in Chapter 4.

Motivations and objectives

In weather routing, uncertainty arises not only from weather conditions but also from the estimation of fuel consumption. Today's ship performance models, especially those involving SFOC exhibit significant uncertainties when estimating fuel consumption. These uncertainties may render voyage optimization results in ineffective applications. This paper aims to investigate this uncertainty of ship fuel consumption due to the ship performance model, and its impact on weather routing. Specifically, this paper aims to investigate the uncertainties in fuel consumption caused by stochastic SFOC.

Results and conclusion remarks

This paper aims to quantify the uncertainty in ship fuel consumption and its impact on weather routing, which involves three main steps: 1) developing a GA-BP model for ship speed-power performance prediction; 2) developing a GPR model for stochastic SFOC prediction; 3) integrating the two models to estimate fuel consumption. In addition, the uncertainty in ship fuel consumption and its impact on weather routing is investigated.

- **Speed-power ship performance prediction**

Figure 6.8 and Figure 6.9 presents the comparison between the GA-BP model's prediction, the actual measurements using the test set, and predictions using a semi-empirical approach (Lang & Mao, 2020). The red dashed lines indicate the ideal fit, corresponding to $R^2 = 1$.

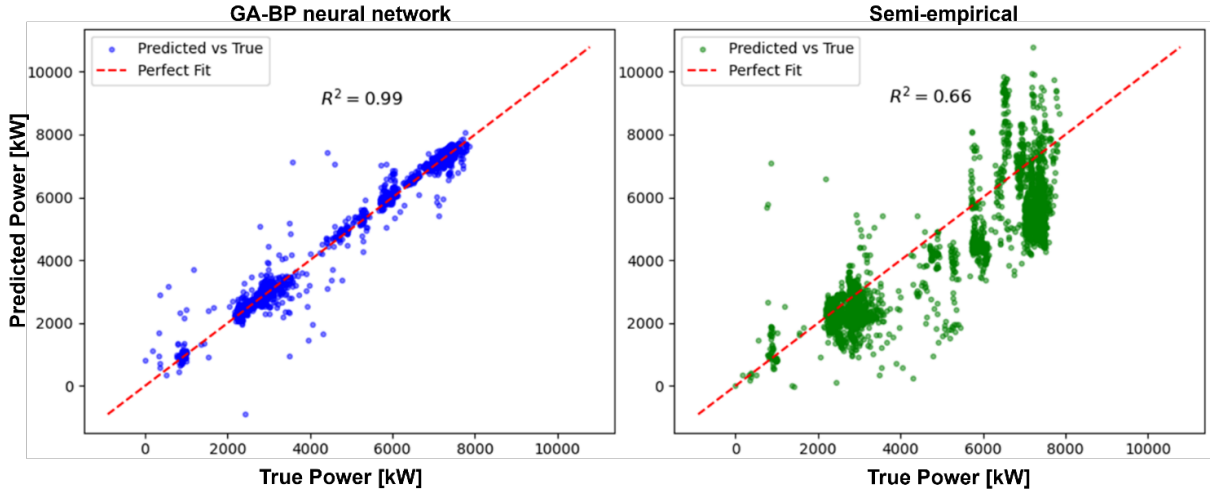

Figure 6.8: Comparison between measurements and predictions for propulsion power using the proposed GA-BP model (left) and the semi-empirical approach (right).

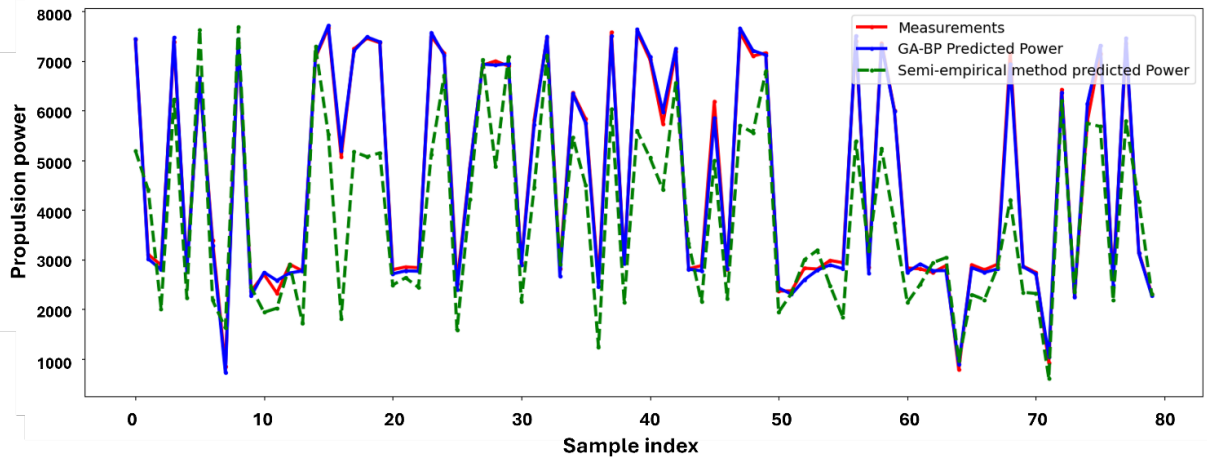

Figure 6.9. Comparison between different methods and true values for 80 samples (2.5% of test set).

The proposed GA-BP model includes some hyperparameters that needed to be first determined, which were obtained using a Bayesian optimization approach (Xuan & Tian, 2021), and those in GA were tuned based on performance. The measurement dataset was split into the training set (70%) and test set (30%), then standardized. Figure 6.8 and Figure 6.9 show that the proposed GA-BP model exhibits excellent prediction performance with $R^2 = 0.99$.

- **Stochastic fuel prediction with SFOC model**

The four-fold cross-validation technique is used to assess the effectiveness of the proposed methods, a common strategy for validating ML methods (Zhang et al., 2023). The dataset was divided into four subsets, with each subset taking turns serving as the validation set while the others are used as the test sets. Evaluating the model with four distinct datasets yields four separate scores, and the final performance metric is calculated as the average of these four validation results. This method effectively prevents overfitting and enhances the model's generalization ability. In this paper, the RMSE of the GPR model is calculated using a four-fold cross-validation framework. As shown in Table 6.7, the results highlight the proposed model's strong predictive power on unseen datasets.

Table 6.7: Validation results using four-fold cross-validation.

Iteration	RMSE
1	2.03
2	3.22
3	2.75
4	3.62
Mean	2.9

- **Uncertainty of fuel consumption in weather routing**

The two proposed models are utilized by the 3DDA to estimate fuel consumption for weather routing. The Monte Carlo experiment is conducted, and the result is presented in this part. Based on an actual route with an ETA of 159 hours, 1000 optimization simulations are conducted starting from its departure to its destination and this ETA. The uncertain SFOC first leads to variations in the waypoints. The probability of distribution of EEOI for the most frequently resulting route is further shown in Figure 6.10, which indicates significant variations. A lower EEOI is preferable, but the average EEOI improved noticeably in simulations that considered the fuel uncertainty. This means that in actual operations, the EEOI can be adversely affected by uncertainties, leading to performance that does not meet the set requirements.

The scenarios with ETAs of 155.25 and 155.5 hours are particularly notable, as shown in Figure 6.11. The expected EEOI is lower for an ETA of 155.5 hours compared to 155.25 hours. This is because to achieve a shorter ETA, ships must travel faster and consume more fuel, which leads to a decrease in EEOI and, thus, less energy efficiency. However, when considering the

likelihood of meeting the EEOI targets, the scenario with the lower expected EEOI (and ETA of 155.5 h) demonstrates a reduced probability of achieving the EEOI standards. This demonstrates the importance of accounting for the uncertainty in fuel consumption during weather routing, to effectively apply the optimization results in practice and meet the energy efficiency goals.

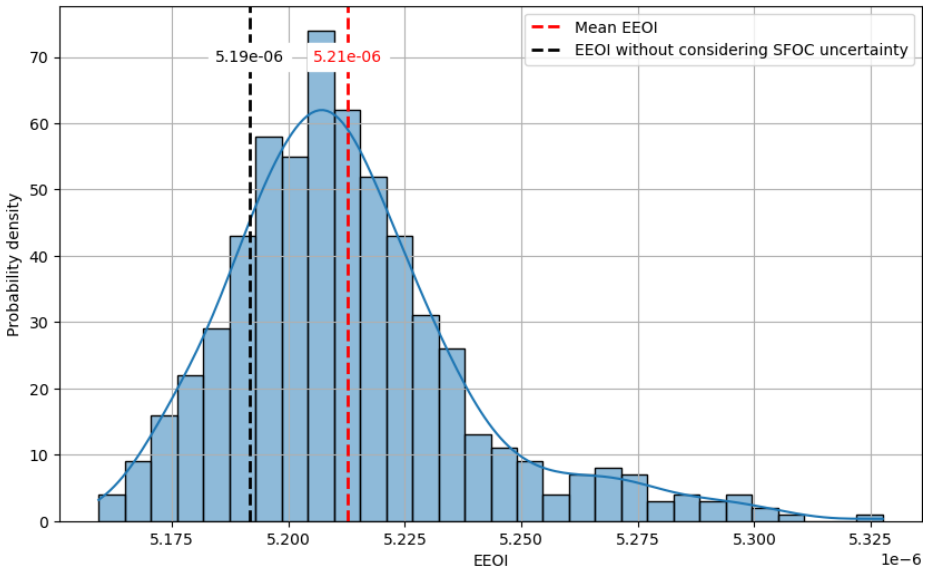

Figure 6.10: Probability distribution of fuel consumption with an ETA of 159 hours.

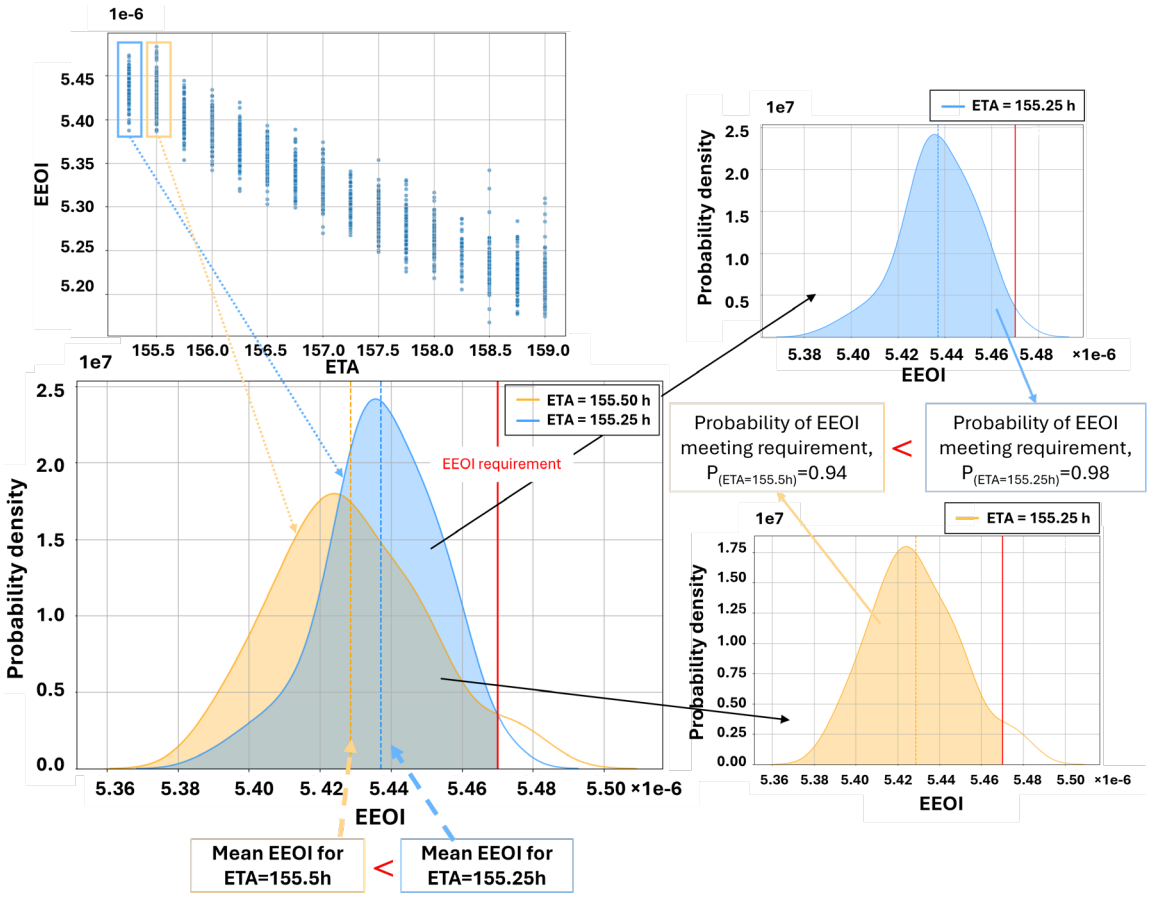

Figure 6.11: Probabilistic analysis of EEOI distribution for ETAs of 155.25 and 155.5 hours.

6.6 Summary of Paper VI

Isochrone-based real-time ship collision avoidance complying with COLREGs in confined waterways.

Paper VI extends the research outcomes of the Isochrone-based real-time optimization algorithm by applying it to the CA problem, as introduced in Chapter 5.

Motivations and objectives

Timely arrivals and accurate ETAs are essential objectives for inland and coastal shipping (Lei et al., 2024), while the CA algorithm is expected to support real-time applications, achieving a balance between real-time performance and optimal outcomes (Zhang et al., 2025; Zhu et al., 2024). These goals motivate this paper to further explore the research of improving the Isochrone method and apply it to the CA problem for both open waters and confined waterways. It seeks to achieve real-time collision avoidance while considering the ETA, assist timely ship operation, and ensure ship safety in traffic. More specifically, this paper aims to enhance the land avoidance capabilities of the Isochrone method to adapt to terrain restrictions and integrate compliance with traffic regulations, such as COLREGs.

Results and conclusion remarks

The proposed method is demonstrated in two scenarios: open water and confined waterways. Demonstration in open water focuses on the effectiveness of the proposed algorithm in complying with COLREGs. Further validation in the confined waterway scenario highlighted the algorithm's CA capabilities in narrow spaces, considering both COLREGs and restrictions, such as land and other inland waterway infrastructures. The OS and TSs are assumed to be 100 meters long and 9 meters wide.

- **Collision avoidance in an open water area**

The proposed method is first demonstrated in open water as shown in Figure 6.12. The area includes static obstacles and three TSs. Static obstacles are simulated as circles with a diameter of 10 meters, with an additional safety distance of 50 meters.

The situation for collision avoidance in the head-on scenario is shown as an example in Figure 6.12. In general, the behaviors of the OS comply with COLREGs for the head-on encountering situation. It can be observed that the OS first turns to starboard as regulated by COLREGs and takes early evasive action to avoid the upcoming TSs. After the encounter, the OS returned to the centerline, then moved left to avoid static obstacles, and finally converged toward the destination. In addition, the entire moving trajectory is smooth without irregular turns, suitable for the ship to follow in operations.

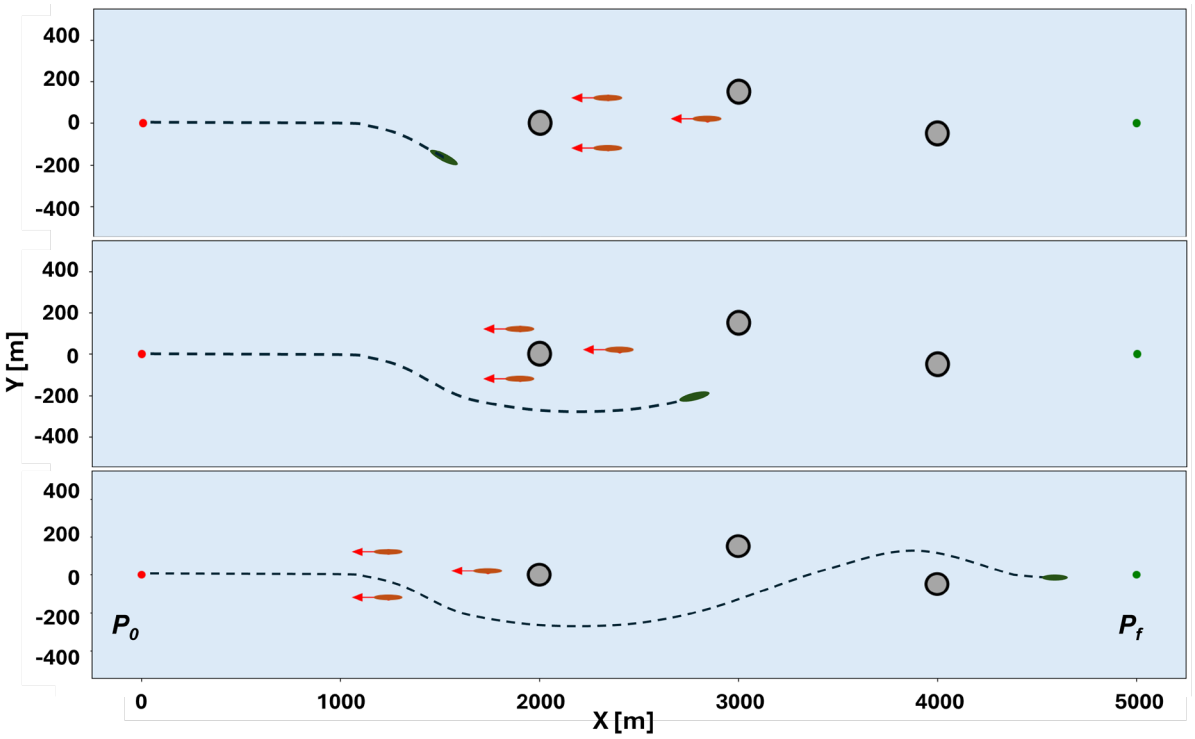

Figure 6.12: CA demonstrations for the head-on scenario in the open water area.

- **Collision avoidance in confined waterways**

The proposed method is further demonstrated in the confined waterway shown in Figure 6.13. The river width is set to 200 to 400 meters. In addition to the same static obstacles as those in Figure 6.12, a 250-meter-long and 10 to 20-meter-wide waterway lock is also simulated. Its dimensions correspond to small to medium-sized locks and it is located along the riverbank and centered within the waterway, as shown in Figure 6.13 (a), occupying 20% of the river width.

In inland traffic, ships rarely cross rivers laterally, thus only head-on and overtaking scenarios are simulated in this confined waterway. As mentioned earlier, the TS trajectories are assumed to be known in advance by the OS. Figure 6.13 (b) and (c) illustrate the TS trajectories for head-on and overtaking scenarios, respectively, where green points indicate target points.

Figure 6.14 illustrates the process of avoiding a head-on collision with TSs. The OS initially follows the reference route (centerline) when no collision is detected. To avoid a collision and prioritize starboard maneuvering, the OS passes through the central waterway lock from its starboard side. After passing through the lock, the two TSs leave the nearby waterway, allowing the OS to return to the centerline and continue toward the target point $\boldsymbol{P}_f$.

The CA process for overtaking two TSs is also shown in Figure 6.14. On the right side of the river, the TSs travel at slower speeds than that of the OS. Similarly, the OS initially follows the centerline while avoiding obstacles. After passing the static obstacles, it begins a starboard turn

and overtakes the two TSs from the right side. Once the overtaking maneuver is complete, the OS returns to the centerline with a relatively smooth turn, converging toward the target point P_f. These two cases in the confined waterway demonstrate the CA capability of the proposed algorithm, which complies with COLREGs while considering the constraints of the waterway's terrain.

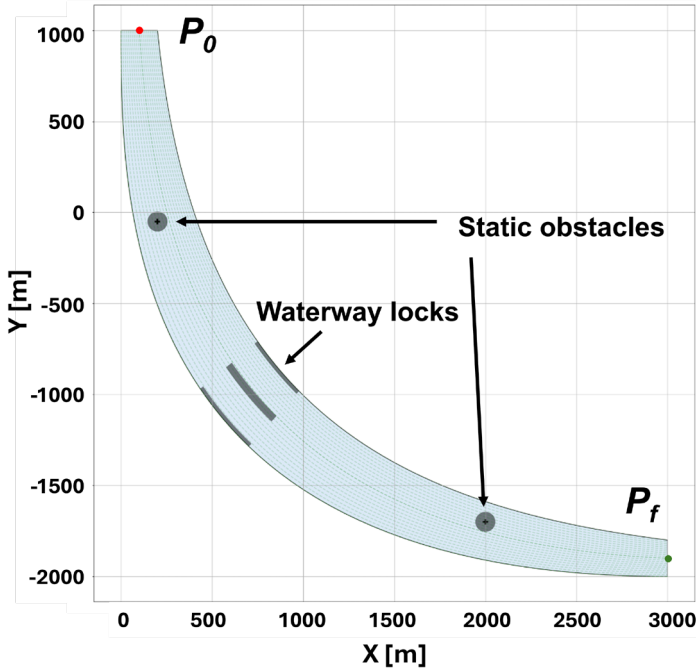

(a)

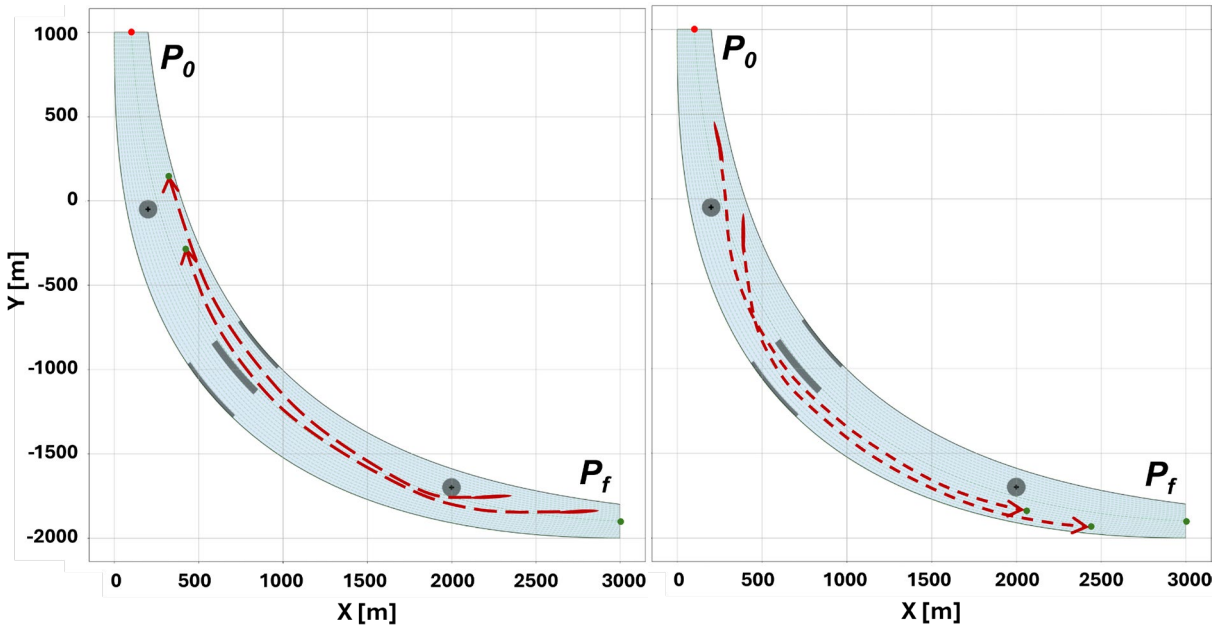

(b) (c)

Figure 6.13: Demonstrations of confined waterway with water waterway locks in (a), and TS's trajectories information in (b) and (c).

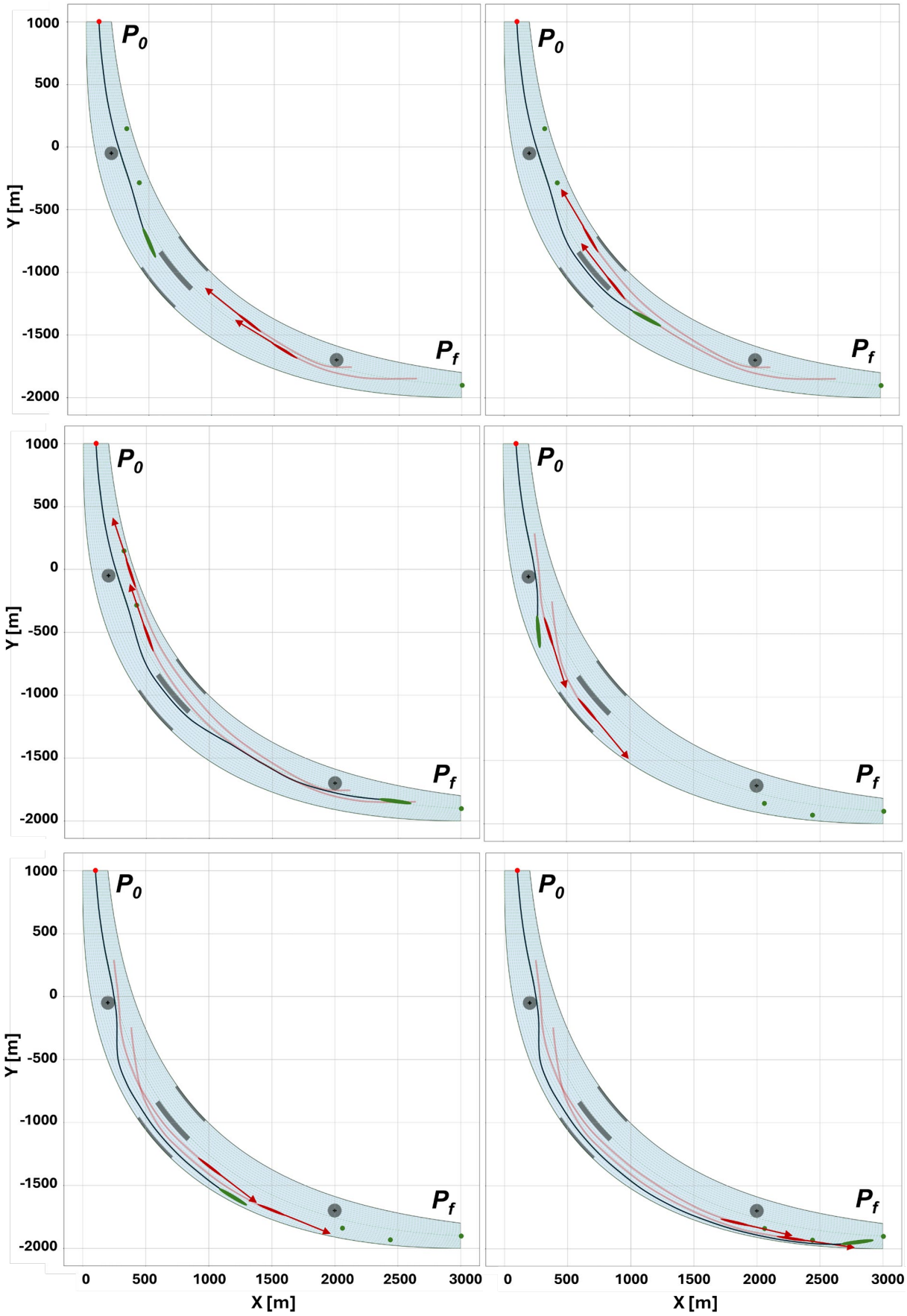

Figure 6.14: Simulations of collision avoidance in head-on and overtaking scenarios in confined waterways.

In summary, for the simulated cases in both open areas and confined waterways, the OS's evasive maneuvers effectively avoid both static and moving obstacles. Additionally, the suggested trajectories comply with COLREGs, ensuring smooth route without sharp turns, making them suitable for practical operations. The computational time for these cases averages less than 10 seconds, including trajectory prediction using the ship dynamics model. By leveraging parallel computing techniques, the computational cost of trajectory prediction can be further reduced, indicating strong potential for real-time applications of the proposed Isochrone-based method.

7 Conclusions

This thesis investigates and develops voyage optimization algorithms to achieve intelligent maritime transportation, i.e., to enhance the decision-making in operations, with a focus on improving energy efficiency in weather routing and ensuring ship operational safety for collision avoidance. It has been found that both the proposed IPO and L-MOEA methods effectively minimize fuel consumption and optimize energy efficiency in weather routing. Furthermore, the application of the real-time IPO method has been extended to effectively address collision avoidance (CA) problems in both open waters and confined waterways.

All the proposed methods can assist seafarers with voyage planning for one voyage before departure based on the information provided, which includes destination and ETA. Weather routing also incorporates weather forecasts. When the ship is en route, the proposed algorithms can also be utilized on board by seafarers to address any uncertainties in real-time or to regularly update the voyage. It can be every 24 to 72 hours for weather routing when the weather forecast is usually updated. For CA, it can be when TSs are found approaching, with updates occurring usually in seconds or minutes depending on the frequency of environmental and traffic data refresh.

Specifically, several tasks have been conducted to meet the following objectives respectively.

1) A systematic review and clarification of terminologies in weather routing and identify opportunities in current research for the development of optimization algorithms (Paper I).
2) Proposal of an effective and efficient algorithm based on the Isochrone method to achieve energy-efficient real-time weather routing (Papers II and III).
3) Adoption of an efficient ML MOEA to address energy-efficient weather routing and consider uncertainties in weather forecast (Paper IV).
4) Investigation of the fuel consumption uncertainty caused by SFOC in ship performance models and its impact on weather routing (Paper V).
5) Application of Isochrone-based algorithms research to address CA problems, to assist on-time transport and ensure ship operational safety for inland and coastal shipping (Paper VI).

Some conclusions on each of the topics investigated are summarized as follows.

Systematic review for optimization algorithms in weather routing

The literature review was conducted in **Paper I**, which reveals that algorithms and models have been the two main research focuses on weather routing research, and ML applications started to emerge after 2020. For optimization algorithms in weather routing, the findings are as follows:

- Isochrone, DP-based, EA/GA, and PSO/ACO are the four major types of optimization algorithms frequently used in weather routing.
- Their recent algorithmic development trends share similarities, focusing on four areas:
    - Enhancing the diversity of candidate solution sets.
    - Preserving superior candidate sets during the process, to enhance the optimization performance of the algorithms, finding a balance between avoiding local optima and excessive divergence.
    - Creating hybrid algorithms that leverage the strengths of different algorithms.
    - Strengthening practical applications to meet specific operational requirements.
- Based on these insights, future directions may also be divided into two aspects:
    - Improving algorithm performance through enhanced heuristics and integrating learning-based methods
    - Enhancing practical applications, such as effectively handling uncertainties and supporting future clean-fuel-driven ships.

Development of optimization algorithms for weather routing

The voyage optimization Isochrone algorithm is improved for real-time energy efficient weather routing, as its computational efficiency is demonstrated in industrial practice. This work is sequentially presented in **Papers II** and **III**. Five strategies are proposed to address the drawbacks of the Isochrone method, e.g., sharp turning and local optimization issues. Based on the findings, the IPO algorithm is proposed to achieve real-time energy efficient ship voyage planning and execution. It has been found that:

- All five improvement strategies can lead to an improved capability compared to the Isochrone method. Among these, two strategies, "Reversed subsector" and "Isochrone-A*", are found to be the most effective.
- The two strategies are integrated with ML-enhanced heuristics, resulting in the IPO method. It has been demonstrated that the IPO method can provide smooth voyages with gradual turns and an average of 5% fuel reduction. Its runtime can be on average 20 seconds including ship performance predictions, allowing for real-time applications.
- Other optimization methods included for comparison either show no fuel savings or less than 5%, or their computational time is at least twice that of IPO.

The application of an advanced ML algorithm, MOEA in weather routing is further investigated in **Paper IV**, to leverage its powerful optimization capability while addressing the convergence inefficiency of a typical MOEA. It has been found that:

- The proposed self-evolving learning network in L-MOEA can capture positive evolutionary directions and conduct efficient searches. Compared with other state-of-the-art optimization methods, the proposed L-MOEA significantly reduces fuel consumption and duration on given voyages.

- An uncertainty-driven module (L-MOEA-U) is proposed to address uncertainties in weather conditions. L-MOEA-U also contributes to providing more robust solutions, with an overall improvement exceeding 20%, ensuring the reliability of voyage optimization results.

SFOC induced uncertain fuel consumption in weather routing

Paper V introduces a ML-based predictive model to estimate uncertain fuel consumption and assesses its impact on weather routing. This consists of three components: (1) a GA-BP model developed to predict ship power; (2) a GPR model developed to predict stochastic SFOC; and (3) Monte Carlo simulations applied to analyze the effects of SFOC induced uncertain fuel consumption on weather routing. It has been found that:

- Under specific operational conditions, a ship's SFOC is not determined but varies within a range.
- Results from Monte Carlo simulations further suggest that the impact of uncertainty on the effectiveness of ship weather routing cannot be ignored in practical applications.
- Moreover, optimization should account not only for the actual fuel consumption but also for the probability of achieving compliance with relevant standards, such as EEOI.

Real-time Isochrone-based collision avoidance in confined waterways

In **Paper VI**, an Isochrone-based CA algorithm developed to ensure ship safety helps meet real-time operations and punctual arrival requirements. In addition to leveraging computational efficiency and ETA considerations of traditional Isochrone algorithms for weather routing, this algorithm specifically enhances land avoidance capabilities to account for terrain/bathymetry. The results reveal the following:

- The proposed Isochrone-based CA method features terrain adaptability and regulatory compliance, including adherence to COLREGs both in confined waterways and open water areas.
- It can recommend an optimized voyage that ensures short-distance sailing and ship safety during collision avoidance.
- Moreover, the algorithm can be executed on average for less than 10 seconds which includes trajectory predictions, allowing for real-time applications.

8 Future work

Weather routing to assist intelligent maritime operations

Intelligence in ship operations indicates a high level of decision-making capability, enabling the generation of optimal plans that can consider various objectives, particularly with the support of data (Sarker, 2022). The current implementation of the IPO assumes constant speed. However, ship speed is not the most direct operational variable in shipping but rather engine speed (RPM). Therefore, engine speed (RPM) should replace ship speed in future adaptations to achieve better practicality. Additionally, 3D algorithms present enhanced optimization performance and better decision-making capabilities; thus, developing a 3D-IPO that incorporates RPM variations may be worthwhile. Although this can lead to an increased computational load due to the greater number of voyage options, such variability may be effectively managed by using ML-based heuristics based on data-driven techniques, to filter and refine the choices.

Additionally, weather routing is a research topic with significant potential in practical application, and the literature review revealed that enhancing its applicability is an important direction. To better support the energy transition in the future, a wider variety of clean-fuel powered ship types will emerge, including hybrid, electric, or wind-assisted propulsion ships (WAPS). Voyage optimization for these ships will take into consideration their specific operational characteristics, such as the wind angle of attack for WAPS. Exploring research developments in this area is also highly worthwhile supporting their smoother implementations. In addition, different fuels may require different engine RPMs, leading to varying optimization outcomes for power or fuel consumption, which may be dependent on the type of fuel used. Future research could further comprehensively explore the differences and impact in optimizing power or fuel in weather routing, and its relationship with the type of fuel used.

Sensitivity of weather routing on various factors

Future work can also investigate the sensitivity of the proposed IPO method to some factors that may have a great impact on its performance. These factors include waypoint resolution in the Isochrone algorithm defined by its parameters, and how that would influence convergence. Additionally, incorporating improved weather forecast models will be critical to enhancing prediction accuracy, leading to enhanced performance. However, the impact of update frequency of weather information on weather routing may need to be further investigated through real-time applications.

Enhanced considerations for real traffic in collision avoidance

The current work on collision avoidance is based on several assumptions. Firstly, ship dynamic models are assumed to be linear, but they can later be replaced with more precise models tailored for inland ships, such as those accounting for the effects of shallow water on ship movement (Zhang et al., 2023b). Additionally, the ship domain is considered static, whereas it should

dynamically adjust based on encounters with other vessels. It is also assumed that the OS knows the movement and trajectory of the TS through communications in traffic. However, more reliable solutions can be considered in practice (Tran et al., 2023), such as using AIS data for trajectory prediction (Rothmund et al., 2022; Zhang et al., 2023a). Lastly, as the shallow water effects are not analyzed, the current method cannot comprehensively estimate the energy consumption of maneuvering and sailing (Zhang et al., 2024a), which should be considered a more realistic and critical objective for optimization. Thus, the existing method uses short distances as a simplified way to estimate energy costs. Future work can consider optimizing energy efficiency in addition to enhanced ship safety for collision avoidance, based on dynamic models for inland ships.

Real case study and validation

The real behavior of traffic ships may be unpredictable with constantly changing trajectories, as their future movements may not be strongly correlated with their previous ones because of varying operational tasks and conditions. Therefore, simulations cannot fully capture the complexity of real traffic situations. Consequently, validating the proposed CA algorithm based on real traffic data is extremely necessary to comprehensively demonstrate its effectiveness, especially for such an operational challenge as collision avoidance.

References

Abdelaal, M., Fränzle, M., & Hahn, A. (2018). Nonlinear Model Predictive Control for trajectory tracking and collision avoidance of underactuated vessels with disturbances. *Ocean Engineering*, *160*, 168-180.

Ahlgren, F., Mondejar, M. E., & Thern, M. (2019). Predicting dynamic fuel oil consumption on ships with automated machine learning. *Energy Procedia*, *158*, 6126-6131.

Alonso-Mora, J., Beardsley, P., & Siegwart, R. (2018). Cooperative Collision Avoidance for Nonholonomic Robots. *IEEE Transactions on Robotics*, *34*(2), 404-420.

Ari, I., Aksakalli, V., Aydogdu, V., & Kum, S. (2013). Optimal ship navigation with safety distance and realistic turn constraints. *European Journal of Operational Research*, *229*(3), 707-717.

Bahrami, N., & Siadatmousavi, S. (2024). Ship voyage optimisation considering environmental forces using the iterative Dijkstra's algorithm. *Ships and Offshore Structures*, *19*(8), 1173-1180.

Baldauf, M., Benedict, K., Kirchhoff, M., Schaub, M., Gluch, M., & Fischer, S. (2018). Energy-efficient ship operation: the concept of green manoeuvring. *Corporate social responsibility in the maritime industry*, 185-218.

Bassam, A. M., Phillips, A. B., Turnock, S. R., & Wilson, P. A. (2023). Artificial neural network based prediction of ship speed under operating conditions for operational optimization. *Ocean Engineering*, *278*, 114613.

Bellman, R. (1952). On the theory of dynamic programming. Proceedings of *The national Academy of Sciences*, *38*(8), 716-719.

Besikçi, E. B., Arslan, O., Turan, O., & Ölçer, A. I. (2016). An artificial neural network based decision support system for energy efficient ship operations. *Computers & Operations Research*, *66*, 393-401.

Chakravarthy, A., & Ghose, D. (1998). Obstacle avoidance in a dynamic environment: A collision cone approach. *IEEE Transactions on Systems Man and Cybernetics Part a-Systems and Humans*, *28*(5), 562-574.

Chen, L. Y., Hopman, H., & Negenborn, R. R. (2018). Distributed model predictive control for vessel train formations of cooperative multi-vessel systems. *Transportation Research Part C-Emerging Technologies*, *92*, 101-118.

Chen, M., & Tan, Y. (2023). SF-FWA: A Self-Adaptive Fast Fireworks Algorithm for effective large-scale optimization. *Swarm and Evolutionary Computation*, *80*, 101314.

Chen, Y., & Mao, W. (2024). An Isochrone-Based Predictive Optimization for Efficient Ship Voyage Planning and Execution. *IEEE Transactions on Intelligent Transportation Systems*.

Choi, G.-H., Lee, W., & Kim, T.-w. (2023). Voyage optimization using dynamic programming with initial quadtree based route. *Journal of Computational Design and Engineering*, *10*(3), 1185-1203.

Clarke, D., Gedling, P., & Hing, G. (1983). The application of manoeuvering criteria in hull design using linear theory.

Coldwell, T. G. (1983). Marine Traffic Behavior in Restricted Waters. *Journal of Navigation*, *36*(3), 430-444.

Coraddu, A., Oneto, L., Baldi, F., & Anguita, D. (2017). Vessels fuel consumption forecast and trim optimisation: A data analytics perspective. *Ocean Engineering*, *130*, 351-370.

Davis, P. V., Dove, M. J., & Stockel, C. T. (1980). A Computer-Simulation of Marine Traffic Using Domains and Arenas. *Journal of Navigation*, *33*(2), 215-222.

De Wit, C. (1990). Proposal for low cost ocean weather routeing. *The Journal of Navigation*, *43*(3), 428-439.

Degiuli, N., Farkas, A., Martić, I., & Grlj, C. G. (2023). Optimization of maintenance schedule for containerships sailing in the Adriatic Sea. *Journal of marine science and engineering, 11*(1), 201.

Deng, S., & Mi, Z. (2023). A review on carbon emissions of global shipping. *Marine Development*, *1*(1), 4.

Dijkstra, E. W. (1959). A note on two problems in connexion with graphs [Article]. *Numerische Mathematik*, *1*(1), 269-271.

DNV. (2018). Maritime Forecast to 2050 - Energy Transition Outlook 2018. www.dnv.com/publications

DNV. (2023). Maritime forecast to 2050 - Energy transition outlook 2023. www.dnv.com/publications

DNV. (2024a). Leading a data-driven transition. https://www.dnv.com/publications/leading-a-data-driven-transition/

DNV. (2024b). Maritime forecast to 2050 - Energy transition outlook 2024. https://www.dnv.com/energy-transition-outlook/key-highlights/

Dong, L., Li, J., Xia, W., & Yuan, Q. (2021). Double ant colony algorithm based on dynamic feedback for energy-saving route planning for ships. *Soft Computing*, *25*, 5021-5035.

Du, W., Li, Y., Zhang, G., Wang, C., Zhu, B., & Qiao, J. (2022a). Energy saving method for ship weather routing optimization. *Ocean Engineering*, *258*, 111771.

Du, W., Li, Y., Zhang, G., Wang, C., Zhu, B., & Qiao, J. (2022b). Ship weather routing optimization based on improved fractional order particle swarm optimization. *Ocean Engineering*, *248*.

Du, W., Li, Y., Shi, J., Sun, B., Wang, C., & Zhu, B. (2023). Applying an improved particle swarm optimization algorithm to ship energy saving. *Energy*, *263*.

Du, Y., Meng, Q., Wang, S., & Kuang, H. (2019). Two-phase optimal solutions for ship speed and trim optimization over a voyage using voyage report data. *Transportation Research Part B: Methodological*, *122*, 88-114.

European Centre for Medium-Range Weather Forecasts. *European Centre for Medium-Range Weather Forecasts (ECMWF)*. https://www.ecmwf.int/

Fabbri, T., & Vicen-Bueno, R. (2021). Decision-making methodology in environmentally-conditioned ship operations based on ETD-ETA windows of opportunity. *Journal of Navigation*, *74*(6), 1219-1237.

Fan, Y., Sun, X., & Wang, G. (2019). An autonomous dynamic collision avoidance control method for unmanned surface vehicle in unknown ocean environment. *International Journal of Advanced Robotic Systems*, *16*(2).

Fang, M.-C., & Lin, Y.-H. (2015). The optimization of ship weather-routing algorithm based on the composite influence of multi-dynamic elements (II): Optimized routings. *Applied Ocean Research*, *50*, 130-140.

Fiorini, P., & Shiller, Z. (1998). Motion planning in dynamic environments using velocity obstacles. *International Journal of Robotics Research*, *17*(7), 760-772.

Fossen, T. I. Python Vehicle Simulator. Retrieved December 2024 from https://github.com/cybergalactic/PythonVehicleSimulator

Fox, D., Burgard, W., & Thrun, S. (1997). The dynamic window approach to collision avoidance. *IEEE Robotics & Automation Magazine*, *4*(1), 23-33.

Fujii, Y., & Tanaka, K. (1971). Traffic Capacity. *Journal of the Institute of Navigation*, *24*(4), 543-&.

Gao, P., Zhou, L., Zhao, X., & Shao, B. (2023). Research on ship collision avoidance path planning based on modified potential field ant colony algorithm. *Ocean & Coastal Management*, *235*.

Gkerekos, C., & Lazakis, I. (2020). A novel, data-driven heuristic framework for vessel weather routing. *Ocean Engineering*, *197*, 106887.

Guo, F., Chen, L., & Wang, Z. (2024). Imbalanced data-oriented probabilistic modeling for fuel consumption uncertainty of marine diesel engine during oceangoing voyages. *Ocean Engineering*, *312*.

Gupta, P., Rasheed, A., & Steen, S. (2022). Ship performance monitoring using machine-learning. *Ocean Engineering*, *254*.

Hagiwara, H. (1989). Weather routing of (sail-assisted) motor vessels. *Ph. D. thesis, Delft Univ. Tech.*

Halim, A. H., Ismail, I., & Das, S. (2021). Performance assessment of the metaheuristic optimization algorithms: an exhaustive review. *Artificial Intelligence Review, 54*(3), 2323-2409.

Hart, P. E., Nilsson, N. J., & Raphael, B. (1968). A formal basis for the heuristic determination of minimum cost paths. *IEEE transactions on Systems Science and Cybernetics*, *4*(2), 100-107.

He, Z., Chu, X., Liu, C., & Wu, W. (2023). A novel model predictive artificial potential field based ship motion planning method considering COLREGs for complex encounter scenarios. *ISA Transactions*, *134*, 58-73.

Holtrop, J., & Mennen, G. (1982). An approximate power prediction method. *International Shipbuilding Progress*, *29*(335), 166-170.

Hörteborn, A., Ringsberg, J. W., Svanberg, M., & Holm, H. (2019). A revisit of the definition of the ship domain based on AIS analysis. *The Journal of Navigation, 72*(3), 777-794.

Hu, Y., Zhang, A., Tian, W., Zhang, J., & Hou, Z. (2020). Multi-Ship Collision Avoidance Decision-Making Based on Collision Risk Index. *Journal of Marine Science and Engineering*, *8*(9).

Hu, Z., Zhou, T., Zhen, R., Jin, Y., Li, X., & Osman, M. (2022). A two-step strategy for fuel consumption prediction and optimization of ocean-going ships. *Ocean Engineering*, *249*.

Huang, L., Wen, Y., Geng, X., Zhou, C., & Xiao, C. (2018). Integrating multi-source maritime information to estimate ship exhaust emissions under wind, wave and current conditions. *Transportation Research Part D: Transport and Environment*, *59*, 148-159.

Huang, Y., Chen, L., Chen, P., Negenborn, R. R., & van Gelder, P. H. A. J. M. (2020). Ship collision avoidance methods: State-of-the-art. *Safety Science*, *121*, 451-473.

IMO. (2020). Just In Time Arrival Guide: Barriers and Potential Solutions (GloMEEP Project Coordination Unit International Maritime Organization).

IMO. (2023). 2023 IMO strategy on reduction of GHG emissions from ships. https://www.imo.org/en/OurWork/Environment/Pages/2023-IMO-Strategy-on-Reduction-of-GHG-Emissions-from-Ships.aspx

James. (1957a). Application of wave forecast to marine navigation. *Washington*.

James. (1957b). Application of wave forecasts to marine navigation. *New York University.*

Jeong, S., Jeong, D., Park, J., Kim, S., & Kim, B. (2019). A voyage optimization model of LNG carriers considering boil-off gas. In *OCEANS 2019 MTS/IEEE SEATTLE* (pp. 1-7). IEEE.

Jiang, L., An, L., Zhang, X., Wang, C., & Wang, X. (2022). A human-like collision avoidance method for autonomous ship with attention-based deep reinforcement learning. *Ocean Engineering*, *264*.

Jimenez, V. J., Kim, H., & Munim, Z. H. (2022). A review of ship energy efficiency research and directions towards emission reduction in the maritime industry. *Journal of Cleaner Production*, *366*, 132888.

Johansen, T. A., Perez, T., & Cristofaro, A. (2016). Ship Collision Avoidance and COLREGS Compliance Using Simulation-Based Control Behavior Selection With Predictive Hazard Assessment. *IEEE Transactions on Intelligent Transportation Systems*, *17*(12), 3407-3422.

Kiran, A., & Vasumathi, D. (2020). Data mining: min–max normalization based data perturbation technique for privacy preservation. Proceedings of *the third international conference on computational intelligence and informatics*: *ICCII 2018* (pp. 723-734). Singapore: Springer Singapore.

Klompstra, M. B., Olsder, G., & Van Brunschot, P. (1992). The isopone method in optimal control. *Dynamics and Control*, *2*(3), 281-301.

Lang, X., Wu, D., & Mao, W. (2021). Benchmark Study of Supervised Machine Learning Methods for a Ship Speed-Power Prediction at Sea. In *International Conference on Offshore Mechanics and Arctic Engineering* (Vol. 85161, p. V006T06A018). American Society of Mechanical Engineers.

Lang, X., & Mao, W. (2020). A semi-empirical model for ship speed loss prediction at head sea and its validation by full-scale measurements. *Ocean Engineering*, *209*, 107494.

Lang, X., & Mao, W. (2022). Big Data-Based Decision Support Systems. In *Encyclopedia of Ocean Engineering* (pp. 143-149). Springer.

Lang, X., Wang, H., Mao, W., Osawa, N., & (2021). Impact of ship operations aided by voyage optimization on a ship's fatigue assessment. *Journal of Marine Science and Technology*, *26*, 750-771.

Lang, X., Wu, D., & Mao, W. (2022). Comparison of supervised machine learning methods to predict ship propulsion power at sea. *Ocean Engineering*, *245*, 110387.

Lang, X., Wu, D., & Mao, W. (2024). Physics-informed machine learning models for ship speed prediction. *Expert Systems with Applications*, *238*, 121877.

Lee, S.-M, Roh, M.-I., Kim, K.-S., Jung, H., & Park, J. J. (2018). Method for a simultaneous determination of the path and the speed for ship route planning problems. *Ocean Engineering*, *157*, 301-312.

Lee, H., Roh, M., & Kim, K. (2021). Ship route planning in Arctic Ocean based on POLARIS. *Ocean Engineering*, 234.

Lee, S., Sun, Q., & Meng, Q. (2023). Vessel weather routing subject to sulfur emission regulation. *Transportation Research Part E-Logistics and Transportation Review*, *177*.

Lei, J., Chu, Z., Wu, Y., Liu, X., Luo, M., He, W., & Liu, C. (2024). Predicting vessel arrival times on inland waterways: A tree-based stacking approach. *Ocean Engineering*, *294*.

Li, P., Wang, H., & He, D. (2018). Ship weather routing based on improved ant colony optimization algorithm. In *2018 IEEE Industrial Cyber-Physical Systems (ICPS)* (pp. 310-315). IEEE.

Li, L., Wu, D., Huang, Y., & Yuan, Z. (2021). A path planning strategy unified with a COLREGS collision avoidance function based on deep reinforcement learning and artificial potential field. *Applied Ocean Research*, *113*.

Li, X., Sun, B., Guo, C., Du, W., & Li, Y. (2020). Speed optimization of a container ship on a given route considering voluntary speed loss and emissions. *Applied Ocean Research*, *94*, 101995.

Li, X., Ding, K., Xie, X., Yao, Y., Zhao, X., Jin, J., & Sun, B. (2024). Bi-objective ship speed optimization based on machine learning method and discrete optimization idea. *Applied Ocean Research*, *148*.

Lin, Y.-H. (2018). The simulation of east-bound transoceanic voyages according to ocean-current sailing based on Particle Swarm Optimization in the weather routing system. *Marine Structures*, *59*, 219-236.

Lin, Y.-H., Fang, M.-C., & Yeung, R. W. (2013). The optimization of ship weather-routing algorithm based on the composite influence of multi-dynamic elements. *Applied Ocean Research*, *43*, 184-194.

Luo, X., Yan, R., & Wang, S. A. (2024). Ship sailing speed optimization considering dynamic meteorological conditions. *Transportation Research Part C: Emerging Technologies*, *167*.

Ma, L., Yang, P., Gao, D., & Bao, C. (2023). A multi-objective energy efficiency optimization method of ship under different sea conditions. *Ocean Engineering*, *290*.

Ma, D., Zhou, S., Han, Y., Ma, W., & Huang, H. (2024a). Multi-objective ship weather routing method based on the improved NSGA-III algorithm. *Journal of Industrial Information Integration*, *38*, 100570.

Ma, W., Lu, T., Ma, D., Wang, D., & Qu, F. (2021). Ship route and speed multi-objective optimization considering weather conditions and emission control area regulations. *Maritime Policy & Management*, *48*(8), 1053-1068.

Majumder, A., & Majumder, A. (2021). Pathfinding and navigation. *Deep Reinforcement Learning in Unity: With Unity ML Toolkit*, 73-153.

Mannarini, G., & Carelli, L. (2019). VISIR-1. b: Ocean surface gravity waves and currents for energy-efficient navigation. *Geoscientific Model Development*, *12*(8), 3449-3480.

Mannarini, G., Salinas, M. L., Carelli, L., Petacco, N., & Orović, J. (2023). VISIR-2: ship weather routing in Python. *EGUsphere*, *2023*, 1-40.

Mao, W., Li, Z., Ogeman, V., & Ringsberg, J. W. (2015). A regression and beam theory based approach for fatigue assessment of containership structures including bending and torsion contributions. *Marine Structures*, *41*, 244-266.

Mao, W., Ringsberg, J. W., Rychlik, I., & Li, Z. (2012). Theoretical development and validation of a fatigue model for ship routing. *Ships and Offshore Structures*, *7*(4), 399-415.

Mao, W., & Rychlik, I. (2017). Estimation of Weibull distribution for wind speeds along ship routes. *Proceedings of the Institution of Mechanical Engineers, Part M: Journal of Engineering for the Maritime Environment*, *231*(2), 464-480.

Mao, W., Ringsberg, J. W., Rychlik, I., & Storhaug, G. (2010). Development of a Fatigue Model Useful in Ship Routing Design. *Journal of Ship Research*, *54*(4), 281-293.

Mao, W., Rychlik, I., Wallin, J., & Storhaug, G. (2016). Statistical models for the speed prediction of a container ship. *Ocean Engineering*, *126*, 152-162.

Marques, C. H., Caprace, J. D., Belchior, C. R., & Martini, A. (2019). An approach for predicting the specific fuel consumption of dual-fuel two-stroke marine engines. *Journal of Marine Science and Engineering, 7(*2), 20.

Mason, J., Larkin, A., & Gallego-Schmid, A. (2023). Mitigating stochastic uncertainty from weather routing for ships with wind propulsion. *Ocean Engineering*, *281*.

Moradi, M. H., Brutsche, M., Wenig, M., Wagner, U., & Koch, T. (2022). Marine route optimization using reinforcement learning approach to reduce fuel consumption and consequently minimize CO_2 emissions. *Ocean Engineering*, *259*, 111882.

National Weather Service Portland. Beaufort Scale. Retrieved January 2025 from https://www.weather.gov/pqr/beaufort

Norouzi, A., Heidarifar, H., Borhan, H., Shahbakhti, M., & Koch, C. R. (2023). Integrating machine learning and model predictive control for automotive applications: A review and future directions. *Engineering Applications of Artificial Intelligence, 120*, 105878.

Park, H., Blanco, C. C., & Bendoly, E. (2022). Vessel sharing and its impact on maritime operations and carbon emissions. *Production and Operations Management*, *31*(7), 2925-2942.

Qian, L., Li, H., Hong, M., Qi, Y., & Guo, Z. (2023). Avoiding sudden maritime risk: A new variable speed route planning model by integrating Spatio-temporal dimension. *Ocean Engineering*, *288*.

Roh, M.-I. (2013). Determination of an economical shipping route considering the effects of sea state for lower fuel consumption. *International Journal of Naval Architecture and Ocean Engineering*, *5*(2), 246-262.

Rothmund, S. V., Tengesdal, T., Brekke, E.F., & Johansen, T.A. (2022). Intention modeling and inference for autonomous collision avoidance at sea. *Ocean Engineering*, 266.

Sarigiannidis, A. G., Chatzinikolaou, E., Patsios, C., & Kladas, A. G. (2016). Shaft generator system design and ship operation improvement involving SFOC minimization, electric grid conditioning, and auxiliary propulsion. *IEEE Transactions on Transportation Electrification, 2*(4), 558-569.

Sarker, I. H. (2022). AI-based modeling: techniques, applications and research issues towards automation, intelligent and smart systems. *SN Computer Science, 3(2)*, 158.

Serigstad, E. (2017). Hybrid collision avoidance for autonomous surface vessels. *Master thesis, NTNU.*

Shah, B. C., Svec, P., Bertaska, I. R., Sinisterra, A. J., Klinger, W., von Ellenrieder, K., Dhanak, M., & Gupta, S. K. (2016). Resolution-adaptive risk-aware trajectory planning for surface vehicles operating in congested civilian traffic. *Autonomous Robots*, *40*(7), 1139-1163.

Shin, Y., Abebe, M., Noh, Y., Lee, S., Lee, I., Kim, D., Bae, J., & Kim, K. (2020). Near-optimal weather routing by using improved A* algorithm. *Applied Sciences*, *10*(17), 6010.

Sidoti, D., Pattipati, K. R., & Bar-Shalom, Y. (2023). Minimum Time Sailing Boat Path Algorithm. *IEEE Journal of Oceanic Engineering*, *48*(2), 307-322.

Simonsen, M. H., Larsson, E., Mao, W., & Ringsberg, J. W. (2015). State-of-the-art within ship weather routing. In *International Conference on Offshore Mechanics and Arctic Engineering* (Vol. 56499, p. V003T02A053). American Society of Mechanical Engineers.

Soner, O., Akyuz, E., & Celik, M. (2018). Use of tree based methods in ship performance monitoring under operating conditions. *Ocean Engineering*, *166*, 302-310.

Storhaug, G. (2007). Experimental investigation of wave induced vibrations and their effect on the fatigue loading of ships. *Ph. D. thesis, NTNU.*

Svec, P., Thakur, A., Raboin, E., Shah, B. C., & Gupta, S. K. (2014). Target following with motion prediction for unmanned surface vehicle operating in cluttered environments. *Autonomous Robots*, *36*(4), 383-405.

Szlapczynska, J., & Szlapczynski, R. (2019). Preference-based evolutionary multi-objective optimization in ship weather routing. *Applied Soft Computing*, *84*, 105742.

Szlapczynski, R., & Szlapczynska, J. (2017). Review of ship safety domains: Models and applications. *Ocean Engineering*, *145*, 277-289.

Tillig, F., & Ringsberg, J. W. (2019). A 4 DOF simulation model developed for fuel consumption prediction of ships at sea. *Ships and Offshore Structures*, *14*(sup1), 112-120.

Tran, H. A., Johansen, T. A., & Negenborn, R. R. (2023). Collision avoidance of autonomous ships in inland waterways–A survey and open research problems. In *Journal of Physics: Conference Series* (Vol. 2618, No. 1, p. 012004). IOP Publishing.

Tran, N. K., & Haasis, H. D. (2018). A Research on Operational Patterns in Container Liner Shipping. *Transport*, *33*(3), 619-632.

Tsai, C. L., Su, D. T., & Wong, C. P. (2021). An empirical study of the performance of weather routing service in the North Pacific Ocean. *Maritime Business Review*, *6*(3), 280-292.

Tsolakis, A., Negenborn, R. R., Reppa, V., & Ferranti, L. (2024). Model Predictive Trajectory Optimization and Control for Autonomous Surface Vessels Considering Traffic Rules. *IEEE Transactions on Intelligent Transportation Systems*.

Tsou, M.-C. (2010). Integration of a geographic information system and evolutionary computation for automatic routing in coastal navigation. *The Journal of Navigation*, *63*(2), 323-341.

Tzortzis, G., & Sakalis, G. (2021). A dynamic ship speed optimization method with time horizon segmentation. *Ocean Engineering*, *226*, 108840.

UNCTAD. (2023). Review of Maritime Transport 2023: towards a green and just transition (UNCTAD/RMT/2023). *U. N. Publications*. https://unctad.org/publication/review-maritime-transport-2023

Wang, K., Guo, X., Zhao, J., Ma, R., Huang, L., Tian, F., Dong, S., Zhang, P., Liu, C., & Wang, Z. (2022). An integrated collaborative decision-making method for optimizing energy consumption of sail-assisted ships towards low-carbon shipping. *Ocean Engineering*, *266*, 112810.

Wang, H., Lang, X., Mao, W., Zhang, D., & Storhaug, G. (2020a). Effectiveness of 2D optimization algorithms considering voluntary speed reduction under uncertain metocean conditions. *Ocean Engineering, 200*, 107063.

Wang, H., Lang, X., & Mao, W. (2021). Voyage optimization combining genetic algorithm and dynamic programming for fuel/emissions reduction. *Transportation Research Part D: Transport and Environment*, *90*, 102670.

Wang, K., Li, J., Huang, L., Ma, R., Jiang, X., Yuan, Y., Mwero, N. A., Negenborn, R. R., Sun, P., & Yan, X. (2020b). A novel method for joint optimization of the sailing route and

speed considering multiple environmental factors for more energy efficient shipping. *Ocean Engineering*, *216*, 107591.

Wang, H., Yan, R., Wang, S., & Zhen, L. (2023). Innovative approaches to addressing the tradeoff between interpretability and accuracy in ship fuel consumption prediction. *Transportation Research Part C: Emerging Technologies*, *157*, 104361.

Wang, H., Mao, W., & Eriksson, L. (2019). A Three-Dimensional Dijkstra's algorithm for multi-objective ship voyage optimization. *Ocean Engineering*, *186*, 106131.

Wang, H., Mao, W., & Eriksson, L. (2020c). Efficiency of a Voluntary Speed Reduction Algorithm for a Ship's Great Circle Sailing. *Transnav-International Journal on Marine Navigation and Safety of Sea Transportation, 14(2)*, 301-308.

Wang, Y., Xu, H., Feng, H., He, J., Yang, H., Li, F., & Yang, Z. (2024). Deep reinforcement learning based collision avoidance system for autonomous ships. *Ocean Engineering*, *292*.

Wisniewski, B. (1991). Methods of route selection for a sea going vessel. *Gdansk: Wydawnictwo Morskie*.

Xuan, A., & Tian, S. (2021). A regional integrated energy system load prediction method based on Bayesian optimized long-short term memory neural network. In *2021 IEEE PES Innovative Smart Grid Technologies - Asia (ISGT Asia)* (pp. 1-5). IEEE.

Xue, H. (2022). A quasi-reflection based SC-PSO for ship path planning with grounding avoidance. *Ocean engineering*, *247*, 110772.

Yan, R., Wang, S., & Du, Y. (2020). Development of a two-stage ship fuel consumption prediction and reduction model for a dry bulk ship. *Transportation Research Part E: Logistics and Transportation Review*, *138*, 101930.

Yan, R., Yang, D., Wang, T., Mo, H., & Wang, S. (2024). Improving ship energy efficiency: Models, methods, and applications. *Applied Energy*, *368*, 123132.

Yang, L., Chen, G., Rytter, N. G. M., Zhao, J., & Yang, D. (2019). A genetic algorithm-based grey-box model for ship fuel consumption prediction towards sustainable shipping. *Annals of Operations Research*, 1-27.

Yu, H., Fang, Z., Fu, X., Liu, J., & Chen, J. (2021). Literature review on emission control-based ship voyage optimization. *Transportation Research Part D: Transport and Environment*, *93*, 102768.

Yuan, Q., Wang, J., Zhao, T.-H. Hsieh, Sun, Z., & Liu, B. (2022). Uncertainty-informed ship voyage optimization approach for exploiting safety, energy saving and low carbon routes. *Ocean Engineering, 266*, 112887.

Zaccone, R., Ottaviani, E., Figari, M., & Altosole, M. (2018). Ship voyage optimization for safe and energy-efficient navigation: A dynamic programming approach. *Ocean engineering*, *153*, 215-224.

Zhang, M., Kujala, P., Musharraf, M., Zhang, J., & Hirdaris, S. (2023a). A machine learning method for the prediction of ship motion trajectories in real operational conditions. *Ocean Engineering*, *283*.

Zhang, C., Zhang, D., Zhang, M., Zhang, J., & Mao, W. (2022). A three-dimensional ant colony algorithm for multi-objective ice routing of a ship in the Arctic area. *Ocean Engineering*, *266*, 113241.

Zhang, C., Ringsberg, J. W., & Thies, F. (2023b). Development of a ship performance model for power estimation of inland waterway vessels. *Ocean Engineering, 287.*

Zhang, C., Ma, Y., Thies, F., Ringsberg, J. W., & Xing, Y. (2024a). Towards autonomous inland shipping: a manoeuvring model in confined waterways. *Ships and Offshore Structures*, 1-13.

Zhang, M., Taimuri, G., Zhang, J., Zhang, D., Yan, X., Kujala, P., & Hirdaris, S. (2025). Systems driven intelligent decision support methods for ship collision and grounding prevention: Present status, possible solutions, and challenges. *Reliability Engineering & System Safety*, *253*.

Zhang, M., Tsoulakos, N., Kujala, P., & Hirdaris, S. (2024b). A deep learning method for the prediction of ship fuel consumption in real operational conditions. *Engineering Applications of Artificial Intelligence*, *130*.

Zhu, Q., Xi, Y., Weng, J., Han, B., Hu, S., & Ge, Y. (2024). Intelligent ship collision avoidance in maritime field: A bibliometric and systematic review. *Expert Systems with Applications*, *252*.

Zhuang, J., Zhang, L., Zhao, S., Cao, J., Wang, B., & Sun, H. (2016). Radar-based collision avoidance for unmanned surface vehicles. *China Ocean Engineering*, *30*(6), 867-883.

Zis, T. P., Psaraftis, H. N., & Ding, L. (2020). Ship weather routing: A taxonomy and survey. *Ocean Engineering*, *213*, 107697.

Życzkowski, M., Krata, P., & Szłapczyński, R. (2018). Multi-objective weather routing of sailboats considering wave resistance. *Polish Maritime Research*, *25*(1), 4-12.

Zyczkowski, M., & Szlapczynski, R. (2023). Collision risk-informed weather routing for sailboats. *Reliability Engineering & System Safety*, *232*, 109015.